Development of novel combinatorial treatment strategies to overcome resistance in breast cancer

Dissertation zur Erlangung des Doktorgrades
der Fakultät für Chemie und Pharmazie
der Ludwig-Maximilians-Universität München

Prajakta Shirish Oak

From Pune, INDIA

Munich, 2012

Dissertation zur Erlangung des Doktorgrades

der Fakultät für Chemie und Pharmazie

der Ludwig-Maximilians-Universität München

Development of novel combinatorial treatment strategies to overcome resistance in breast cancer

Prajakta Shirish Oak

From Pune, INDIA

Munich, 2012

Erklärung

Diese Dissertation wurde im Sinne von § 7 der Promotionsordnung vom 28. November 2011 von Professor Dr. Ernst Wagner von der Fakultät für Chemie und Pharmazie vertreten.

Eidesstattliche Versicherung

Diese Dissertation wurde eigenständig und ohne unerlaubte Hilfe erarbeitet.

München, am 26.01.2012

.....

(Unterschrift des Autors / der Autorin)

Dissertation eingereicht am …….

1. Gutacher: Prof. Dr. Ernst Wagner

2. Gutacher: PD Dr. Manfred Ogris

Mündliche Prüfung am ……..

सर्वतीर्थमयी माता सर्वदेवमयः पिता|
मातरं पितरं तस्मात् सर्वयत्नेन पूजयेत्||

(Mother is the embodiment of all pilgrimages, father is the embodiment of all deities. Hence, mother and father are to be revered with all the efforts)

Dedicated to my parents and brother

"Somewhere, something incredible is waiting to be known."

….**Carl Sagan**

TABLE OF CONTENTS

1. INTRODUCTION

1.1 Breast cancer - An overview

1.1.1 Breast cancer facts and figures

The global burden of cancer continues to increase mostly because of the aging, factors like exposure to UV radiation, pollution and a rise in the adoption of cancer-causing behaviors (obesity, poor diet, smoking habits etc.). Breast cancer is the most frequently diagnosed cancer and the second leading cause of cancer death among females [1]. Latest statistics estimated almost 230,480 new cases of the invasive breast cancer occurring among women during 2011 and about 2,140 new cases in men. For the year 2012, almost 39,970 deaths due to breast cancer are expected along with 226,870 new cases (Figure 1) [2].

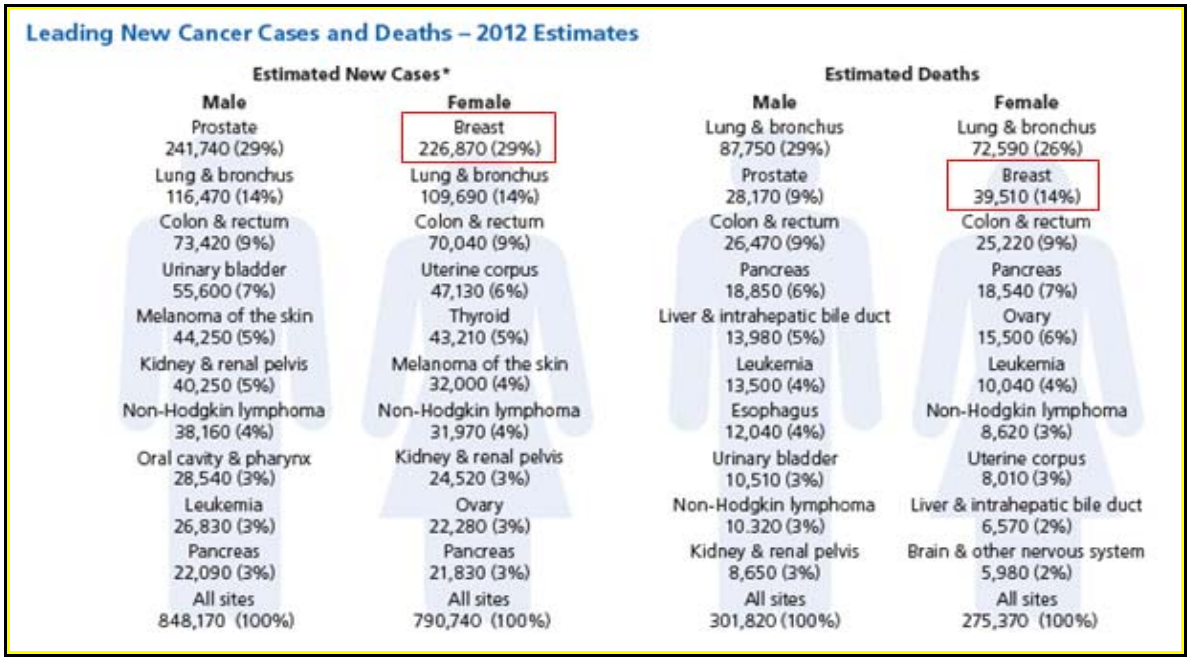

(Adapted from: Cancer Facts & Figures 2011, Atlanta: American Cancer Society, 2011, copyright 2012 by American cancer society inc., surveillance research)

Figure 1. Statistical representation of cancer cases and deaths in the year 2012. Highlighted areas (Red bordered box) show number of breast cancer deaths and cases estimated in 2012 [2].

1.1.2 Breast cancer development and types

Almost 95% of the breast cancers arise from epithelial cells and hence are termed carcinomas [3]. They can be classified in the following two major types:

A. Non-invasive breast cancer. This category consists of cancer types that are localized to the ducts or the lobules. These are further characterized based on the location. The *ductal carcinoma in situ* (DCIS) is defined by a mass of proliferating cancer cells confined to ducts, with no evidence of invasion through the basement membrane [3]. It is one of the prevalent types of breast cancer showing a dramatic increase in the number of cases since the year 1970. The second type of non-invasive carcinoma is *lobular carcinoma in situ* (LCIS) that arises and is confined to the milk producing glands or lobules. The proportion of LCIS in benign breast disease is low, ranging between 0.5% and 4%, but the majority of these lesions are multicentric, suggesting a more widespread process [4].

   Furthermore, Paget's disease of the nipple is the third type of non-invasive cancer which is a rare form of breast cancer, accounting for just 1% of all cases.

B. Invasive breast cancer. This is the type of cancer that spreads outside the membrane of the lobule or duct into the breast tissue. Consequently, the cancer cells will either remain localized to the breast or metastasize to other parts of the body, such as lymph nodes in the armpit or beyond, to the brain, bones, liver, or lungs hence giving rise to metastatic breast cancer (MBC). Strikingly, about 80% of all breast cancers are *invasive ductal carcinomas* (IDC) spreading through the cells of the ducts. On the other hand, *invasive lobular carcinoma* (ILC) starts spreading through lobules. It accounts for only 10–14% of all breast carcinomas. Its incidence is greater than that of invasive cervical carcinoma [5]. Furthermore, invasive breast carcinoma (IBC) is a form of rapidly progressive locally advanced breast cancer (approximately 3-5% of all breast cancers) characterized by discoloration ranging from red to purple and affecting at least one third of the breast, thickening and/or fine dimpling, warmth, and a palpable ridge present at the margin of indurations.

1.1.3 Molecular classification of breast cancer

Breast cancer is a heterogeneous disease, comprising of numerous distinct cell types having different biological features and clinical behavior. Therefore, classification of breast cancer cannot be limited to the one based on localization and the extent of the tumor. To further classify breast cancer on molecular basis, various groups utilizing different molecular techniques and comprehensive gene profiling analysis have revealed five major subtypes of breast cancer: basal-like, luminal A, luminal B, $HER2^{+}/ER^{-}$, and normal breast–like [6-9]. Such molecular differences lead to distinct clinical outcomes and responses to treatment. Amongst the subtypes, luminal A-type tumors have the best prognosis and are low-grade tumors [8]. On the other hand, luminal B type tumors are usually more aggressive demonstrating more proliferation and hence are high-grade tumors. Besides, basal-like tumors show relatively poor prognosis and express some molecules found in the basal/ myoepithelial compartment of normal breast tissue. These tumors are frequently negative for (Estrogen Receptor) ER and HER2 [10]. The better insight of the molecular subtypes of breast cancer eases the choice of therapy regimen for the patients and ensures more sensitivity to the treatment. Besides, molecular heterogeneity as described in this section forms the basis of this thesis in characterizing chemoresistance mechanisms.

1.2 Regular treatment options

In the recent years, life-saving treatment strategies for breast cancer advanced dramatically bringing new hope and excitement. Instead of just one or two, various treatment options are available for breast cancer. Furthermore, a choice of treatment based on the factors like age, physiological condition of patients and stage of cancer is possible. Treatment options for the breast cancer could be characterized as follows

1.2.1 Local treatment options

This type of treatment specifically targets the tumor and rest of the body parts remains unaffected. It constitutes the following procedures.

A. Surgery. Surgical removal is suggested to patients having a localized tumor below 4 cm. *Lumpectomy* is a type of surgery referring to surgical removal of the tumor in breast along with negligible amount of surrounding tissue. Another version, *partial mastectomy* is extensive and removes more amount of normal tissue surrounding the tumor. This is also referred to as *quadrantectomy*. These two surgical procedures constitute the 'breast conserving surgery' as the removal of complete breast is avoided. Furthermore, patients with a more advanced stage of breast cancer may undergo a *total mastectomy* or complete removal of breast with a sentinel lymph node biopsy. For a more advanced tumor *radical mastectomy* is advised that includes removal of breasts along with removal of lymph nodes in the armpits and chest. Surgeries are the preferred mode of treating breast cancer when accompanied with radiotherapy or chemotherapy.

B. Radiation therapy. Surgical removal of tumor is often followed by radiation therapy to remove residual microscopic cells [11]. Superiority of this combination can be proved by data demonstrating a recurrence rate of 14.3% for those patients undergoing breast conservation therapy followed by radiation as compared to 39.2% for those undergoing surgery alone [12].

1.2.2 Systemic treatment options

Molecular classification of breast cancer has made it possible to administer specific enzymes, drugs, antibodies and hormones for treating cancer. When these compounds are administered either through blood vessels or orally, it is characterized as systemic therapy.

A. Chemotherapy. Chemotherapy is usually recommended for all women with an invasive breast cancer that is hormone receptor-negative. It is usually administered through blood steam or given orally. On the other hand, *regional chemotherapy* is the administration of drugs directly into the cerebrospinal fluid, an organ, or a body cavity such as the abdomen, mainly affecting cancer cells in those areas. Several therapeutic drug options are available for the treatment through chemotherapy and are discussed later in the introduction.

B. Hormone therapy. Hormone therapy removes hormones or blocks their action and stops cancer cells from growing. For example, hormone therapy with tamoxifen is often given to patients with early stages of breast cancer and those with metastatic breast cancer [13]. Moreover, hormone therapy with an aromatase inhibitor is given to some postmenopausal women who have hormone-dependent breast cancer.

C. Targeted therapies. Therapies targeting a specific downstream protein or a metabolite comes under this category and is being studied extensively. Figure 2 summarizes all targeted drug possibilities established or under study. Some of the frequently used therapeutic strategies are targeting HER2 and VEGF protein that play important role in tumor progression and chemoresistance. There are a lot of hopeful drug candidates used commonly for the targeted therapies now a day like bevacizumab (an anti-VEGF-A antibody), everolimus (an inhibitor of mTOR), sunitinib and sorafenib (multitarget drugs) [14]. Furthermore, lapatinib (HER1 and HER2 dual inhibitor), pertuzumab, trastuzumab-DM1 and neratinib constitute promising drugs/ antibodies used for targeting HER2. In addition to these drugs, many others drugs have been developed or are being developed that target hallmarks of cancer specifically e.g. sustaining proliferative signaling, avoiding immune destruction, activating invasion and metastasis, resisting cell death and so on [15].

1.2.3 Common adjuvant chemotherapy regimens

Cancer treatment is often a combination of different types of therapies to ensure eradication of the entire tumor. Likewise, chemotherapeutics are administered in combination for better effect and treatment. AC/TAC (adriamycin and cyclophosphamide/ taxol, adriamycin (doxorubicin) and cyclophosphamide), CMF/CAF (cyclophosphamide, methotrexate and fluorouracil/ cyclophosphamide, adriamycin and fluorouracil), EC/CEF (epirubicin and cyclophosphamide/ cyclophosphamide, epirubicin and fluorouracil) and TC/TCH (taxotere and cyclophosphamide/ taxotere, cyclophosphamide and herceptin) are the examples of some combinations frequently used in clinics. These combinations reach response rates from 60% to 100% when administered in a primary or adjuvant setting [12,16]. In

spite of this fact, in about 40% of the breast cancer cases a relapse is seen accompanied by a decline in chemotherapy response rates to only 20% [17].

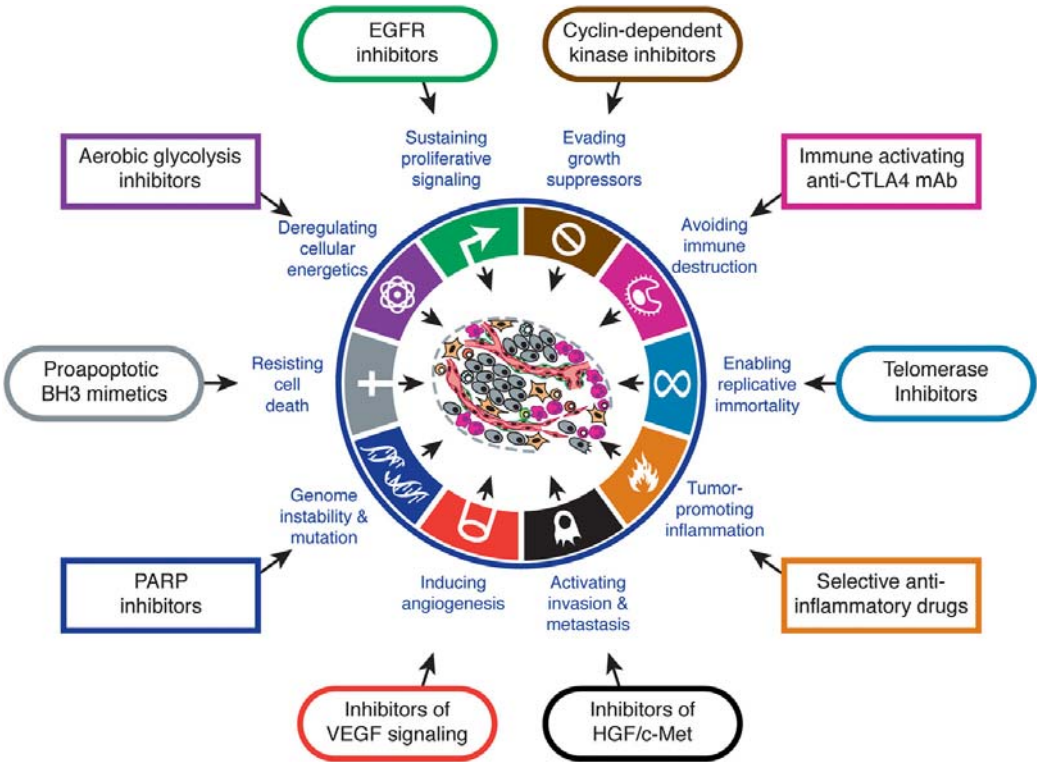

(Adapted from: Hallmarks of cancer: the next generation, Hanahan D, Cell, 2011, 144(5), p 668, copyright 2011 by Elsevier inc.)

Figure 2. Targeting hallmarks of cancer for therapy. Summary of all the possible therapeutic target proteins/metabolites opening up new therapeutic field for cancer. Some of these targeted therapies are already being used and others are understudy or clinical trials [15].

1.2.4 Chemotherapeutics and their mode of action

One of the hallmarks of cancer is high proliferation of cells. Therefore, targeting proliferation is one of the logical approaches towards treatment. The drugs targeting genetic material of the cells and hence proliferation, come under category of *DNA altering agents*. DNA alkylators or cross-linkers (platinum-based drugs) form major part of this category [18]. *Cisplatin* is the most effective drug that is in the clinical use since 1972 to treat a variety of cancer types [19]. All alkylating agents form covalent linkages with macromolecules having nucleophilic centre. As the end result of this treatment DNA replication is blocked that in turn may discontinue RNA replication and protein synthesis [20].

Furthermore, *anthracyclin* drugs are also frequently utilized drugs termed *antitumor metabolites*. *Doxorubicin* and *daunorubicin* are among the most important drugs from this category in terms of the clinical activity [21]. Anthracyclins intercalates in the major groove between the base pairs of the DNA double helix and RNA that in turn leads to interference with the DNA replication, RNA transcription, translation, and inhibition of enzyme activities and proper membrane functioning. Likewise, *epirubicin (adriamycin* analogue) and *Mitoxantrone* (anthracenedione antibiotic) are used in combination with other drugs and can replace anthracyclines [22,23].

Additionally, *antimetabolites* have been in use for the treatment of the malignant disease for 50 years, since their discovery [24]. These drugs interfere with normal metabolic processes and include *5-fluorouracil* (5-FU) a nucleoside analogue and *methotrexate* a dihyrofolate reductase inhibitor that are clinically approved drugs [25].

Further, *antimicrotubule agents* are among the most frequently used drugs for breast cancer chemotherapy, with proven efficacy in both localized and metastatic disease. It is well known that *paclitaxel*, one of the taxanes, binds to the microtubules in cells and arrests cells in mitosis by stabilizing mitotic spindle microtubules [26].

1.3 Resistance to chemotherapy and targeted therapies

Several mechanisms generating chemoresistance in breast cancer are summarized in Figure 3 [27]. The mechanisms highlighted with a red bordered box are the ones examined in this study.

1.3.1 Activated hormone receptors

Many studies have shown involvement of hormones like estrogen receptor (ER) in causing chemoresistance [28,29]. For instance the ER^- breast tumors were found to be chemosensitive as compared to the ER^+ tumors to six anti-cancer drugs [30]. Likewise, a lot of mechanisms lead to chemoresistance via ER^+ upregulation. Association with inactivation of p53, ABC transporter mediated drug resistance, enhanced β-tubulin expression etc. are few reasons for chemoresistance caused by ER activation [29].

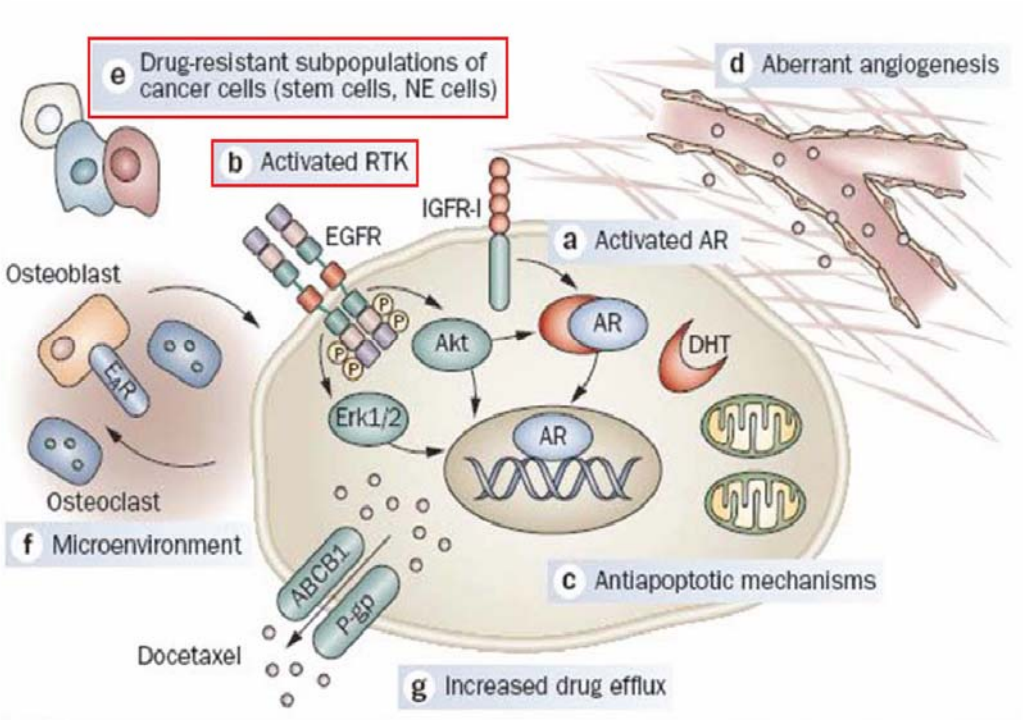

(Adapted from: Drug resistance in metastatic castration-resistant prostate cancer, Seruga B, Nat Rev Clin Oncol., 2011, 8(1), copyright 2010 by Nature Publishing group)

Figure 3. General mechanisms of chemoresistance. Summary of the common mechanisms leading to chemoresistance in cells. (a) Activation of hormone receptors (androgen receptor in case of prostate cancer as shown here and estrogen receptor in case of breast cancer) leading to activation of downstream signaling. (b) Activation of receptor tyrosine kinases which in turn causes activation of pro-survival signals. (c) Activation of anti-apoptotic mechanisms usually driven by bcl-2, bcl-xl and IAPs. (d) Aberrant angiogenesis causing survival and progression of tumor. (e) Involvement of cancer stem cells in resistance. (f) Interactions with microenvironments causing pro-survival signal transduction. (g) Increased drug efflux through drug transporters as ABC transporters. The highlighted one (red bordered box) are the mechanisms examined for this study [27].

1.3.2 Anti-apoptotic mechanisms

The key players in the apoptosis are Bcl-2 family regulator proteins. Anti-apoptotic proteins like Bcl-2 and Bcl-xl play a major role in acquiring chemoresistance. For instance, an overexpression of these anti apoptotic factors was demonstrated in colon cancer cells resistant to 5-FU [31]. Furthermore a study of ovarian cancer cells revealed high expression of Bcl-xl *in vitro* and *in vivo* after treatment with cisplatin, paclitaxel, topotecan, and gemcitabine [32]. In contrast treatment of ovarian cancer cells with Bcl-2 and Bcl-xl inhibitor ABT-737 in the combination with chemotherapeutics displayed more efficacy than the chemotherapeutic treatment alone [33]. Likewise, there is a preclinical evidence supporting a synergistic therapeutic role of the anti-sense therapies of Bcl-xl and Bcl-2 with cytotoxic agents in a wide

spectrum of the human cancers, including breast, lung, colon, prostate, gastric, epidermis, bladder, hepatoma, cholangiocarcinoma, lymphoma, acute and chronic leukemia and melanoma [34,35]. Extending this finding to the "inhibitor of apoptosis proteins" (IAPs), X-linked inhibitor of apoptosis protein (XIAP) is found to be associated with the resistance to 5-FU and gemcitabine in the pancreatic cancer [36]. Moreover, another IAP Survivin also plays a key role in chemoresistance of endothelial cells hence, making it a target for current therapies [37].

1.3.3 Increased drug efflux

Studies and the clinical investigations verify that the initially responsive tumors show relapse and resistance to one or multiple drugs used for the treatment. One of the mechanisms associated with it is the enhanced drug efflux through the membrane transporters. One such transporter family that is extensively studied in terms of the drug resistance is the ATP binding cassette (ABC) transporter family. This phenomenon of displaying resistance to more than one drug is termed as *multiple drug resistance (MDR)* [38]. The ABC family proteins p-glycoprotein, MRP1 and ABCG2 are the three major proteins that protect cell from endogenous and exogenous molecules and are thus the major contributors to absorption, distribution and excretion of the clinically administered drugs [39]. A number of ABC transporters have been identified that are associated with the breast cancer chemoresistance. Table 1 gives an overview of these transporters and their respective drug targets hence verifying the vast diversity of these transporter proteins [40]. Strikingly, the major drugs used in therapy like adriamycin (doxorubicin), paclitaxel, 5FU etc. are the targets of the ABC transporter family hence causing resistance to therapies.

Gene	Protein	Tissue	Chemotherapeutic drugs effluxed by transporter	None chemotherapeutic substrates
ABCB1	PGP/MDR1	Intestine, liver, kidney, placenta, blood-brain barrier, most tissues	Colchicine, doxorubicin, etoposide, vinblastine, paclitaxel	Neutral and cationic organic compounds, digoxin, saquinavir, many commonly used drugs
ABCC1	MRP1	All tissues	Doxorubicin, daunorubicin, vincristine, etoposide, colchicines, camptothecins, methotrexate	Glutathione and other conjugates, organic anions, leukotriene C4, rhodamine
ABCC4	MRP4	Prostate, testes, ovary, intestine, pancreas, lung, kidney, most tissues	6-mercaptopurine and 6-thioguanine and metabolites, methotrexate	Nucleotide analoges, organic anions,
ABCC5	MRP5	Most tissues	6-mercaptopurine and 6-thioguanine and metabolites	Nucleotide analogues, cyclic nucleotides, organic anions
ABCC10	MRP7	Low in all tissues except pancreas		Nucleoside analogues
ABCC11	MRP8	Low in all tissues except kidney. Spleen, colon, brain	5-fluorouracil	
ABCC12	MRP9	Breast, testes, brain, skeletal, ovary	Not known	Not known
ABCG2	BCRP	Liver, breast	Mitoxantrone, topotecan, doxorubicin, daunorubicin, irinotecan, imatinib, methotrexate	Prazosin, pheophorbide A, Hoechst 33342, rhodamine

(Adapted from: Multidrug Resistance in Breast Cancer: From In Vitro Models to Clinical Studies, Holen I, International journal of breast cancer, 2011, (2011), p 2, copyright 2011 by N. S.Wind and I. Holen)

Table 1. An overview of ABC transporters and their target drugs [40].

1.3.4 Interactions with microenvironment

The effect of micro-environmental factors on chemoresistance can be described in two ways. The factors like receptor tyrosine kinases, platelet derived growth factor, insulin like growth factor, proteins like TGFβ, cytokines etc. can interact with and modulate each other and in turn act cooperatively on several levels [41-44]. Secondly there is a crosstalk between the intracellular signaling pathways and pathways of adhesion molecules. This crosstalk regulates the intensity and the duration of the activation of related pathways leading to complexity. Therefore, it is difficult to overcome the survival advantage by blocking only a single target [45]. A study demonstrated generation of the resistant subclones of mice bearing mammary tumors when treated with alkylating agents. After administration of these subclones

to other mice, a cross chemoresistance to alkylating agents was observed and this effect was restricted to *in vivo* conditions[46]. Likewise, the orthotopic human small cell lung cancer developed orthotopically in mice were sensitive to cisplatin and resistant to mitomycin D. These tumors when injected subcutaneously demonstrated resistance to cisplatin and sensitivity to mitomycin D suggesting the role of microenvironment in acquiring the resistance [47]. Similar results were obtained for other types of cancer [48,49]. Hence, targeting more than one components of the signaling pathways and the interaction cascades is necessary to overcome the resistance.

1.3.5 Receptor tyrosine kinases causing resistance to chemotherapy and targeted therapies

Receptor tyrosine kinases interact with a number of downstream processing factors and hence are involved in activating/suppressing a complex network of pathways leading to tumor progression, aggressiveness and chemoresistance. One example of the receptor tyrosine kinase is discoidin domain receptor 1 (DDR1). It interacts with cyclooxygenase 2 and activates the NFκB pathway hence conferring chemoresistance [50]. Furthermore Src tyrosine kinase activation is associated with the 5-FU resistance that is reverted by Src inhibitor PP2 [51]. Apart from this, the activation of the epidermal growth factor receptor family especially HER2 is involved extensively in chemoresistance [52]. For instance, HER2 transfected lung cancer cells showed enhanced resistance to chemotherapies [53]. Furthermore, the amplification of the HER2 gene and overexpression of HER2 protein occurs in 20-25% of breast cancers and is often associated with poor prognosis [54-56]. Likewise, HER2 overexpression is also exhibited by the ovarian cancer patients showing resistance to chemotherapeutics [57].

Moreover, the primary adjuvant therapy for the HER2 positive cancers is the treatment with trastuzumab that targets HER2. Trastuzumab is a humanized monoclonal antibody that binds to the extracellular domain of the HER2 receptor and is the first HER2-targeted agent approved for clinical use in breast cancer. Although it is one of the most effective treatments in oncology, a significant number of patients show resistance to this treatment. Some of the mechanisms of trastuzumab

resistance are prevention of trastuzumab binding due to a truncated HER2 receptor, the upregulation of HER2 downstream signalling pathways, signalling through alternate pathways as PI3K, Akt, IGFR, VEGF etc. and the failure to trigger an immune mediated destruction of tumor cells [58-60]. A summary of all these mechanisms is shown in Figure 4 [61].

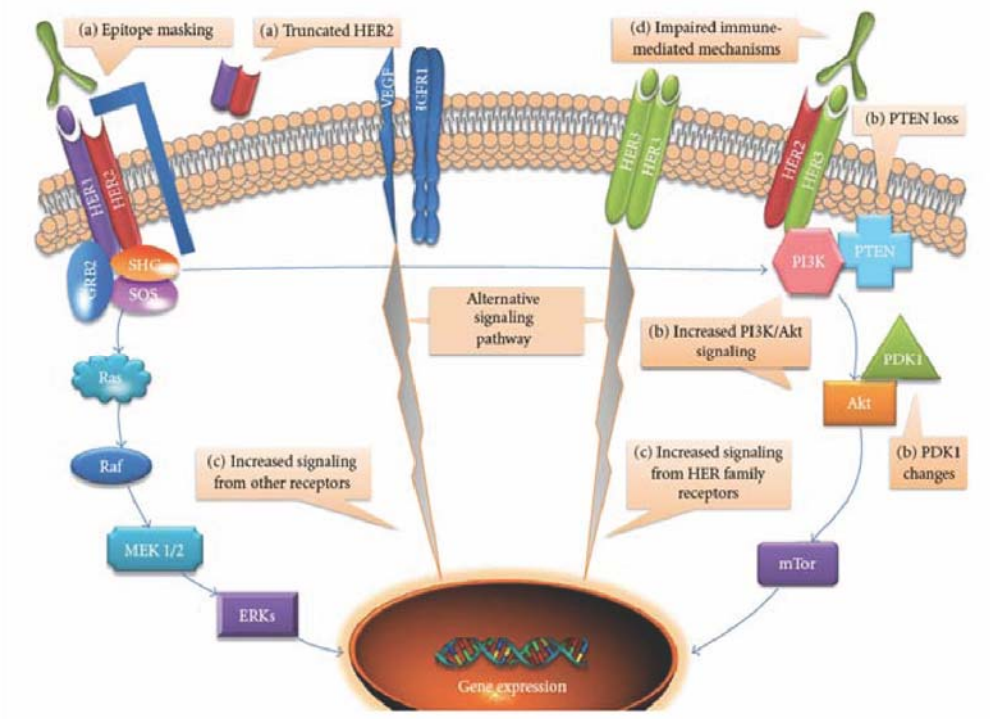

(Adapted from: Molecular Mechanisms of Trastuzumab Resistance in HER2 Overexpressing Breast Cancer, Gabriel L, International journal of breast cancer, 2011, (2011), p 4, copyright 2011 by G. L. Fiszman and M. A. Jasnis)

Figure 4. Mechanisms of trastuzumab resistance. This figure summarizes the mechanisms leading to trastuzumab resistance. (a) Impaired binding of trastuzumab to the receptor. (b) Increased downstream Pro-survival signaling. (c) Increased signaling from dimerization of receptor with other receptors of same family. (d) Impaired immune mediated mechanisms [61].

1.3.6 Involvement of cancer stem cells (CSCs)

An emerging concept leading to the chemoresistance is involvement of a less differentiated population in escaping the therapies. These cells called cancer stem cells or tumor initiating cells or stem cell-like cells have certain properties related to stem cells. One of the properties of these cells is “quiescence” or slow proliferation that confers resistance to chemotherapeutics [62]. Likewise, these cells are present as a subpopulation termed as “side population”. It is verified by in cancer cell lines that

the side population cells express high amount of ABCG2 and MDR1 transporters propelling toxic drugs out of the cells [63-65].

Stem cell-like population correlated with certain markers like $CD44^+/CD24^-$ population from MCF-7 and SKBR3 cells showed resistance to adriamycin and epirubicin [66]. Likewise, $CD44^+/CD24^-$ subset from MCF-7 and MDA MB-231 also showed resistance to radiotherapy [67]. Overexpression of another cancer stem cell marker ALDH1 is associated with resistance to cyclophosphamide in leukemia and colon cancer cells [68,69]. Hence, there is a need to develop novel therapeutic strategies that can target this potential chemoresistant population.

1.4 Heterogeneity: a new dimension to chemoresistance

1.4.1 Cancer stem cells leading to heterogeneity

Human breast cancers are highly heterogeneous group of tumors consisting of several morphologically different subtypes [70]. A number of factors leading to the heterogeneity of breast cancer have been hypothesized and are under study. Upcoming mechanism leading to heterogeneity is involvement of cancer stem cells causing the same [70-72]. Supporting this hypothesis, most of the tumors that arise from a single cell eventually end up in constituting cells with different characteristics and types. In fact some cells in a tumor are infiltrating normal cells proposed to support the growth of cancer cells [73].

Moreover, to describe the involvement of cancer stem cells in the tumor progression and recurrence, researchers put forward two models. The model of the *"clonal evolution"* proposes that every cell in a tumor being genetically instable has a potential to undergo mutations. Selection of most adaptive phenotype to adverse conditions will lead to formation of new tumors and recurrence. This model is applicable to many solid tumors like breast, brain, prostrate etc.

The model of *"cancer stem cells"* suggests presence of stem cells from the commencement of tumors. The stem cells eventually skip therapies due to certain properties like *"quiescence"* and give rise to new tumors. It is also termed as "*hierarchical model of cancer stem cells*" [74]. Figure 5 describes the two models for involvement of stem cells in formation of new tumors.

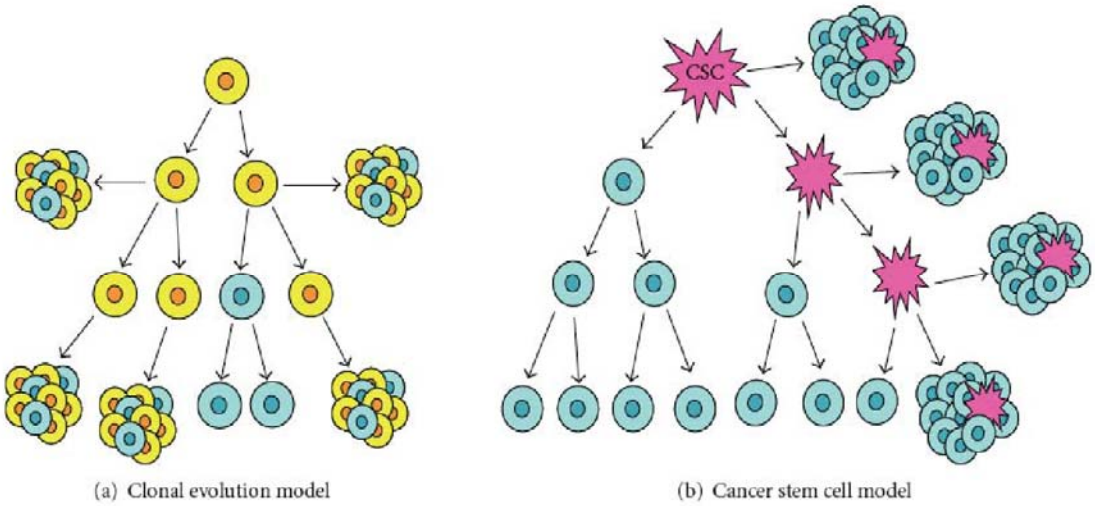

(Adapted from: The Controversial Clinicobiological Role of Breast Cancer Stem Cells, Casarsa C, Journal of oncology, 2008, (2001), p 3, copyright 2008 by 2008 Claudia Casarsa et al.)

Figure 5. Models for heterogeneity in solid cancers. (a) The clonal evolution model puts forward the hypothesis that every tumor cell has a potential to undergo mutation and give rise to new tumors. The cells adapted to survive adverse conditions (yellow) will dominate and form new tumors. (b) The cancer stem cell model depicts that certain population of cells showing stem cell like properties i.e. cancer stem cells (pink) exist in the tumor right from the beginning. These cells skip therapy and give rise to new tumors [74]

Residual cancer cells after administration of chemotherapy are termed cancer stem cells or tumor initiating cells because of their ability to give rise to the new tumors and are therefore responsible for the relapse [62,75]. Several markers are explored that define this CSC subset [76-80]. One of the extensively studied breast cancer stem cell subtypes is $CD44^{+}/CD24^{-}$. The stem cell-like behavior of this subset was verified by demonstrating tumor formation after the injection of as few as 200 cells into the mammary fat pad of nonobese diabetic/severe combined immunodeficient mice [69,76]. Apart from this subset, $Lin^{-}/CD29^{high}/CD24^{+}$ was found in p53 null mice that showed potential to initiate the tumor formation [81]. Additionally, this population also generated entire mammary gland when injected in the mouse mammary fat pad further proving its stem cell-like behavior [82]. Likewise, ALDH1, MUC1, Sca1 etc. constitute additional markers associated with cancer stem cells [55,83,84]. Moreover, NANOG, OCT4, and SOX2 correlate to the poorly differentiated breast cancers enriched for the cancer stem cells [85]. Besides, their ability to induce pluripotency and association with the chemoresistant cancer stem cell subset from ovarian cancer and osteosarcoma nominates them as upcoming markers for determining cancer stem cells [86-89]. In addition, 3 dimensional spheroids or mammospheres also displayed enrichment for

this subset. Furthermore, their 3D architecture resembles tumors better hence making them a relevant tool to study cancer stem cells and heterogeneity [78,90,91].

1.4.2 EMT inducing metastasis and heterogeneity

Epithelial cell plasticity can generate distinct cellular subpopulations that contribute to the intratumoral heterogeneity in breast cancer. Early studies verified that the breast cancer cell lines with the increased invasiveness *in vitro* and displaying metastatic potential *in vivo*, exhibited expression of the mesenchymal intermediate filament protein and marker vimentin [92]. This can be explained by the phenomenon termed epithelial to mesenchymal transition (EMT). The emergence of EMT is associated with the loss of cellular polarity, partial to total destabilization of cell–cell junctions, remodeling and replacement of cytoskeletal components, the onset of cell migration and the suppression of apoptosis [93]. Figure 6 indicate roles of EMT and "mesenchymal to epithelial transition"(MET) in tumor progression and metastasis [94]. Studies suggest that only a small percentage of tumor cells undergo a total transition and these cells are presumably the source of the actively metastatic cells [95,96]. Moreover, recent data verifies association of EMT not only with the invasiveness and metastasis but also with the heterogeneity and cancer stem cells [97]. Therefore, EMT could be utilized as one of the therapeutic targets to minimize heterogeneity, metastasis and the progression of tumors.

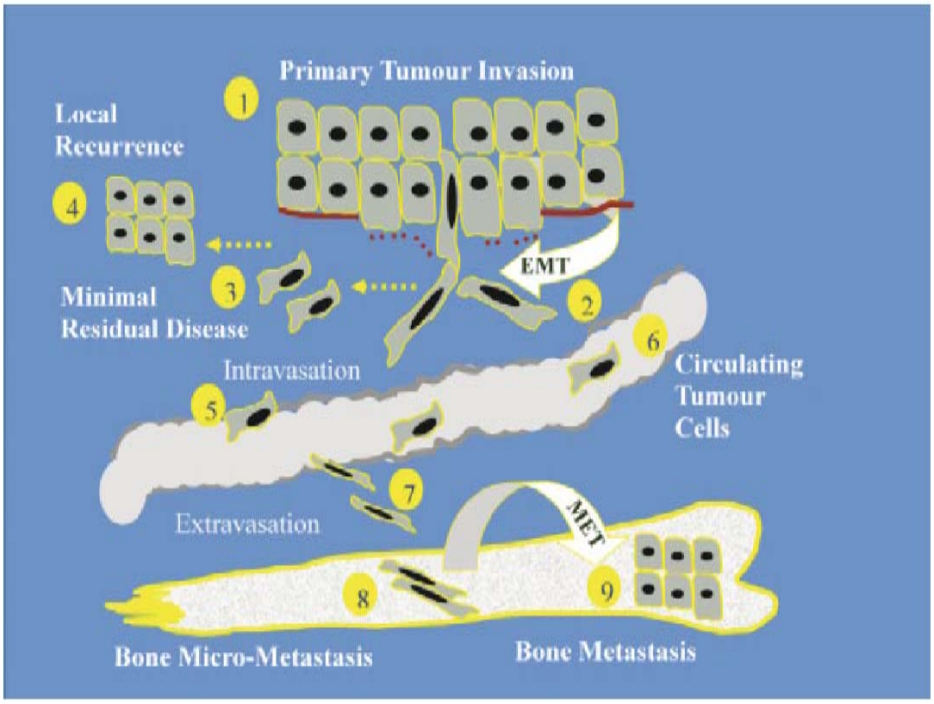

(Adapted from: Epithelial—Mesenchymal andMesenchymal—Epithelial Transitions in Carcinoma Progression, Hugo H, Journal of Cellular Physiology, 2007, 213, p 381, copyright 2007 by Wiley-Liss, Inc..)

Figure 6. EMT and MET phenomenon in cancer progression and heterogeneity. Tumor consisting of epithelial cell mass undergoes the transition from epithelial to mesenchymal cells hence giving rise to a heterogeneous tumor (1). Mesenchymal cells then disseminate and migrate (2). Some residual cells are left back for the recurrence of epithelial tumor (3, 4). Some migrating cells invade blood steam and while maintaining their mesenchymal state gets transported through blood (5, 6). This will aid their extravasation and persist there as micrometastases after undergoing MET to form epithelial tumors at secondary sites (7, 8) [94].

1.4.3 Interplay of EMT, CSC and RTKs to generate chemoresistance

Cancer stem cells were first discovered in acute myeloid leukemia [98]. Since then, the cancer stem cells (CSCs) have been identified in most types of the hematopoietic malignancies and recently, CSCs have also been identified in solid tumors, such as breast [76,99], brain [100], Colon [101] and prostate cancer [102]. Recently, it is shown that $CD44^+/CD24^-$ marker, which is associated with CSCs also describes significantly higher relative invasion index than the $CD44^+/CD24^+$ cells[103]. Likewise, Al-Hajj *et al.* reported that the cells with this phenotype isolated from either primary breast cancers or from clinically apparent metastatic lesions have stem cell properties [76]. Furthermore, data revealed $CD44^+$ cells from both primary tumors and lung metastases are highly enriched for tumor initiating cells [104]. This complex array of

data indicates an association between EMT and CSC that eventually leads to the acquisition of chemoresistance. One of the reasons for this association could be involvement of pathways like Wnt, notch, hedgehog etc. in EMT as well as in maintaining undifferentiated state of stem cells [105].

Furthermore, receptor tyrosine kinases associated with the chemoresistance are also correlated to CSC markers suggesting another crosslink in heterogeneity of breast cancer. For instance, HER2, a RTK responsible for tumor progression, metastasis and chemoresistance is related with CSC markers as ALDH1 and Notch1 [55,106]. In another study it was found that HER-2 overexpressed in MDA-MB-231 breast cancer cells, co-operated with TGF-β to induce an enhanced pro-invasion, angiogenesis, and EMT signature correlating HER2 over-expression with EMT [107].

The interplay amongst phenomenon/ processes taken together induces different subpopulations with complex interactions and signalling leading to the chemoresistance. Therefore, targeting one of the subpopulation will not eradicate entire tumor. Since the current therapies against cancer mainly target the terminally differentiated proliferating cancer cells more effectively, investigation of more specific treatment regimens is a must for complete eradication of tumor.

1.5 Salinomycin: a potential drug to overcome resistance to classical therapies

Salinomycin is a 751 Da transmembrane potassium ionophore obtained from bacterium *Streptomyces albus*. Because of its antibacterial activity it has been used widely to control coccidiosis. Being a potassium ionophore, it rapidly embeds in biological membranes such as the cytoplasmic and mitochondrial membranes [108,109]. Gupta *et al.* demonstrated the eradication of $CD44^+$ cancer stem cells isolated from E-cadherin knockdowns of human mammary epithelial cells utilizing salinomycin hence proving its potential effect against cancer stem cells for the first time [110]. In line with this observation, a recent publication showed elimination of side population and $CD133^+$ pancreatic cancer stem cells after treatment with salinomycin [111]. Likewise, salinomycin also inhibited osteosarcoma by selectively targeting the tumor initiating cell population positive for OCT4 and SOX2 [112]. Although its specific effect and mechanism of action are yet to be discovered, a latest study showed that it enhances apoptosis via increased DNA damage and reduced p21 protein levels through

proteasome activity [113]. Furthermore, its action is also linked to the ROS generation in turn leading to mitochondrial dysfunction and apoptotic cell death [114]. A part of this thesis intends to target a less differentiated population hence, making salinomycin as the drug of choice for the study.

1.6 Aims of the thesis

Functional heterogeneity of the cells within a tumor or selection barriers like treatment with chemotherapeutic drugs generate diverse cancer cell populations escaping systemic therapy administered routinely in clinics. The residual cells survived after the therapy then give rise new tumors. The basic aim of this study was to get insight into the process of chemoresistance acquisition for a better understanding of the cell types involved in the same. Furthermore, due to their architectural resemblance to tumors and the enrichment for cancer stem cell subpopulation, utilization of 3D spheroids or mammospheres to study chemoresistance had to be evaluated. Additionally, the thesis aimed to determine the less differentiated and resistant cancer stem cell population based on the interplay between cancer stem cells and membrane receptor tyrosine kinase HER2.

Recent studies highlighted the potential of an antibiotic salinomycin in specifically targeting cancer stem cells/ dedifferentiated cells from tumors [110,112]. Hence, its role in targeting the identified resistant population was also investigated. Further goal was to verify the ability of this drug in combinatorial treatment of heterogeneous breast tumor models. All these observations in turn should provide a basis for development of novel combinatorial treatment strategies to overcome resistance caused against classical therapeutics.

Moreover, it was shown previously that salinomycin eradicated E-cadherin low mesenchymal cells from head and neck squamous carcinomas. Hence, the last part of the thesis intended to explore effect of salinomycin on the mesenchymal-like breast cancer cell lines. Since the mesenchymal-like cells display aggressiveness and metastasis; the effect of salinomycin on migration (basic property of metastatic cells) of these cell lines was further investigated.

2. MATERIALS AND METHODS

2.1 Materials

2.1.1 Cell lines

MCF-7	Cell line Services, Germany (# 300273)
MDA MB-231	Cell line Services, Germany (# 300275)
BT-474	Kindly provided by Prof. A. Ulrich, MPI, Munich, Germany
MDA MB-436	
MDA MB-435	
MDA MB-453	
MDA MB-157	
MDA MB- 468	
SKBR-3	Kindly provided by Prof. A. Vollmar, LMU, Munich, Germany

2.1.2 Media

DMEM high glucose	Biochrom AG, Berlin, Germany
L-15 Leibovitz Medium	Biochrom AG, Berlin, Germany
RPMI 1640	Biochrom AG, Berlin, Germany
Hams F 12	Biochrom AG, Berlin, Germany
Mc Coy's 5A modified medium	Biochrom AG, Berlin, Germany

2.1.3 Chemicals and solutions

Fetal Bovine serum	Gibco/Invitrogen, Karlsruhe, Germany
(Heat inactivated)	(#10500-064)

Trypsin EDTA solution	Biochrom AG, Berlin, Germany (# L2153)
Glutamine	Gibco/Invitrogen, Karlsruhe, Germany
Sodium Pyruvate	Biochrom AG, Berlin, Germany (# L0473)
polyHydroxyethylmethacrylate	Sigma Aldrich, Steinheim, Germany (#P3932)
Cell dissociation solution	Sigma Aldrich, Steinheim, Germany (# C5789)
Hoechst 33342	Sigma Aldrich, Steinheim, Germany (# B2261) dissolved in distilled water.
Verapamil	Sigma Aldrich, Steinheim, Germany (# V4269)
Matrigel	BD Biosciences, Heidelberg, Germany (# 354248)
Paraformaldehyde	Sigma Aldrich, Steinheim, Germany (# 158127)
Triton X 100	Sigma Aldrich, Steinheim, Germany (# X100)
Gelatin solution	Sigma Aldrich, Steinheim, Germany (# G1393)
FlourSave mounting reagent	Merck KGaA, Darmstadt, Germany (# 345789)
DNAase I (Rnase free)	PEQLAB Biotechnologie GMBH, Erlangen, Germany (# 10169)
Cell Stain	Millipore S.A.S, France (# 90144)
Diaminobenzidine	Sigma Aldrich, Steinheim, Germany (# D8001)
HEPES sodium salt	Sigma Aldrich, Steinheim, Germany (# H3784)
Tissue Tek	Saruka Finetek Europe B.V, Netherlands (# 1023000032)
VSP Super Mega-Cassette® White	Saruka Finetek Europe B.V, Netherlands (# VSP-5-9060)

2.1.4 Drugs/ Chemotherapuetics

Doxorubicin	Sigma Aldrich, Steinheim, Germany (# 44583)
Paclitaxel	Sigma Aldrich, Steinheim, Germany (# T7042)
Trastuzumab	Kindly provided by Dr. Pjotr Knyazev, MPI, Munich, Germany
Salinomycin	Sigma Aldrich, Steinheim, Germany (# S6201)

2.1.5 Antibodies

SOX2 (H-65)	rabbit polyclonal, Santa Cruz Biotechnology, USA (# sc 20088)
OCT4	mouse monoclonal, Santa Cruz Biotechnology, USA (# sc 5279)
E-Cadherin	mouse polyclonal, BD Transduction Laboratories™, Heidelberg, Germany (# 610181)
	rat monoclonal, Abcam, UK, (# ab11512)
Vimentin (V9)	mouse monoclonal, Santa Cruz Biotechnology, USA (# sc 6260)
HER2 (c-neu/Ab-2)	mouse monoclonal, Oncogene Research, USA (# OP 14)
Donkey anti mouse Cy3	Thermo Scientific, UK (#PA1-29773)
Goat anti mouse Al488	Life Technologies GmbH, Germany (#A11001)
Donkey anti rat (Cy TM 3)	Jackson ImmunoResearch, UK, (# 712-165-153)

Donkey anti rabbit (DyLight tm 488)	Jackson ImmunoResearch, UK, (# 711-485-152)
Polyclonal Goat anti rabbit immunoglobulins / Biotinylated	Dako Denmark A/S (# E0432)
Polyclonal Goat anti mouse immunoglobulins / Biotinylated	Dako Denmark A/S (# E0433)

2.1.6 qPCR Primers (Roche Germany)

GAPDH (UPL Probe #60)	left: ctctgctcctcctgttcgac
	right: gcccaatacgaccaaatcc
HER2 (UPL Probe #4)	left: gggaaacctggaactcaccta
	right: ccctgcacctcctggata
NANOG (UPL Probe #69)	left: atgcctcacacggagactgt,
	right: agggctgtcctgaataagca
OCT4 (UPL Probe #35)	left: agcaaaacccggaggagt
	right: ccacatcggcctgtgtatatc
SOX2 (UPL Probe #35)	left: ttgctgcctctttaagactagga
	right: ctggggctcaaacttctctc

2.1.7 Mouse models

Crl:SHO-Prkdc^{scid} HR^{hr} double homozygous SCID hairless out bred mice supplied by Charles River Laboratories international, inc. USA.

2.1.8 Kits

Cell titer Glo for cell viability	Promega, Germany, (# G7571)
Vectastain Elite ABC Kit	Vector labs, UK, (# PK-6200)
miRCURY RNA Isolation Kit	Exiqon, Denmark (# 300110)

Transcriptor High Fidelity cDNA Synthesis Kit	Roche applied sciences, Germany (#05081955001)

2.1.9 Special instruments and plasticware

Phase contrast microscope	Carl Zeiss Axiovert 200, Germany
Fluorescence microscope	Carl Zeiss Axiovert 200, Germany
Laser scaning microscope	Carl Zeiss Laser Scanning Microscope LSM 510 Meta, Germany
Time Lapse microscope	Axiovert Carl Zeiss MicroImaging, Germany
FACS machines	FACSCanto™ II, BD Biosciences, Germany
	CyAn™ ADP, Dako cytomations, Germany
	FACSAria™ II, BD Biosciences, Germany
Real time PCR system	LightCycler 480 system, Roche, Germany
Luminometer	Lumat LB9507 instrument, Berthold, Bad Wildbad, Germany
FastPrep-24 Tissue/ cell homogenizer	MP Biomedicals Gmbh, Germany (# 6004-500)
Hybaid PCR thermal cycler	Thermo electro corporation, UK
Well plates (96, 24, 6 well plate)	TPP Techno Plastic Products AG, Switzerland
96 well plates (white for luminescence)	Nunc (Nalgene labware), USA
48 well plates	Nunc (Nalgene labware), USA
Plastic dishes (60mm, 100mm)	Nunc (Nalgene labware), USA
Plastic dishes (150mm)	Sarstedt AG & Co., Germany
Coverslips	Gerhard Menzel GmbH, Germany (# BB024024A1)
Slides	Gerhard Menzel GmbH, Germany (# AA00008332E)
40um nylon cell strainer	BD falcon, NJ, USA (#352340)
Transwell (cell culture inserts 8 µm)	BD Biosciences, NJ, USA (# 353097)

2.1.10 Softwares used

Flowjo 7.6.3 (Flow cytometry analyses).
Zeiss image browser version 3.2.0.115 (LSM analysis).
AxioVision image analyses software from Carl Zeiss Microscopy system (immunohistochemical analyses).
AxioVision image analyses software from Carl Zeiss Microscopy system AxioVs40 V 4.8.1.0 (analyses of phase contrast images).
Infinity capture Infinity2-3C colour 172765 (capture phase contrast images).
Capture camera camera MicroMAX, Roper Scientific, Germany using the MetaMorph software, Universal Imaging (time lapse microscope).
Image J software NIH, USA and Chemotaxis and migration tool, Ibidi, Germany (analyses of time lapse images).

2.2 Methods

2.2.1 In vitro cell culture assays

2.2.1.1 Maintenance of cell lines

All breast cancer cell lines were cultivated as per instructions from purchasing company. Briefly, the cell line MCF-7 was cultivated in DMEM high glucose supplemented with 20% FBS and 2mM Glutamine. BT-474 was grown in RPMI 1640 medium supplemented with 10% FBS and 2mM Glutamine. Both these cell lines were incubated at 37^0 C and 5% CO_2 humidified atmosphere. Cell lines MDA MB-231, MDA MB-453, MDA MB-436, MDA MB-157 and MDA MB-468 were cultivated in L-15 Lebovitz medium supplemented with 10% FBS and 2mM Glutamine and were incubated at 37^oC without CO_2 humidified atmosphere. SKBR-3 was cultivated in Mc Coy's 5A modified medium supplemented with 10% FBS and 2mM Glutamine. MDA MB-435 cells were grown in were cultivated in DMEM/Ham's F-12 medium 1:1 supplemented with 10% FCS and 2mM stable glutamine. These cell lines were

incubated at 37°C and 5% CO_2 humidified atmosphere. 1X trypsin EDTA solution was used for splitting of all the cell lines.

2.2.1.2 Freezing and thawing of cells

By addition of an anti-freezing compound like DMSO, eukaryotic cell lines can be stored in liquid nitrogen for several years. To store cells in liquid nitrogen, cells were spun down at 1000rpm for 5 min at room temperature. Then freezing medium containing 90% medium and 10% DMSO was added to cell pellet. Cells were then kept first at -80°C at least for 24 hrs before transferring it into liquid nitrogen.
For reculturing of the frozen cells, the cell suspension was defrosted at 37°C and 10 ml of medium was added to dilute out DMSO. After centrifuging at 1000 rpm for 5 min at room temperature, fresh medium was added to cell pellet and incubated.

2.2.1.3 Mammospheres generation and cultivation

Mammospheres were generated as described previous [91]. Briefly, dishes were coated with 50 µg/ml PolyHEMA. Medium from the 2D cells grown to a confluency of 80-85% was taken as conditioned medium for growing mammospheres. Single cells were seeded in conditioned medium into polyHEMA coated dishes at the concentration of 40,000 cells/ml. Splitting and passaging of mammospheres was performed as stated earlier [115]. Mammospheres were harvested, incubated with non enzymatic cell dissociation solution at 37°C. Cells were dispersed by pipetting gently and passing through 40um nylon cell strainer once to obtain single cell suspension. After centrifugation at 900 rpm for 5 min at room temperature cells were resuspended in conditioned medium and seeded.

2.2.1.4 Cell viability assay

To check the effect of different drugs on different cell lines this assay was performed. 5000 cells per well of a 96 well plate were seeded. Mammospheres were divided in two parts. One half was trypsinized and cells were counted to a final concentration of 5000 cells per well. Accordingly, whole mammospheres were seeded in a 50 µg/ml Polyhema coated 96 well plate (Figure 14 a). Treatment was performed after 24 hrs of seeding. Treatment were performed as follows

Treatment	Cells	Time
Doxorubicin/ Paclitaxel	2D cells and mammospheres	72 hrs
Trastuzumab/ Salinomycin	Sorted populations	7 days
Combinatorial (Trastuzumab and Salinomycin)	mammospheres	7 days (first with trastuzumab and after 96 hrs salinomycin was added)
Doxorubicin/ Salinomycin	Epithelial/ mesenchymal 2D cells	72 hrs
Combinatorial (Doxorubicin and Salinomycin)	Mixture of epithelial and mesenchymal 2D cells	72 hrs

Cell titer Glo assay was performed for cell viability according to the manufacturer's instructons. This assay utilizes the detection of ATP content of cells thereby directly indicating the no. of live cells in sample. The luminescence was recorded with a Luminometer.

To check effect of the drugs on mammospheres, mammospheres were divided in two halves. One half was trypsinized into single cells followed by counting the amount required to seed 5000 cells/well and accordingly whole mammospheres were seeded in poly HEMA coated 96. Treatment was performed after 24 hrs (Figure 15 a). Cell viability was determined after the treatments.

2.2.1.5 Mammosphere forming potential assay (MFP)

To identify the property of cells to sustain the formation of mammospheres over the passages, this assay was performed. 5000 single dissociated cells of 2D cell line were seeded in polyHEMA coated 60 mm dishes. After 7 days i.e. at passage 0, no. of mammospheres generated was counted. Mammospheres were dissociated into single cells using non enzymatic cell dissociation solution and cell strainer and above procedure was repeated until passage 2 (P2) [116]. Graph was plotted after calculations were performed for P0, P1 and P2.

2.2.1.6 Molecular evolution assay (MEA)

This assay was developed to characterize the resistance of cells to the chemotherapeutics. BT-474 and MDA MB-468 cell lines were treated with 0.5µM doxorubicin (DXR) in cycles. This concentration of doxorubicin was selected as it eradicated almost 50% of the cells. The treatment was performed for 72 hrs followed by change in media and recovery phase for the cells. After each round of recovery, cells were analyzed for their response to doxorubicin and were subjected to functional assay like the quantification of mRNA level of certain genes, the ability of cells to form mammospheres and the percentage of side population (Figure 7).

2.2.1.7 Proliferation assay

5000 sorted cells of $HER2^{high}$ and $HER2^{low}$ fractions of MCF-7 2D and MCF-7 mammospheres (7 days old) were seeded and counted using counting chamber (Fuchs-Rosenthal counting chamber) at day 2, 4, 6 and 8.

2.2.1.8 3D Matrigel Assay

3D Matrigel assay was performed as described previously [117]. Briefly, 8 well chamber slides were coated with 100µl of pure Matrigel and were allowed to polymerize at 37^0 C for 15-20 min. 5000 cells were added in a small volume of medium and allowed to adhere to the coating for 2-5 min. Then 75µl medium with 20% Matrigel was added on top of it. 50µl of medium was supplemented once a week and the no. of colonies formed were counted after 7 days. Phase contrast microscopic images with 10X objective were taken using Infinity capture (Infinity2-3C colour 172765) software and were analysed using Axiovision Rel 3.1 software.

2.2.1.9 Wound healing assay for cell migration

MDA MB-436 cells were seeded in a 6 well plate. When 96-98% confluency was reached, a small scratch was made using melted pasture pipette tip (bulb shaped). Floating and dead cells were washed out using media without FCS and respective media was added to wells. One well was kept untreated as control followed by addition of 0.05µM doxorubicin to second well and 0.05µM salinomycin to the third

well. Migration of cells in the wound was assayed with a live-cell imaging setup consisting of a microscope equipped with a 10X 0.3NA objective, motorized scanning table and a stage incubator (EMBL Precision Engineering) at 37°C and under 5% CO2 atmosphere. Images were captured with a cooled charge-coupled-device camera (MicroMAX; Roper Scientific, Germany) using the MetaMorph software (Universal Imaging) for microscope control and data acquisition. Images were taken after every 15 min for 72 hrs and the data was analyzed using Imaje J software (NIH, USA) and Chemotaxis and migration tool (Ibidi, Germany). This assay was performed utilizing concentrations of drugs at which only 15-20% apoptosis or cell death was observed after 72 hrs treatment as determined by Cell titer Glo assay.

2.2.1.10 Transwell migration assay

This assay for confirmation of cell migration was performed as described earlier [118]. Briefly, Cell culture inserts i.e. transwells (8 µm pore size), were placed in wells of 24 well plate containing 10% FBS in medium plus or minus 10µM doxorubicin or 0.05µM salinomycin. Cells suspended in 0.2 ml serum free medium (plus or minus drugs) were added to the top of each chamber followed by incubation at 37^{o}C with 1% CO2 for MDA MB-436 cells. After 18 hrs the chambers were washed with dH2O and the cells removed from the topside of the chamber with a cotton swab. Migrating cells were fixed and stained using the cell stain solution. The average number of migrating cells from fifteen representative fields (10X objective of phase contrast microscope, three wells per condition) was obtained. Graph was plotted according to the readings obtained. This assay was performed utilizing concentrations of drugs at which only 10-15% apoptosis or cell death was observed after 18 hrs treatment as determined by Cell titer Glo assay.

2.2.1.11 Generation of in vitro mimic of metastatic breast tumor

MCF-7 single cells and MDA MB-436 single cells were mixed in a ratio 1:1 and seeded in dishes in mixture of DMEM medium with 20% FCS and L-15 Lebovitz medium with 10 % FCS in ratio 1:1. Cells were incubated at 37^{o}C and 5% CO_2 humidified atmosphere. Images were captured using phase contrast microscope.

For cell viability assays, MCF-7 and MDA MB-436 cells were mixed in 1:1 ratio and 5000 cells were seeded/ well of 96 well plate. Cells were treated either with DMSO

(as control), doxorubicin and salinomycin either individually or in combination. Cell titer Glo assay was performed after 72 hrs of treatment.

2.2.2 Histological and Immunofluorescence methods

2.2.2.1 Side population analysis

Side population analysis of BT-474 cells and MDA MB-468 cells was performed as suggested in Goodell *et. al* [119]. Single cells were resuspended at 10^6 cells/ ml in prewarmed DMEM solution (Appendix2). One set was kept unstained as control. To one set Hoechst 33342 was added at the concentration of 1 µg/ 10^6 and to another set both Hoechst 33342 and verapamil (50 µM/ sample) were added. Samples were incubated incubated for 90 min at 37^0 C in waterbath. After Hoechst staining, cells were pelleted and maintained at 4^0 C before analyzing with Flow cytometry (CyAn^{TM} ADP Flow cytometer). Percent side population (% SP) was counted by subtracting the % SP in only Hoechst stained samples with % SP of samples stained with both Hoechst and verapamil.

2.2.2.2 Flow cytometry and Fluorescence-activated cell sorting

Single cell suspension of 2D cell lines and 3D mammospheres was prepared using non enzymatic cell dissociation solution. For indirect immunofluorescence cells were fixed with 4% paraformaldehyde (PFA) for 15 min at room temperature, permeabilized with permeabilization solution (Appendix 2) for 10 min and blocked with blocking solution (Appendix 2) for 45 min at room temperature. Cells were incubated with indicated primary antibodies (1:100) and labeled with appropriate fluorescence coupled secondary antibodies (1:200). Fluorescence was acquired using FACSCanto^{TM} II flow cytometer.

For cell sorting, single cell suspension was prepared under aseptic conditions. Cells were blocked using FBS for 30-40 min on ice. Incubations with primary (1:100) and secondary antibodies (1:200) were performed for 1 hr each on ice. Just before sorting of cells 20U/ml DNAaseI enzyme was added to avoid clumping of cells due to remains of genomic DNA and 1µg/ml propidium iodide was added to exclude out the

dead cells. Cell sorting was performed using indicated antibodies with a FACSAria^{TM} II cell sorter.

2.2.2.3 Immunocytology and microscopy

100, 000 cells of 2D cell lines were seeded on coverslips in 6 well plates. After they reached confluency of 70-80% cells were fixed with 4% PFA for 15 min. Whole mammospheres were centrifuged at 1000 rpm for 5 min for collection and fixed with 4% PFA for 20 min. Samples were then permeabilized with permeabilization solution (Appendix 2) for 10 min (2D cells) and 15 min (mammospheres) followed by blocking with blocking solution (Appendix 2) for 45 min. Incubation with indicated primary antibodies (1:100) was performed for 1 hr followed by incubation with respective secondary antibodies (1:200) for 1 hr. Nucleus was stained with DAPI for 10-15 min. All incubations were performed at room temperature and for mammospheres cell pelletting was performed at 1000 rpm for 5 min. For 2D cells coverslips were mounted using FlourSave mounting medium and were stored at 4^{o}C. Images were captured using 63 X 1.4 Oil DIC objective of Laser Scanning Microscope LSM 510 Meta and analyzed using Zeiss image browser version 3.2.0.115.

2.2.2.4 Immunocytochemistry of tissue sections

5-7μM tissue sections were prepared from xenografts of MCF-7 2D and MCF-7 mammospheres injected subcutaneously in female immunodeficient mice after 170 days. The tissue tek layer was removed and the sections were fixed with 4% paraformaldehyde for 10-15 min. After blocking with 5% FBS in PBS twice for 10 min, HER2 antibody (1:200) was added for 2 hrs. Secondary antibody (1:400) and DAPI (1:1000) were added for an hour and sections were treated with FluorSave reagent. Results were captured using 63 X 1.4 Oil DIC objective of Carl Zeiss Laser Scanning Microscope LSM 510 Meta and analysed using Zeiss image browser version 3.2.0.115.

2.2.2.5 Immunohistochemistry of tissue sections

Immunohistochemical analysis was performed as described [120]. Slides (5-7µM sections) were incubated for 15 minutes with 0.3 % H_2O_2 in methanol (for Oct 4) and 1.5 % H_2O_2 in PBS (for HER 2) to quench endogenous peroxidase. An antigen retrieval step was performed using 10mM Sodium citrate buffer, pH 6.0 and cooking the tissue in the microwave for few (15 minutes for HER 2 and 10 minutes for OCT 4). After cooling down at room temperature for at least 30 to 45 minutes, the sections were washed with tap water and three times for five minutes each with PBS. Before incubation with the primary antibody, the sections were blocked for few hours (from 30 minutes to 2 hours) at room temperature with the appropriate serums, Triton X-100 in PBS. The primary antibody is diluted in the blocking solution in appropriate concentrations (1:100) and was incubated at 4°C overnight. Next day the sections were washed three times for five minutes each with PBS. The secondary antibody (biotinylated) was diluted 1:200 in blocking solution and the sections were incubated for few hours (1 to 2 hours). Before applying the A+B reagent (Vectastain Elite ABC Kit) that was prepared 30 minutes before 1:1 for 40 minutes at room temperature, the sections were washed again three times for five minutes each with PBS. Afterwards, the sections were washed again three times for five minutes each with PBS and incubated with DAB (1ml DAB + 0.8ul of 30% H2O2, Hydrogen peroxide) until the appearance of brown colour. The reaction was stopped with tap water for 5 minutes and afterwards the tissue was counterstained shortly with hematoxylin , washed with tap water, dehydrated and mounted with Entellan. Control sections were processed without primary antibody. Images were captured via the Version 4.7 of the AxioVision image analysis software from Carl Zeiss Microscopy system.

2.2.3 Molecular biology methods

2.2.3.1 mRNA Isolation

mRNA isolation was performed by miRCURY^{TM} RNA isolation kit (Exiqon). To describe the procedure for cell lines, cells were washed with 1X PBS and cells lysis solution (350µl-1000µl depending on size of dish) was added. At this stage the

lysates can be stored at -70^{o}C for few hrs or days. After addition of 200µl of 95-100% ethanol lysates were vortexed for 10 sec and the whole mixture was transferred to the column. After centrifugation for 1 min at 14,000g, wash 400µl of solution was applied to the column and was again centrifuged. For elution of the total RNA, 50µl of elution buffer was applied to the column and it was centrifuged for 2 min at 14,000g. At this step purified RNA samples could be stored at -20^{o}C for a few days or -70^{o}C for longer period.

For preparing RNA from tissue sample, tumors were homogenized in FastPrep-24 Tissue and cell homogenizer while in lysis buffer and the lysates were subjected to similar RNA isolation procedure.

2.2.3.2 cDNA preparation

cDNA was isolated from the RNA by using Transcription High Fidelity cDNA Synthesis Kit (Roche). Random hexamer primer and PCR grade water was added. The sample was heated in thermo cycler (with a heated lid) at 65^{o}C for 10 min to denature the template followed by chilling on ice. To this mixture, remaining contents of RT mix (buffer, protector, dNTPs, DTT, Reverse Transcriptase) were added to the final volume of 20µl and the mixture was kept in thermocycler with heated lid at 29^{o}C for 10 min. and then at 48^{o}C for 60 min. The reverse transcriptase was inactivated by heating to 85^{o}C for 5 min and reaction was halted by placing the tube on ice. The cDNA prepared was then stored at -20^{o}C for longer perdios before using it for qPCR reaction.

2.2.3.3 qPCR analysis

Quantitative real-time PCR was performed using UPL Probes (Roche) and Probes Master (Roche) on a LightCycler 480 system with *GAPDH* as control. Primers used include GAPDH, HER2, NANOG, OCT4, SOX2. Experiments were performed in triplicates and the obtained average C_T values of target genes were normalised to control as ΔC_T. Changes in expression levels were shown either as fold increase or as ratio (target gene/ control).

2.2.4 In vivo xenograft experiments

1 x 10^5 immunosorted MCF-7 $HER2^{low}$ and $HER2^{high}$ cells were injected subcutaneously into the right flank of 5 – 7 weeks old female Crl:SHO-$Prkdc^{scid}$ HR^{hr} double homozygous SCID hairless out bred mice (7 mice per group). Before inoculation cells were resuspended in PBS and Matrigel (1:1). Tumor volume was measured once or twice a week using a calliper beginning at day 9 of injection. The volumes were calculated by the formula 0.5 x d^2 x D (where d represents the smaller and D represents the larger diameter). For growth curve data points were expressed as average tumor volume [mm^3] +/- SD per group ($HER2^{low}$ and $HER2^{high}$). After 145 days, mice were sacrificed and tumors were resected for cryosections and qPCR.
For xenografts of MCF-7 2D cell line and MCF-7 mammospheres, 1 x 10^6 single cells were injected subcutaneously into the right flank of female Crl:SHO-$Prkdc^{scid}$ HR^{hr} double homozygous SCID hairless out bred mice (5 mice per group). Mice were sacrificed after 170 days and cryosections were prepared from the resected tumors in tissue tek medium using mega cassette. All animal procedures were approved and controlled by the local ethics committee and carried out according to the guidelines of the German law of protection of animal life.

3. RESULTS

3.1 Evolution of chemoresistance to classical chemotherapeutics in vitro

Most of the chemotherapeutics used in the clinics these days affect fast proliferating cells. Since, at the time of treatment not all tumor cells are in the same phase of cell cycle, chemotherapy is administered in cycles. A cycle of chemotherapy (which is typically 21 or 28 days) refers to the time it takes to give the treatment and then allow the body to recover from the side effects of the medicines. The period of recovery can give rise to resistant cells that are able to skip therapy and hence cause recurrence of tumor. To mimic this clinical system and to characterize the evolution of resistance to chemotherapeutics, we designed an assay named 'Molecular evolution assay' (MEA). A schematic representation of MEA is shown in figure 7. Briefly, two representative epithelial breast cancer cell lines BT-474 and MDA MB-468 were treated with 0.5μM doxorubicin (DXR) in cycles. This concentration of doxorubicin had been selected as it eradicated almost 50% of the cells. The treatment was performed for 72 h followed by change in media and recovery phase for the cells. After each round of recovery, cells were analyzed for their response to doxorubicin and were subjected to functional assay like the quantification of mRNA level of certain genes, the ability of cells to form mammospheres and the percentage of side population.

Recovered cells from each round of MEA were analyzed for their acquired resistance to doxorubicin. Comparison of cell viability assay displays evolution of resistant cells in round 3 (R3) and round 4 (R4) for both BT-474 and MDA MB-468 (Figure 8 a and b).

Additionally, the IC50 values indicate R3 and R4 cells acquired resistance against doxorubicin as compared to R1 cells for both cell lines (Table 2).

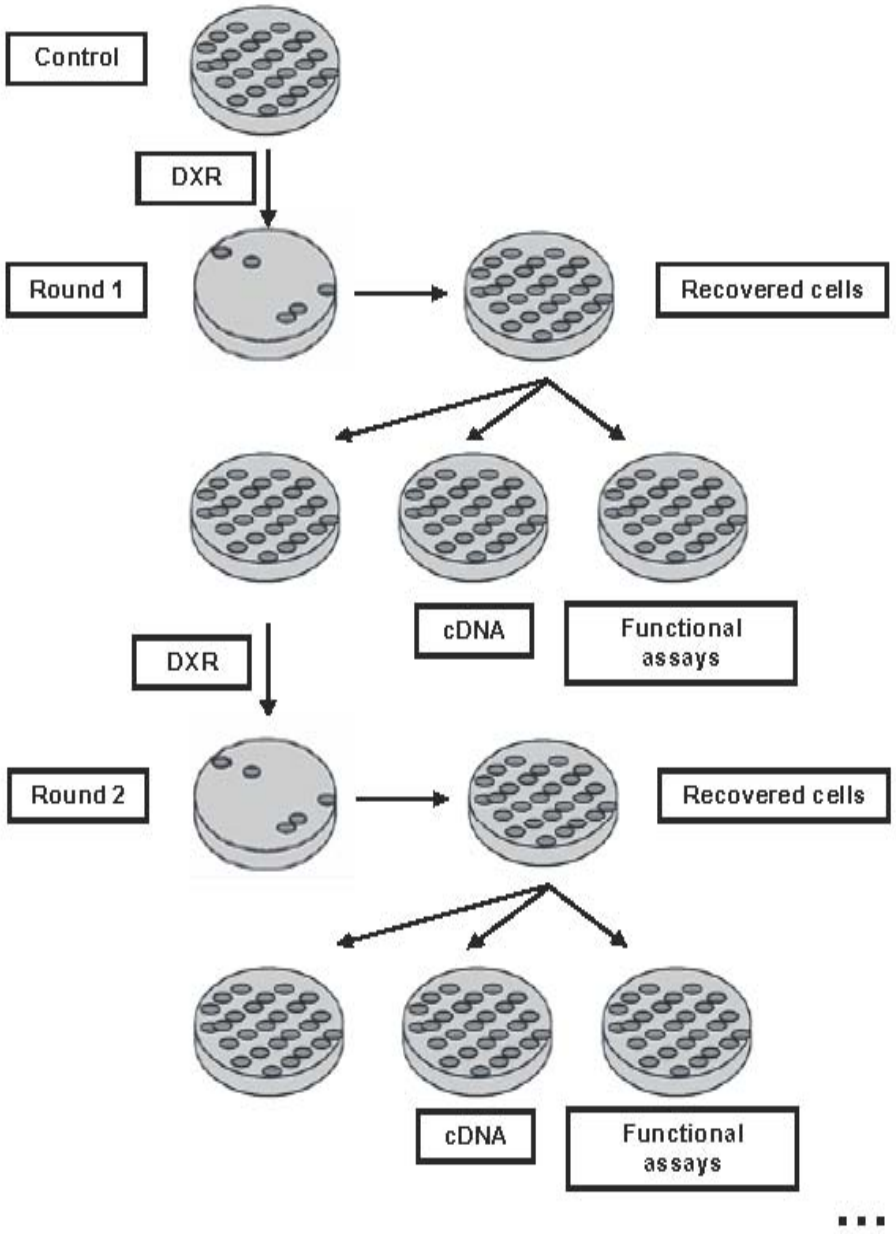

Figure 7. Schematic representation of the Molecular Evolution Assay (MEA). BT-474 and MDA MB-468 cells were treated with 0.5 μM doxorubicin for 72 h followed by a recovery phase. Recovered cells were subjected to qPCR analysis and functional assay like cell viability assay, side population analysis and mammospheres forming potential analysis. Four treatment rounds were performed for each cell line (R1-R4).

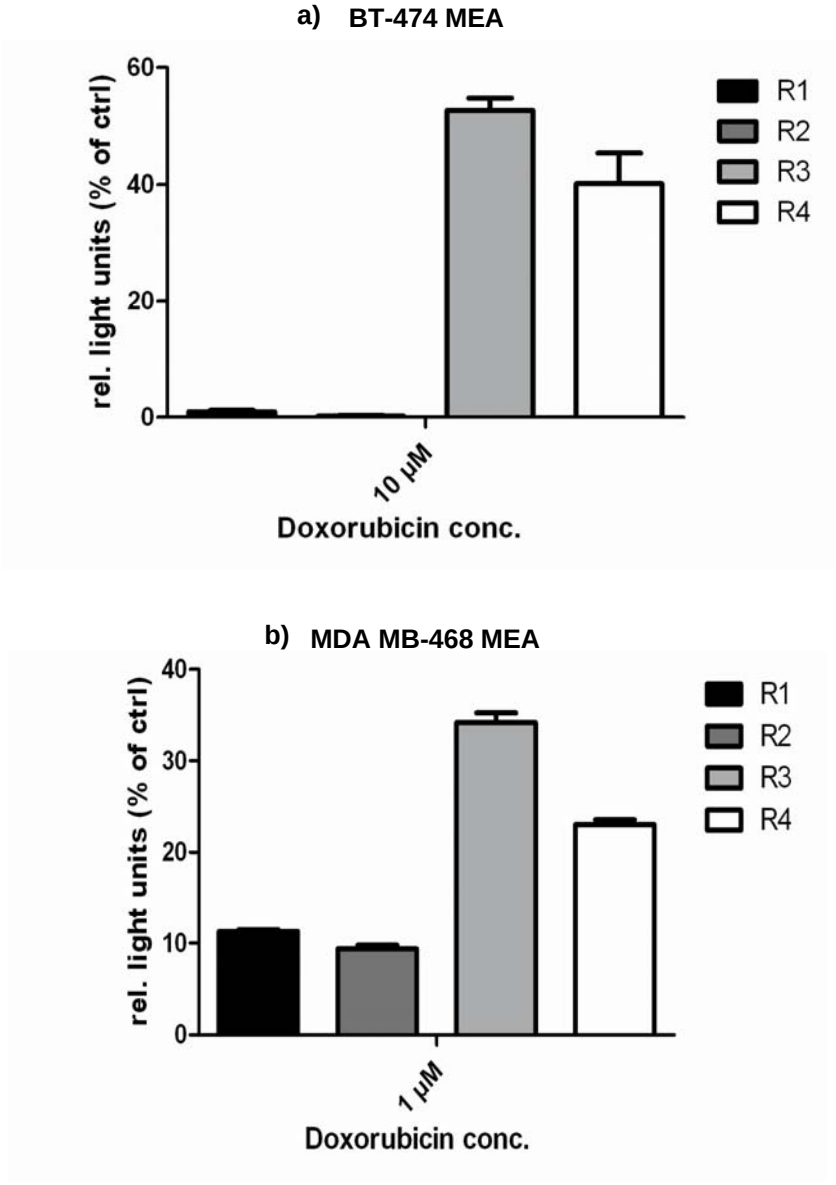

Figure 8. Cell viability assays of recovered cells from each MEA round against doxorubicin. Recovered cells from each round of MEA (Figure 7) were treated with doxorubicin for 72 h and Cell titer Glo assay was performed. Each treatment was done in triplicates. (a) Cell titer Glo assay results for BT-474 cells recovered from each round of MEA (R1-R4). (b) Cell titer Glo assay results for MDA MB-468 cells recovered from each round of MEA (R1-R4). Representative graphs of one concentration are shown here.

DXR (µM)	R1	R2	R3	R4
IC50 BT-474	0.08	0.03	0.38	0.39
IC50 MDA MB-468	0.1	0.09	0.4	0.2

Table 2. IC50 values of doxorubicin for BT-74 and MDA MB-68 cells of R1-R4.

The percentage of side population (SP) of the cells indicates the amount of ABC transporters present in the cells, which in turn help in pumping out the drugs and skipping the therapy. Percentage SP analysis of BT-474 and MDA MB-436 showed a gradual increase in ABC transporters over the rounds for both cell lines indicating evolution of resistant cells after cycles of treatment with doxorubicin (Figure 9 a and b).

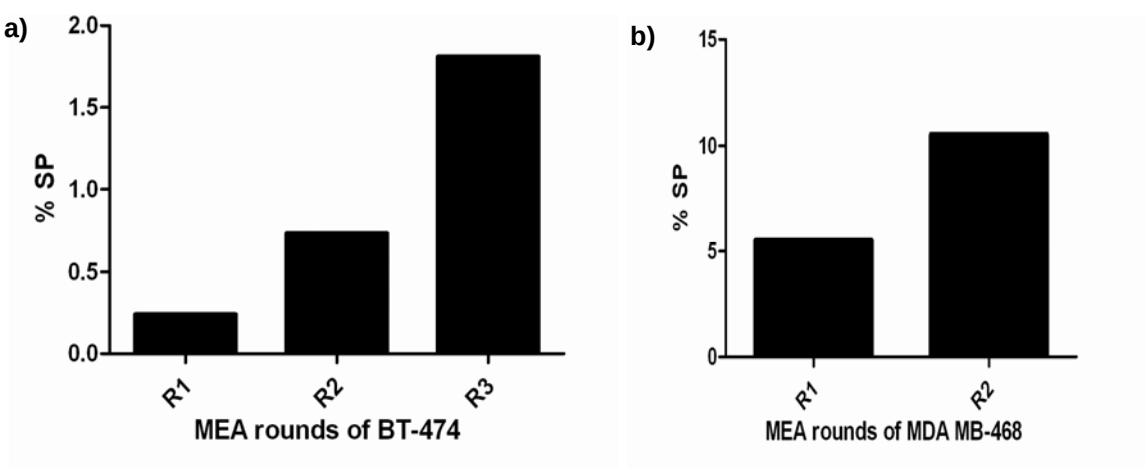

Figure 9. Percentage side population of BT-474 and MDA MB-468 cells obtained from rounds of MEA (Figure 7). (a) Percentage side population of BT-474 cells obtained from round 1 (R1), round 2 (R2) and round 3 (R3). (b) Percentage side population of MDA MB-468 cells obtained from round 1 (R1) and round 2 (R2).

After confirming the increased drug resistance over the rounds of the MEA by performing different assays, we wanted to check the effect of the treatments on the formation of mammospheres (detailed explanation in chapter 3.2) of both cell lines. Therefore we performed a ‘mammosphere forming potential’ (MFP) assay up to 3

passages of cells after each round of the treatment. For the cell line BT-474, treatment round 1 showed a constant MFP with around 200 mammospheres formed per passage. But in treatment round 2, cells showed decreased no. of mammospheres over passages and cells from treatment round 3 and 4 could not generate any mammospheres (Figure 10 a and b). Similar pattern was observed for MDA MB-436 cells where no. of mammospheres decreased over passages and over rounds. No mammospheres were formed for cell from round 3 and 4 (Figure 10 c and d).

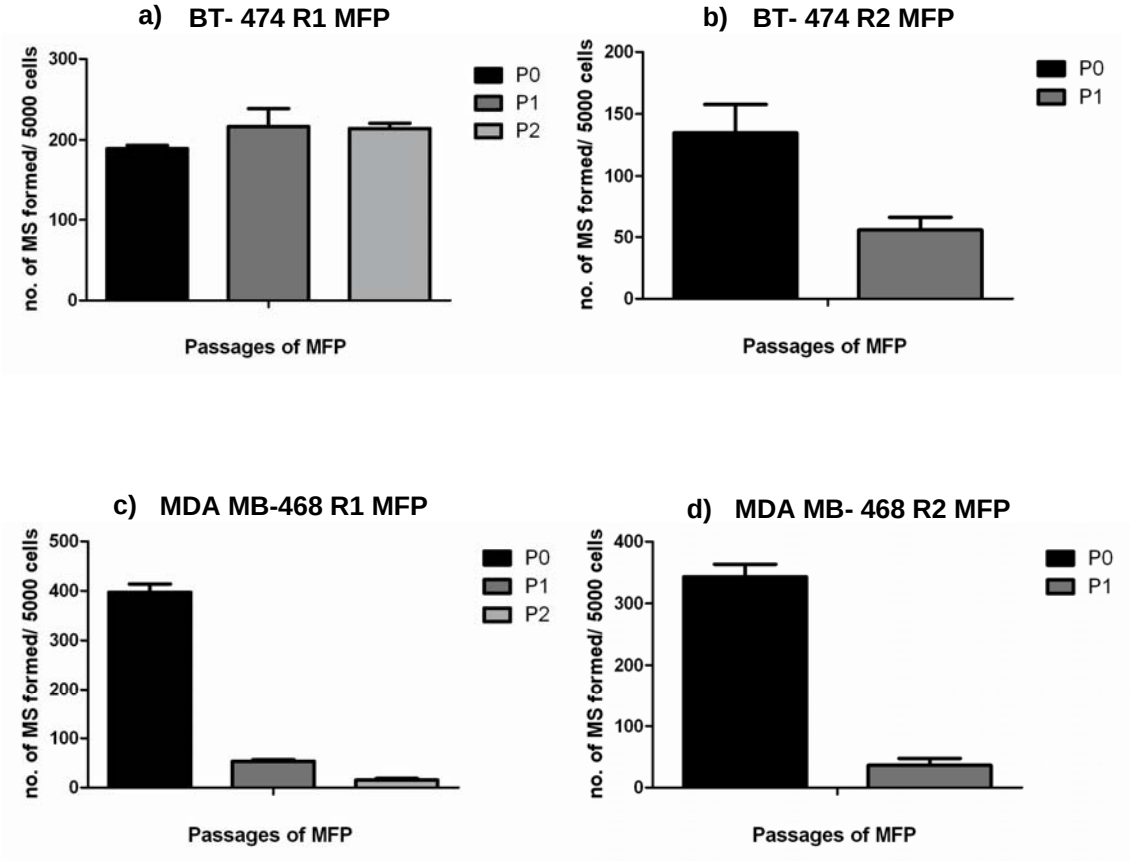

Figure 10. Mammosphere forming potential (MFP) of BT-474 and MDA MB-468 cells obtained from rounds of MEA. (a) MFP of round 1 (R1) cells of BT-474. (b) MFP of round 2 (R2) cells of BT-474. R3 and R4 cells showed no mammospheres formation. (a) MFP of round 1 (R1) cells of MDA MB-468. (b) MFP of round 2 (R2) cells of MDA MB-468. R3 and R4 cells showed no mammospheres formation. All experiments were performed in triplicates (n=3).

3.2 Generation and utilization of mammospheres as tools to study chemoresistance

Three dimensional spheroids of the breast cancer cells or mammary cells are known as mammospheres (MS). 3D architecture confers certain properties that distinguish mammospheres from 2D cell lines. Additionally, these spheroids resemble the tumors better because of their cellular heterogeneity. Furthermore, mammospheres are also enriched in certain markers conferring a chemoresistance phenotype on them. Considering all these properties, mammospheres were taken as tools to study chemoresistance in this thesis.

As shown in Figure 11, different breast cancer cell lines gave rise to different types of mammospheres. Based on the morphologies, mammospheres were divided into categories (Table 3). Epithelial cell lines like MCF-7 and BT-474 showed tight spheroids with merged cellular boundaries and defined spheroid shape. On the other hand, aggressive cell lines like MDA MB-436 and MDA MB-231 showed formation of aggregates. The aggregates were further divided in two categories loose aggregates as shown by MDA MB-231, MDA MB-157 and MDA MB-468 as well as tight aggregates shown by MDA MB-435, MDA MB-436 and MDA MB 453. The mammospheres structures of cell lines like MDA MB-231 and MDA MB-436 owing compromised cell–cell adhesion, acquisition of EMT like characters, and increased invasiveness demonstrated invasive and protrusive structures. In support to these results, a study showed appearance of MDA MB-231 mammospheres as aggregates due to invasive nature of the cell line. These aggregates eventually formed tight spheroids after addition of reconstituted basement membrane [121]. Furthermore, Shaw *et. al, 2004* also discuss loss of polarity of mammospheres after reduction in E-cadherin levels [122].

MCF-7 2D

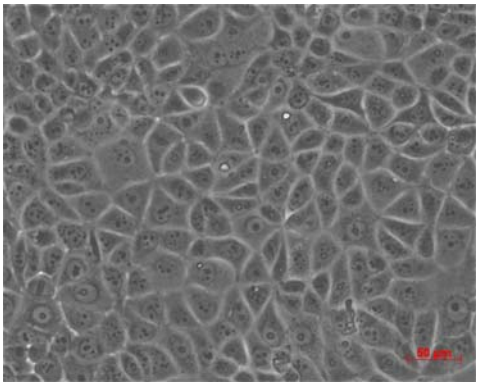

MCF-7 MS

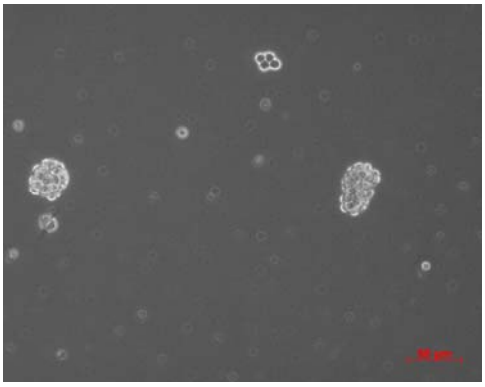

BT-474 2D

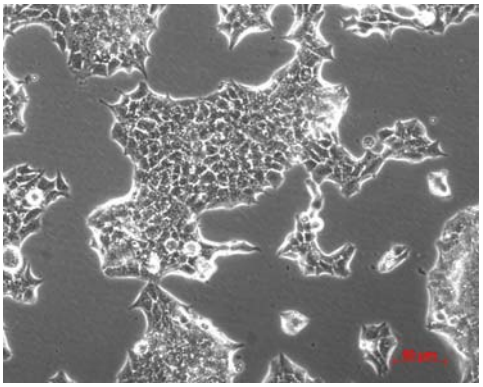

BT-474 MS

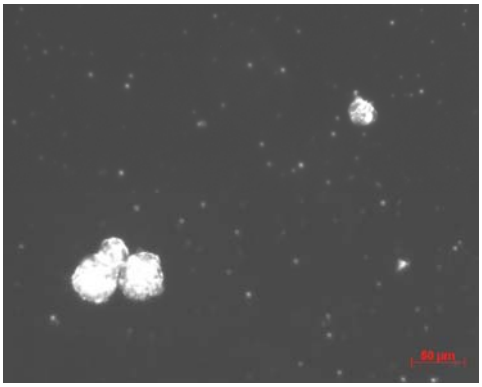

MDA MB-435 2D

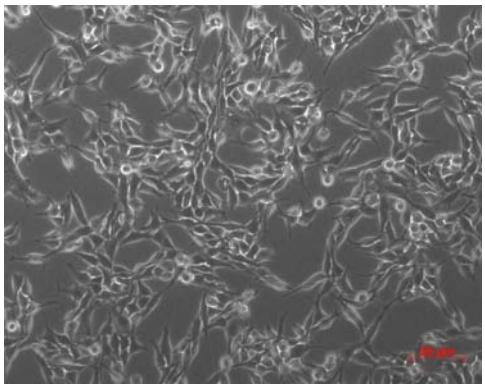

MDA MB-435 MS

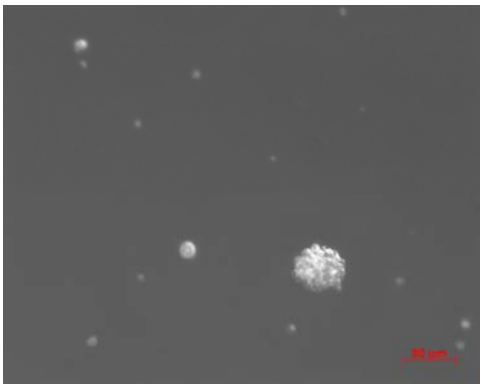

MDA MB-436 2D

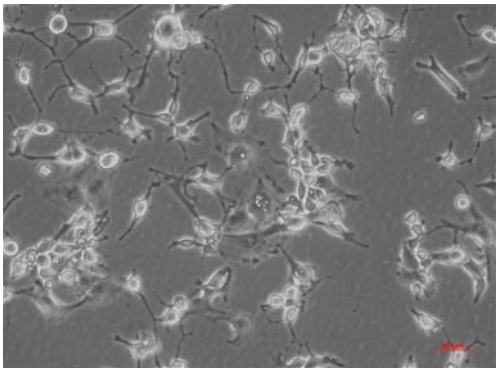

MDA MB-436 MS

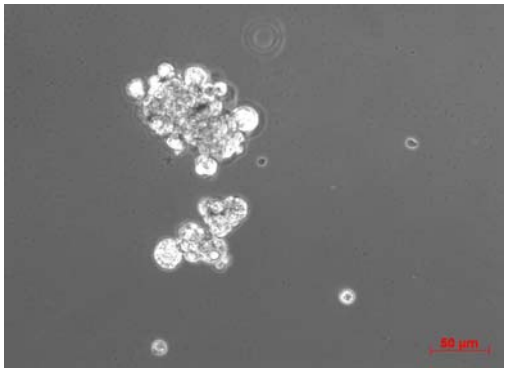

MDA MB-453 2D

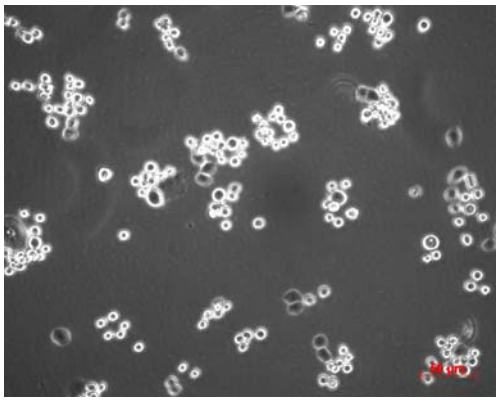

MDA MB-453 MS

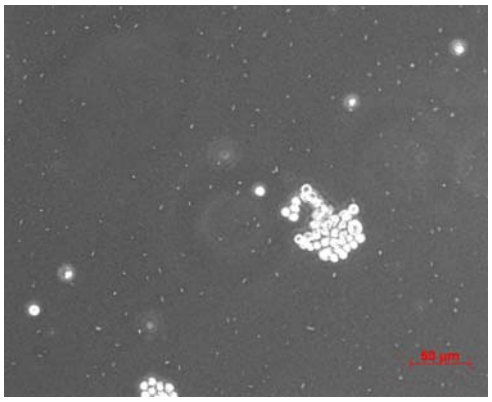

MDA MB-231 2D

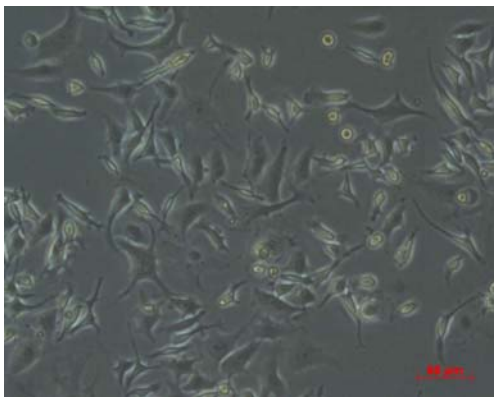

MDA MB-231 MS

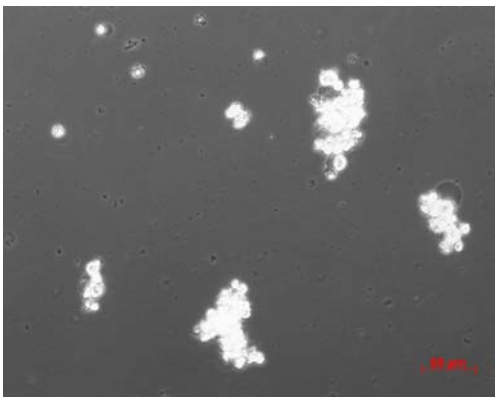

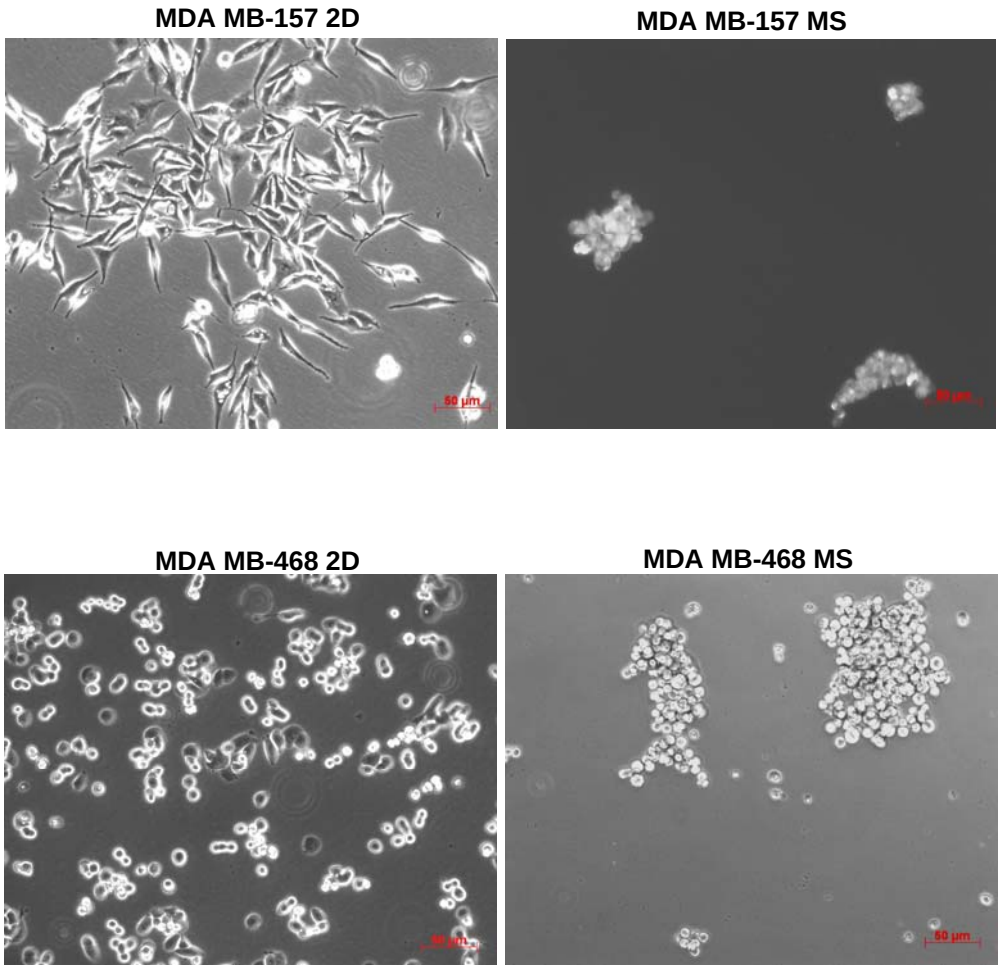

Figure 11. Morphology of different breast cancer cell lines and their mammospheres. Different morphologies of mammospheres were obtained based on different cell types and properties. MCF-7 and BT-474 displayed tight spheroids. MDA MB-435, MDA MB-436 and MDA MB-453 showed tight aggregates. MDA MB-231, MDA MB-157 and MDA MB-468 demonstrated loose aggregates. For 2D cells the images were captured at 48 h and for mammospheres the images were captured after 7 d of seeding.

Spheroids	Tight aggregates	Loose aggregates
MCF-7	MDAMB-435	MDAMB-231
BT-474	MDAMB-453	MDAMB-468
	MDAMB-436	MDAMB-157

Table 3. Classification of mammospheres of different breast cancer cell lines.

To check the ability the cell lines to form and propagate heterogeneous mammospheres, mammosphere forming potential (MFP) assay was performed. Moreover in this assay mammospheres were generated utilizing as low as 5000 single cells (passage 0). Cell from mammospheres were dissociated into single cells and seeded again to form mammospheres of passage 1 (P1). The assay was performed till passage 2 (P2). Cell lines with high E-cadherin expression (MCF-7 and BT-474) showed more or less constant MFP (Figure 12 a). On the contrary invasive cell lines like MDA MB-231, MDA MB-436, MDA MB-468 and MDA MB-157 showed decreased MFP (Figure 12 b). Furthermore, MDA MB-453 showed presence of far less mammospheres and hence seeding for passage 1 was not possible. MDA MB-435 was the only exception that showed increased MFP (Figure 12 c).

a) Constant MFP

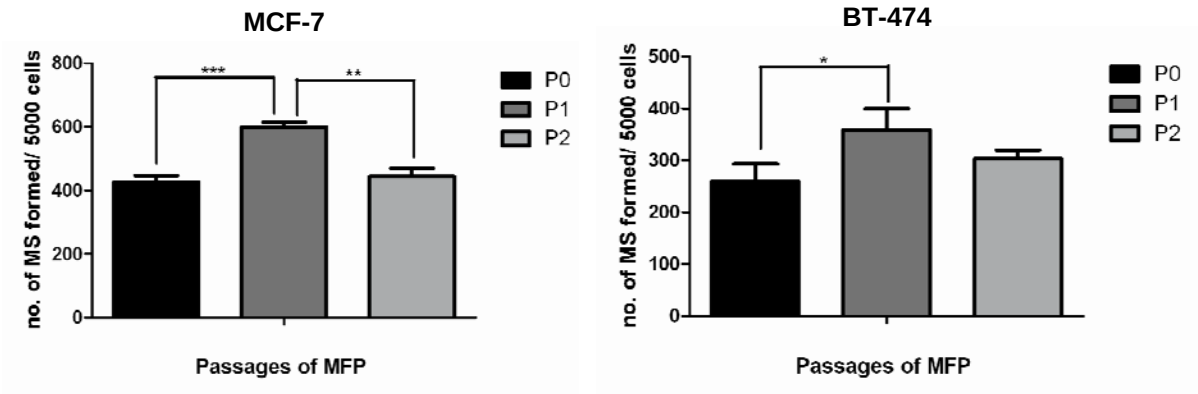

b) Decreasing MFP

MDA MB-231

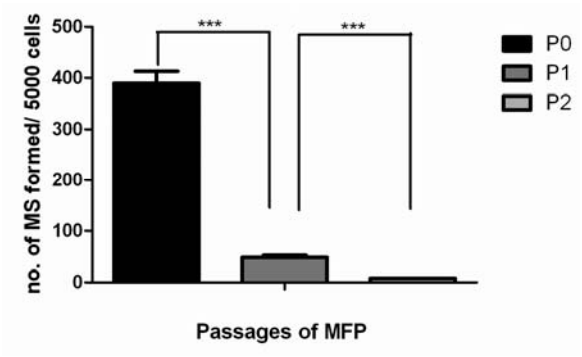

MDA MB-436

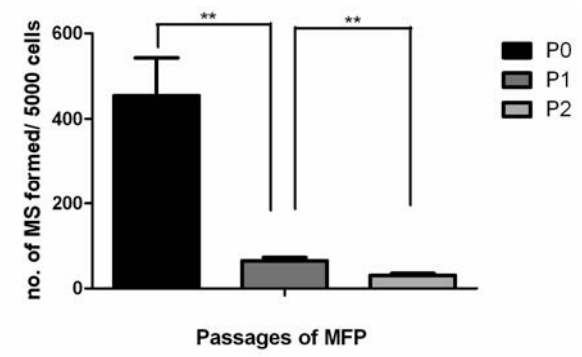

MDA MB-468

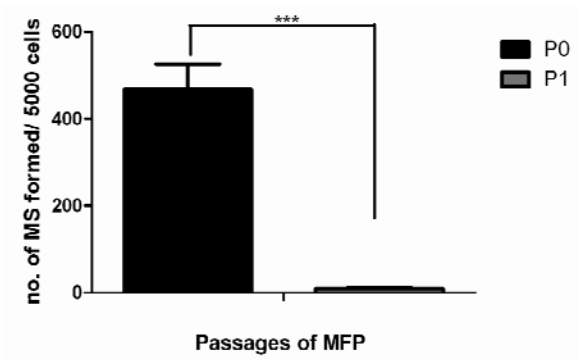

MDA MB-157

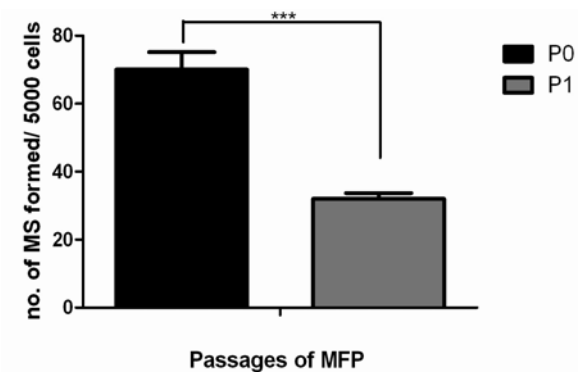

MDA MB-453

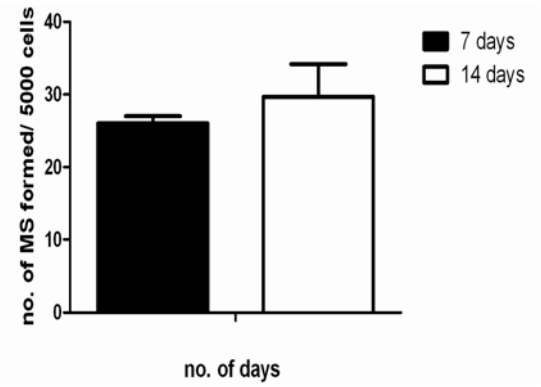

c) Increasing MFP

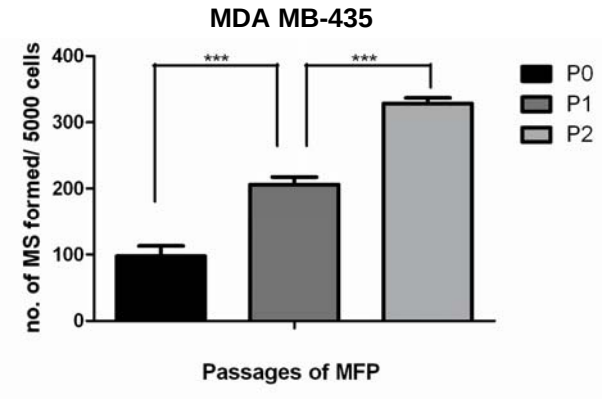

Figure 12. Mammosphere forming potential (MFP) of breast cancer cell line mammospheres upon passaging. (a) Constant MFP of MCF-7 and BT-474 from passage 0 (P0) to passage 2 (P2). (b) Decreasing MFP of MDA MB-231, MDA MB-436, MDA MB-468, MDA MB-157 and MDA MB-453. (c) Increasing MFP of MDA MB-435. For each passage mammospheres were counted after 7d of seeding. Student's t test is performed to determine the significance (*** P-values <0.001, ** P-values <0.01, * P-values <0.05)

Furthermore, to correlate breast cancer chemoresistance, investigation of stem cell-like character in mammospheres was performed. NANOG, OCT4 and SOX2 (NOS) genes were selected as stem cell markers. Figure 13 a shows qPCR analysis of expression of the three genes in mammospheres. Mammospheres of all three cell lines namely MCF-7, MDA MB-435 and MDA MB-231 show up-regulation of NOS genes as compared to 2D cells. Amongst the mammospheres of three cell lines, MCF-7 mammospheres demonstrated highest levels of these genes NANOG (4.5 fold), OCT4 (1.5 fold) and SOX2 (8 fold) as compared to 2D MCF-7 cell line. To confirm qPCR data, FACS staining for SOX2 marker was performed. An over-expression of SOX2 gene was depicted in MCF-7 and MDA MB-453 mammospheres by FACS analysis (Figure 13 b).

a)

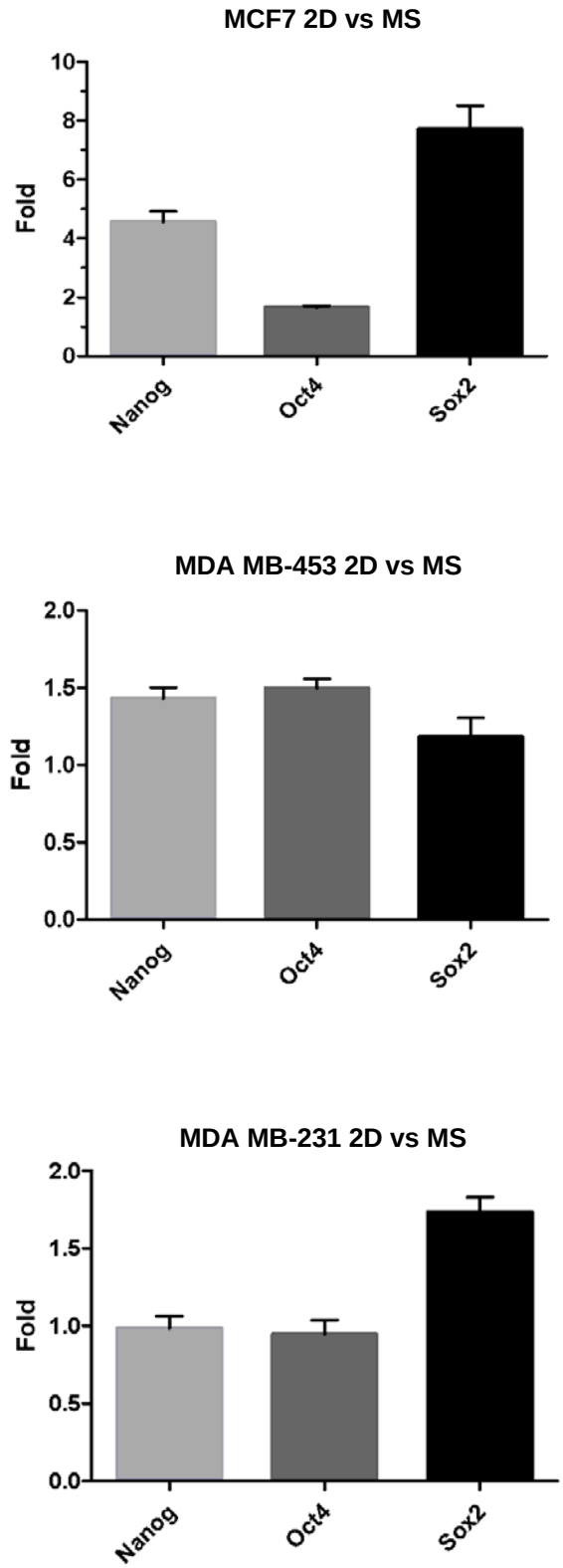
MCF7 2D vs MS
Fold
10
8
6
4
2
0
Nanog
Oct4
Sox2
MDA MB-453 2D vs MS
Fold
2.0
1.5
1.0
0.5
0.0
Nanog
Oct4
Sox2
MDA MB-231 2D vs MS
Fold
2.0
1.5
1.0
0.5
0.0
Nanog
Oct4
Sox2

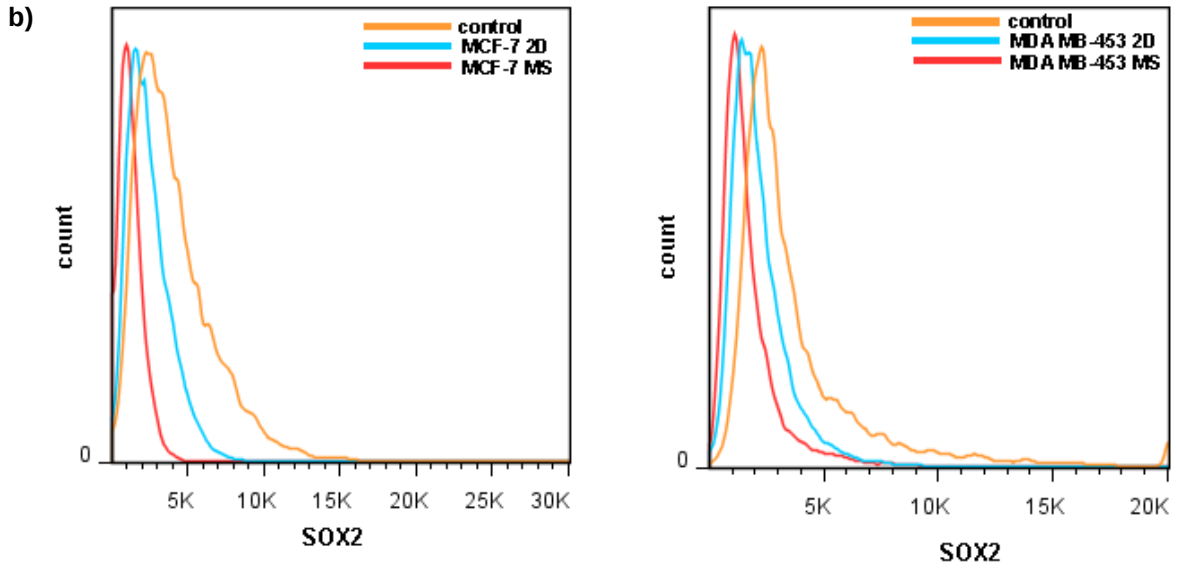

Figure 13. Enrichment of stem cell markers in mammospheres (MS) as compared to 2D cells. (a) qPCR analysis of markers NANOG, OCT4 and SOX2 in mammospheres of MCF-7, MDA MB-453 and MDA MB-231 as compared to 2D cells. The results here are displayed as fold increase of markers in mammospheres as compared to 2D cells. (b) FACS analysis of marker SOX2 in mammospheres as well as 2D cells of MCF-7 and MDA MB-453. Total SOX2 levels are shown in the overlay.

After demonstrating enrichment of stem cell-like cells in mammospheres, their sensitivity to chemotherapeutics was analyzed. MCF-7 mammospheres and 2D cells were subjected to treatment with different classical chemotherapeutics. Briefly, MCF-7 mammospheres were divided in two halves. One half was trypsinized into single cells followed by counting the amount required to seed 5000 cells/well and accordingly whole mammospheres were seeded in poly HEMA coated 96. Treatment was performed after 24 hrs of seeding for 72 hrs (Figure 14 a). Mammospheres showed significant resistance to doxorubicin and paclitaxel as compared to 2D MCF-7 cells (Figure 14 b and c). *In toto,* these results indicate potential of mammospheres as tools to study chemoresistance due to their morphological phenotype, resemblance to tumors and enrichment for stem cell-like cells.

a)

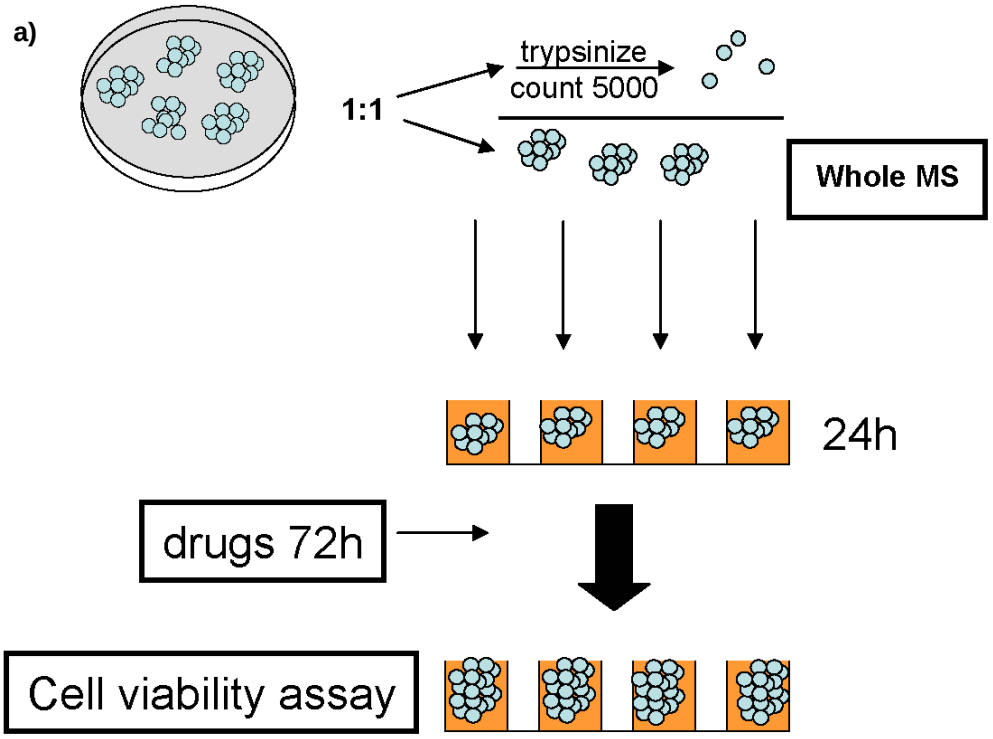
1:1
trypsinize
count 5000
Whole MS
24h
drugs 72h
Cell viability assay

b)

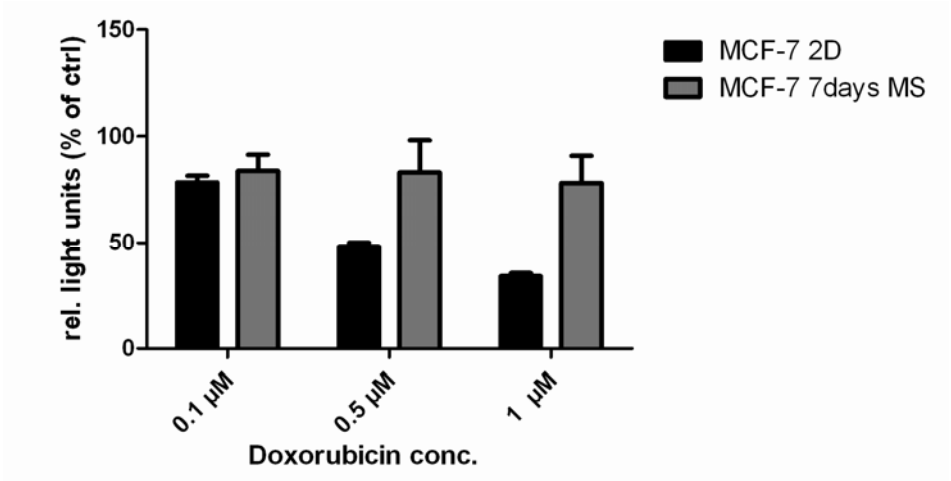
MCF-7 2D
MCF-7 7days MS
rel. light units (% of ctrl)
150
100
50
0
0.1 µM
0.5 µM
1 µM
Doxorubicin conc.

c)

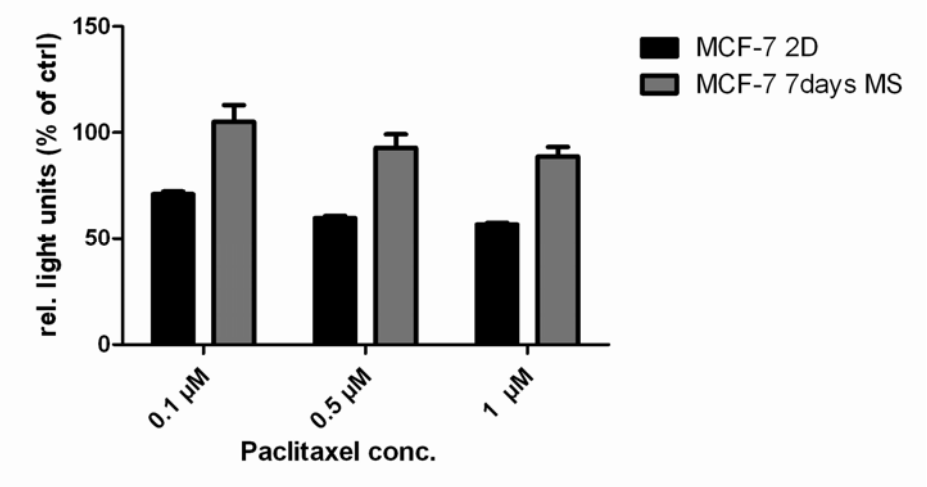

Figure 14. Utilization of mammospheres as tools to study chemoresistance. (a) Scheme for studying effect of chemotherapeutics on mammospheres. Treatment was performed as stated in the text for both 2D cells as well as mammospheres and cell viability was checked through Cell titer Glo assay. (b) Effect of doxorubicin on MCF-7 2D cells and 7 d old MS. (c) Effect of paclitaxel on MCF-7 2D cells and 7 d old. Each treatment was performed in triplicates (n=3).

3.3 Elevation of membrane receptor tyrosine kinase HER2 in mammospheres

Pickl and Ries demonstrated a difference in molecular signaling of HER2 in mammospheres and 2D cell lines [123]. HER2 is an extensively studied growth and survival marker in breast cancer and is associated with the chemoresistance making it one of the intriguing proteins for this study. An analysis of HER2 expression in mammospheres was further performed in this study. Strikingly, MCF-7 and MDA MB-453 mammospheres corroborated increased expression of HER2 at mRNA as well as protein levels as compared to respective 2D cell lines (Figure 15 a and b). Additionally, tissue sections from xenografts obtained by injecting single cells from mammospheres in mice exhibited expression of HER2 which was absent in tissue sections of injected MCF-7 2D cells (Figure 15 c).

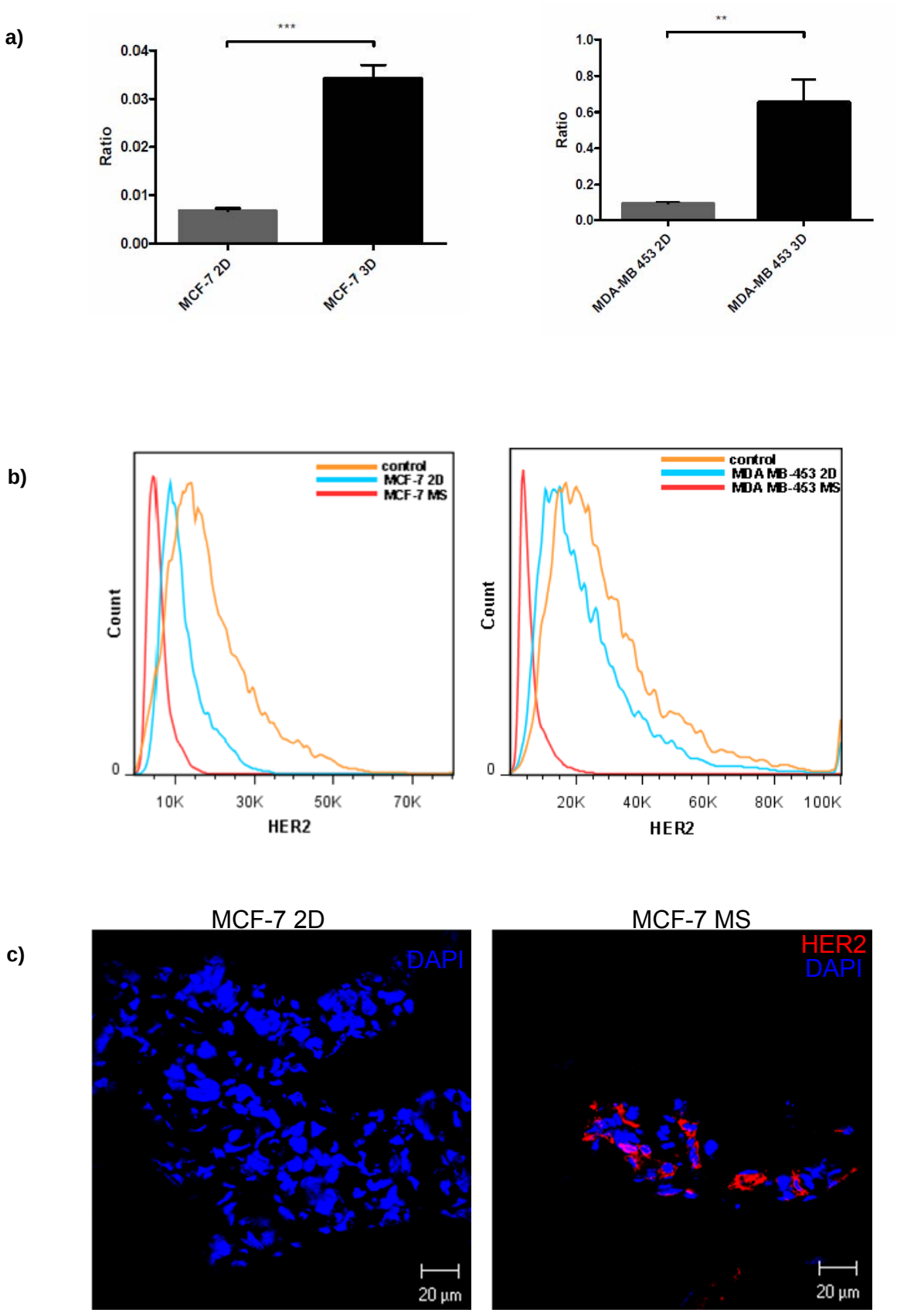

Figure 15. Up regulation of HER2 protein in MCF-7 MS. (a) qPCR analysis of HER2 levels in MCF-7 and MDA MB-453 mammospheres as compared to 2D cell lines. The experiment is performed in

triplicates (n=3). Student's t test is performed to determine the significance (*** P-values <0.001, ** P-values <0.01). (b) FACS analysis of protein HER2 in mammospheres as well as 2D cells of MCF-7 and MDA MB-453. Total HER2 levels are shown in the overlay. (c) Cells of MCF-7 2D and MCF-7 mammospheres were injected subcutaneously in the right flank of female immunodeficient mice and cryosections were prepared after 171 d of injection. Tissue sections were stained for HER2 protein (red) and the nucleus is stained with DAPI (blue). A section of 20 µm is shown here.

Laser scanning microscopic images of MCF-7 and MDA MB-453 mammospheres stained for HER2 displayed differential membrane expression in individual cells of mammospheres (Figure 16 a and b). Some cells showed strong membrane localized HER2 expression (white arrows) whereas some showed no or little HER2 expression (red arrows). To characterize these populations and identify the role of HER2 in mammospheres, two cell fractions were immunosorted.

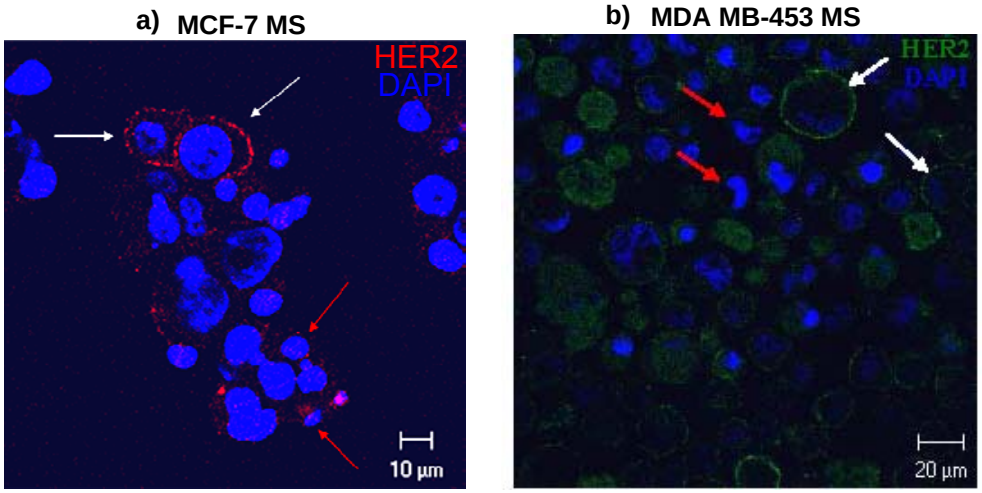

Figure 16. Differential expression of HER2 protein in mammospheres. (a) Laser scanning microscopic images of MCF-7 mammospheres stained for HER2 (red). Nucleus is stained with DAPI (blue). White arrows show membrane staining of HER2 and red arrows indicate $HER2^{low}$ cells. (b) Laser scanning microscopic images of MDA MB-453 mammospheres stained for HER2 (green). Nucleus is stained with DAPI (blue). White arrows show membrane staining of HER2 and red arrows indicate $HER2^{low}$ cells. A section of 10µm is shown here.

10% of the cell population containing highest HER2 levels as $HER2^{high}$ and 10% of cells with the lowest HER2 expression as $HER2^{low}$ were sorted from MCF-7 mammospheres. Accordingly, analysis of the location of these two fractions in forward scatter and sideward scatter plot of the whole population showed $HER2^{low}$ as a small cell fraction (Figure 17).

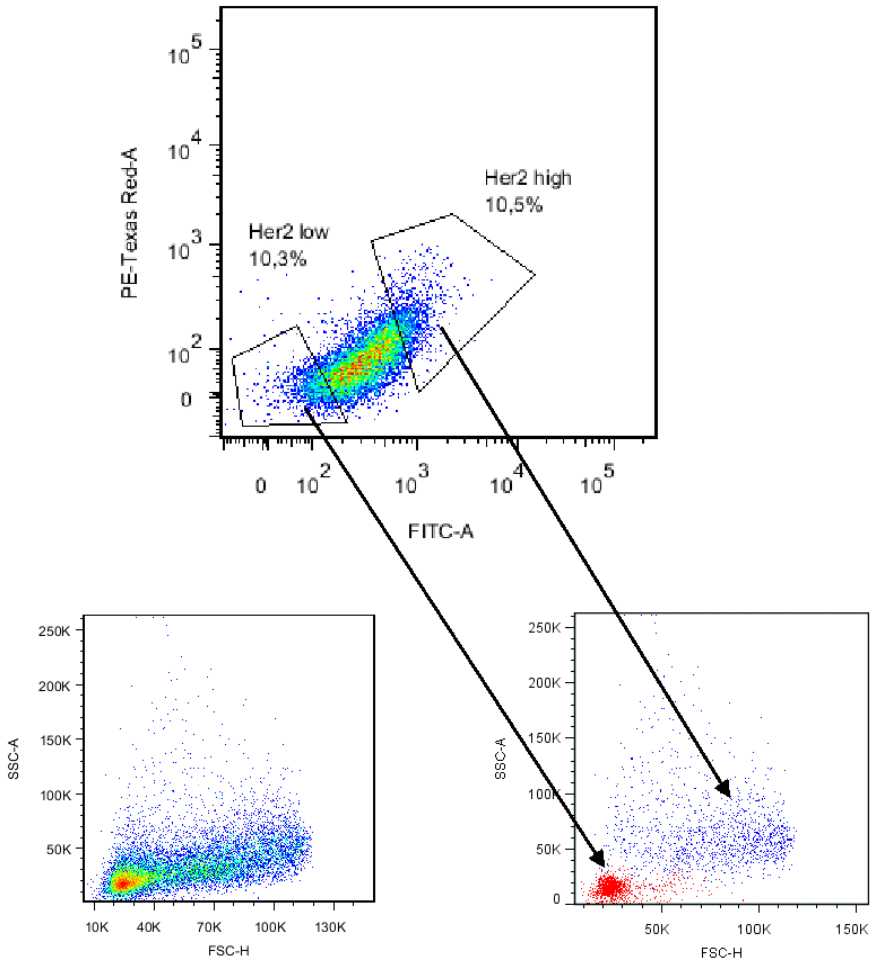

Figure 17. Strategy to immunosort HER2^{low} and HER2^{high} cells from MCF-7 MS.
10 % of HER2^{high} and 10 % of HER2^{low} cells were sorted from 2D cell line and mammospheres of MCF-7 grown for 24 h and 7 d. HER2^{low} is distinctly present in the small cell fraction and HER2^{high} is primarily present in the big cell fraction as analyzed in forward scatter and sideward scatter plot.

To determine the role of HER2 protein expression in formation of mammospheres, these two immunosorted populations from 7 d old mammospheres of MCF-7 were subjected to the MFP analysis. In accordance with the study of Hanssen *et al.* 2010, HER2^{high} fraction showed significantly high number of mammospheres formed even at passage 2 (P2) as compared to those formed by HER2^{low} fraction [124]. In addition HER2^{low} fraction showed gradual decrease in the number of mammospheres formed starting from passage 0 (P0) to passage 2 (P2) (Figure 18 a and b). This data suggests involvement of HER2 in anoikis resistance and formation of mammospheres.

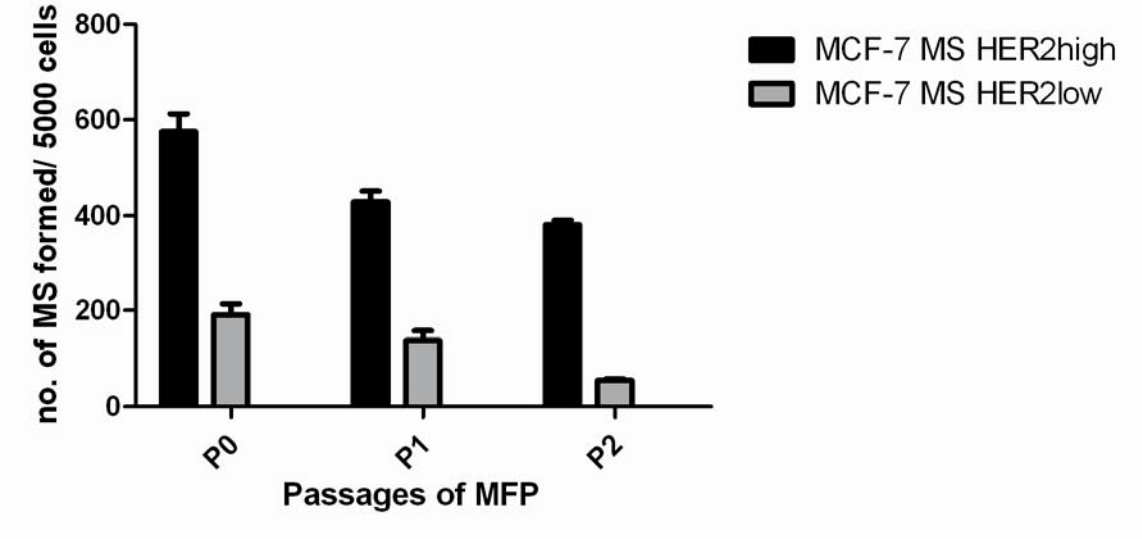

Figure 18. MFP of HER2^{high} and HER2^{low} sorted populations from MCF-7 MS. MFP of HER2^{high} and HER2^{low} sorted cells from MCF-7 mammospheres from P0 to P2. Experiments were performed in triplicates (n=3). Student's t test is performed to determine the significance (*** P-values <0.001, ** P-values <0.01, * P-values <0.05)

3.4 Involvement of cancer stem cells in resistance to therapy and their specific targeting with salinomycin

In addition to its association with poor prognosis and aggressiveness, HER2 protein has been associated with chemoresistance and cancer stem cells [55,106]. As shown in previous results, mammospheres are enriched for cancer stem cells. Therefore, to identify the cancer stem cell populations, sorted cells were first subjected to analysis of stem cell markers. qPCR analysis of stem cell markers in these two fractions of MCF-7 2D cells, 24 h old mammospheres and 7 days old mammospheres demonstrated almost equal expression levels of NANOG, OCT4 and SOX2 in 2D as well as in the 24 h old mammospheres. In contrast, the mammospheres grown for 7 days expressed 4.5 fold, 5 fold and 2.5 fold more NANOG, OCT4 and SOX2 respectively in HER2^{low} cells (Figure 19). Hence, a time-dependent upregulation of NOS markers in HER2^{low} cells of the MCF-7 mammospheres was observed suggesting an evolution of these markers over time during the formation of mammospheres.

Since there was an elevation of the stem cell markers in *HER2^{low}* population of the mammospheres, stem cell like phenotype of this fraction was confirmed by

physiological assays. matrigel, HER2^{low} population displayed presence of ductal-like outgrowths after 7 days (Figure 21 a).

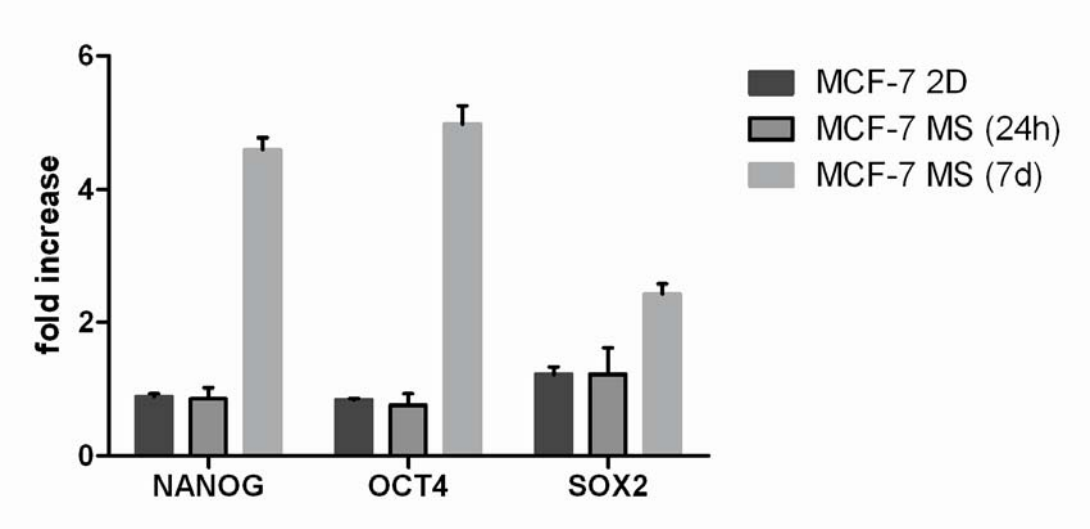

Figure 19. Expression of stem cell markers in HER2^{low} and HER2^{high} fraction of mammospheres. qPCR analysis of NANOG, OCT4 and SOX2 for HER2^{low} and HER2^{high} population sorted from MCF-7 2D cells, mammospheres of MCF-7 grown for 24 h and 7 d. The graph shows expression levels of markers in the HER2^{low} fraction normalized to expression levels in the HER2^{high} fraction.

Proliferation analysis of these two populations shown in Figure 20, exhibits slow proliferation of the HER2^{low} cells in mammospheres of MCF-7. Additionally, the no. of colonies obtained with HER2^{low} population in matrigel, was higher than that obtained from HER2^{high} (Figure 21 b). This data suggests that the HER2^{low} population manifests properties similar to stem cells or poorly differentiated cells such as slow proliferation, ductal-like outgrowth in matrigel and higher colony formation ability.

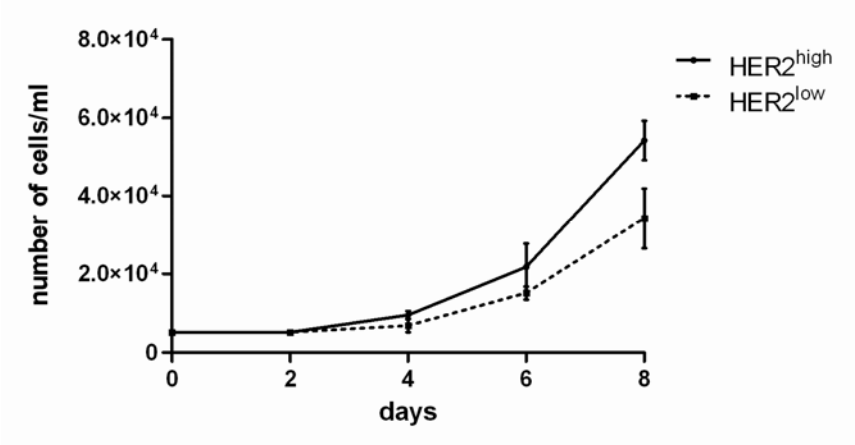

Figure 20. Proliferation of HER^{low} and HER2^{high} populations of MCF-7 MS. Growth curve of HER2^{high} and HER2^{low} sorted populations of MCF-7 mammospheres. Experiment was performed in triplicates (n=3).

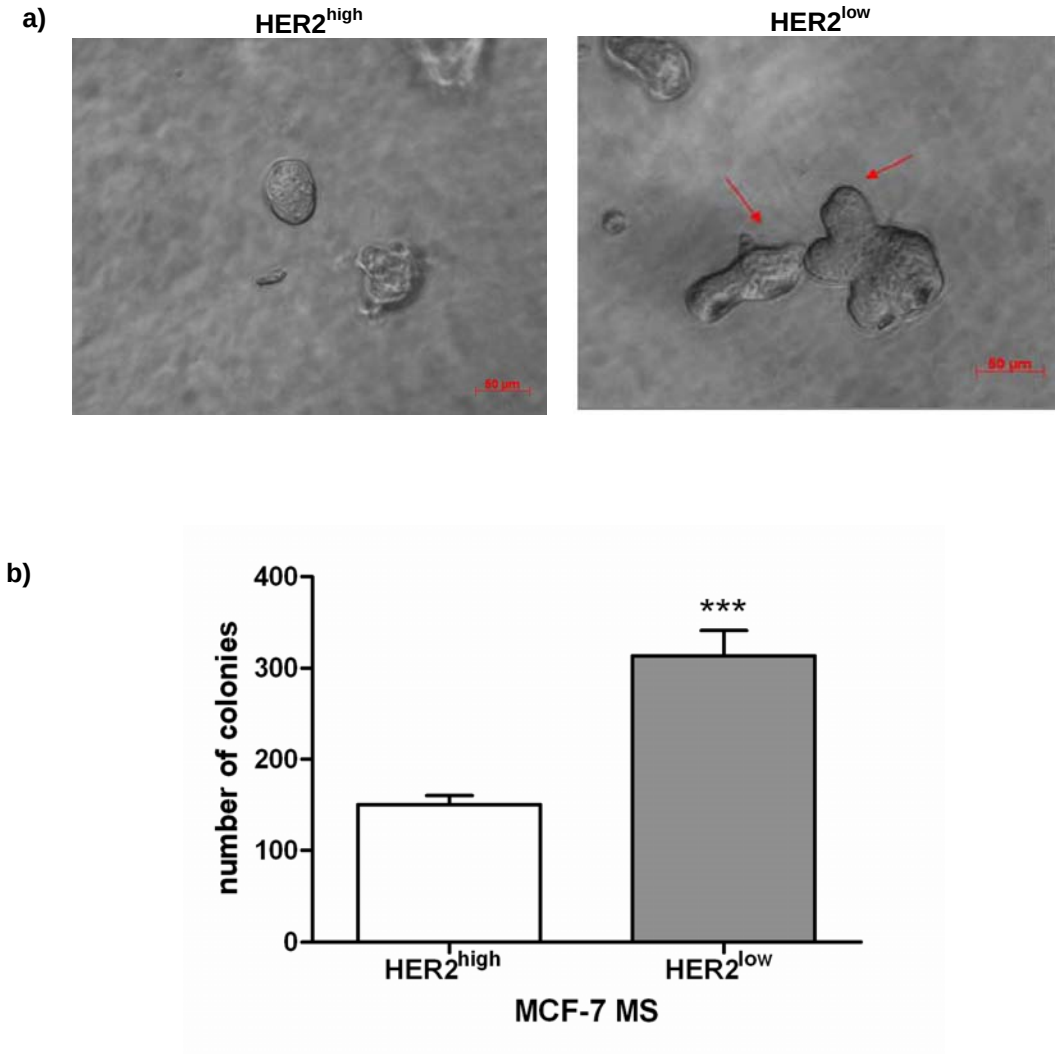

Figure 21. Classification of stem cells in HER2low cells using matrigel growth pattern. (a) Matrigel outgrowths of HER2^{high} and HER2^{low} sorted populations of MCF-7 mammospheres. A section of 50µm is shown here. (b) The colonies formed in matrigel were counted manually after 7 d. The experiment was performed in triplicates (n=3). Student's t test was performed to determine the significance (*** P-values <0.001).

Further to confirm this observation *in vivo*, we injected HER2^{low} and HER2^{high} immunosorted cells from MCF-7 mammospheres subcutaneously in immunodeficient mice (performed by Florian Kopp). The take rate was similar for both the groups. However, monitoring the growth of these tumors over 145 days demonstrated that HER2^{low} cell fraction formed visible tumors 6 weeks before tumors of HER2^{high} cells (Figure 22). In accordance with Figure 20, tumors from HER2^{low} cells demonstrated slow proliferation rate as compared to tumors from HER2^{high} cells.

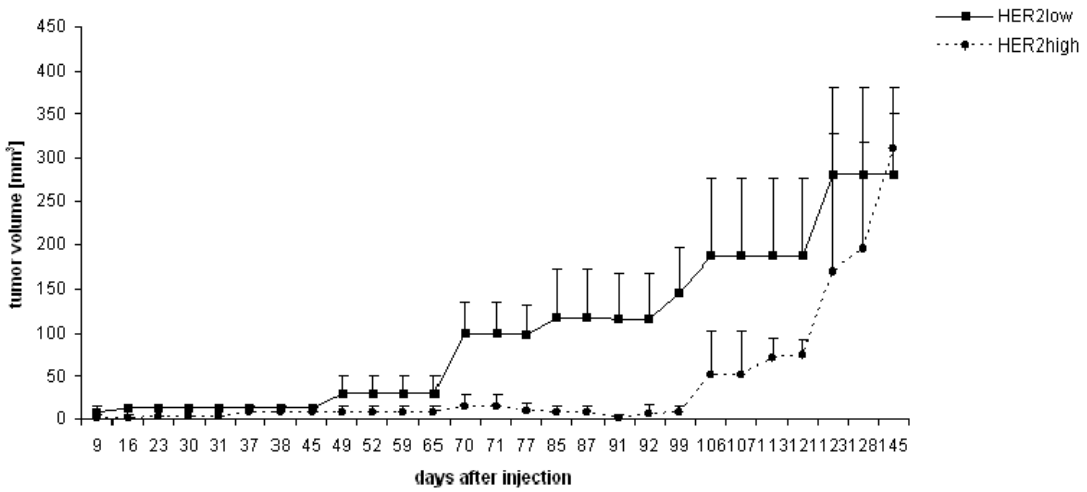

Figure 22. Growth curve of tumors from HER2low and HER2high sorted population injected in mice. Sorted HER2^{low} *and* HER2^{high} cells from 7 d old MCF-7 mammospheres were injected subcutaneously in the right flank of female immunodeficient mice (7 mice per group). For HER2^{low} xenografts, 2 mice developed tumors and for HER2^{high} xenografts 3 mice developed tumors. The growth curve calculated over 145 days after injection is shown here.

HER2 expression in xenografts was performed by immunohistochemistry for the HER2 protein. HER2^{high} tissue sections displayed some feebly expressed extra cellular HER2 while *HER2*^{low} showed no expression of HER2 depicting the authenticity of the sorted cells. Moreover, the HER2^{low} cryosections showed abundant expression of OCT4 while that of HER2^{high} showed no expression (Figure 23). Besides, an upregulation in NANOG, OCT4 and SOX2 was seen at mRNA level too in xenografts of HER2^{low} cells as compared to those of HER2^{high} cells (Figure 24).

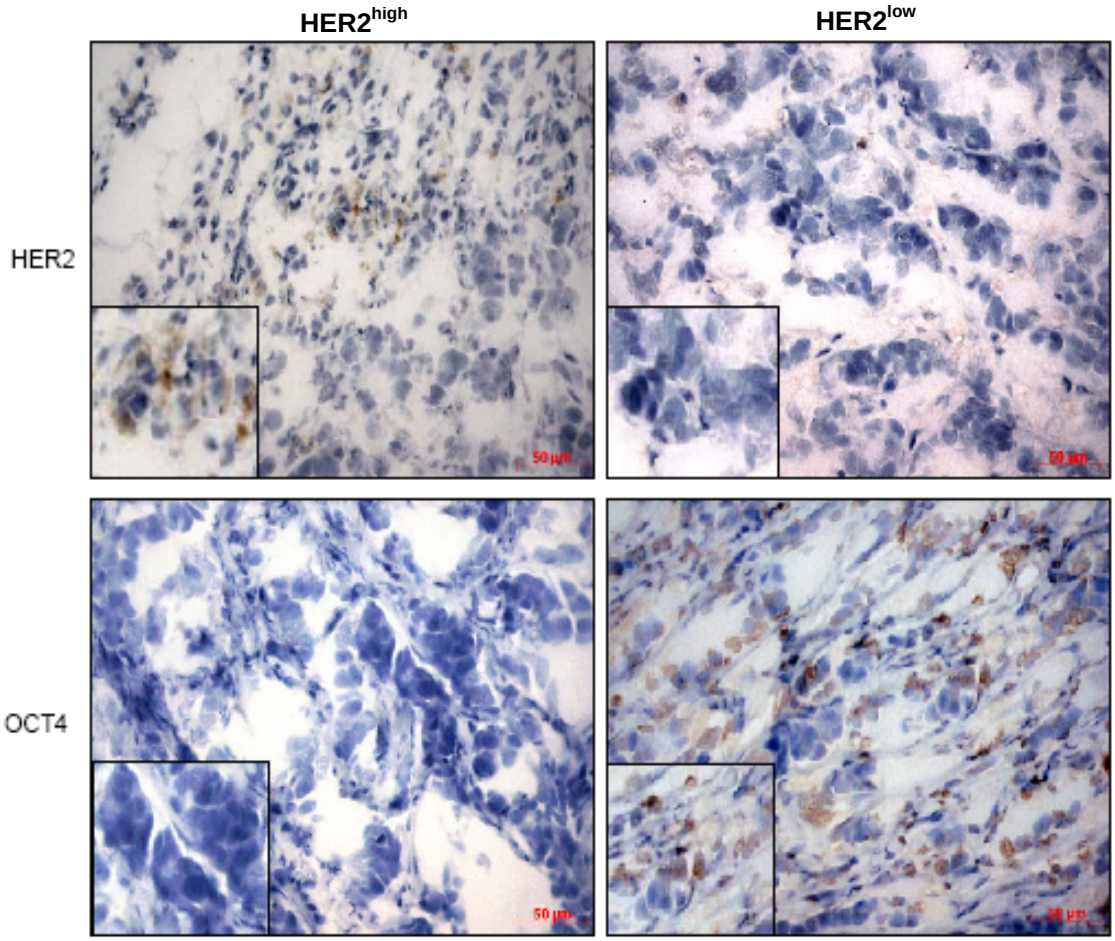

Figure 23. Immunohistochemical analysis of tissue sections obtained from tumors of sorted fractions of MCF-7 MS. Immunohistochemical analysis of cyosections of tumors from injected $HER2^{low}$ and $HER2^{high}$ cells stained with HER2 and OCT4 antibodies. An image taken with 40X objective is shown here with an enlarged section in lower left corner. A section of 50µm is shown here.

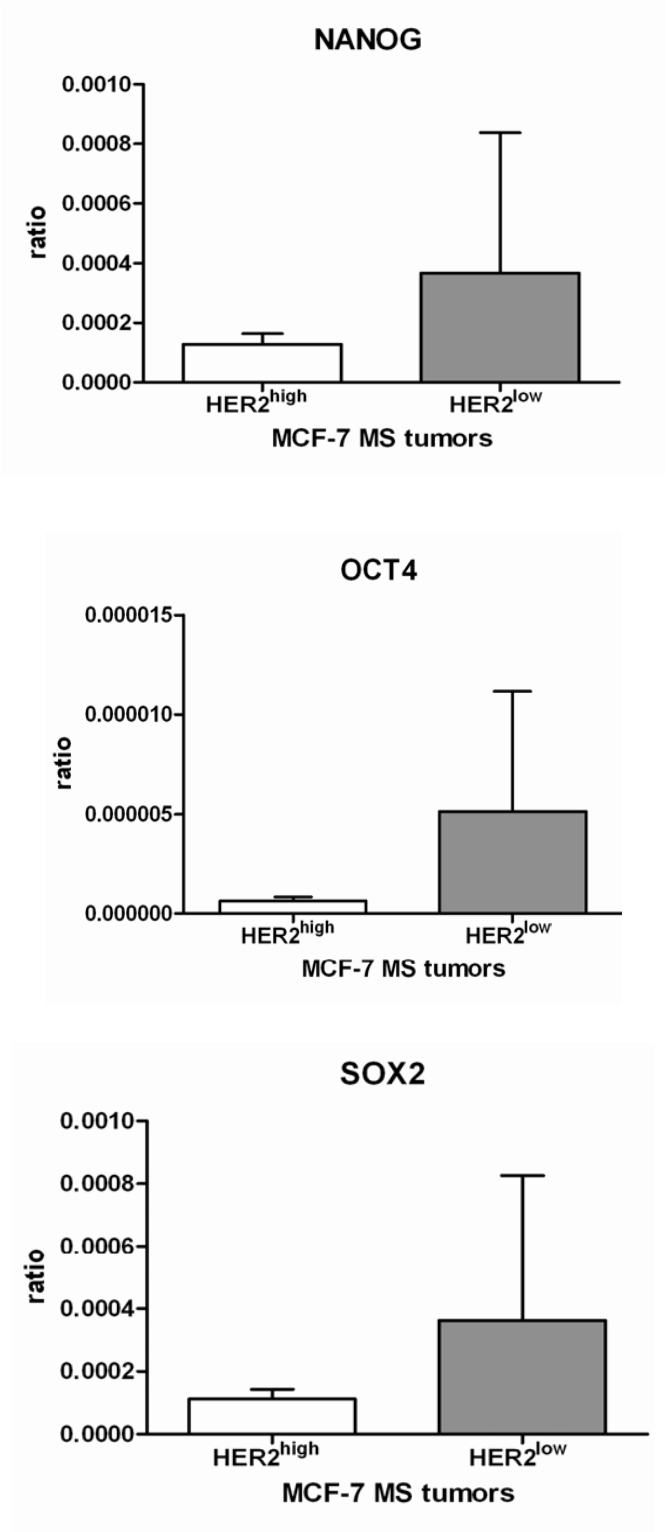

Figure 24. qPCR analysis of stem cell markers in tumors obtained by injection of sorted populations. qPCR analysis of tumors obtained from injection of $HER2^{low}$ and $HER2^{high}$ sorted populations in immuno-compromised mouse. The experiment is performed in triplicates (n=3).

Further aim was to target specifically these two cell fractions $HER2^{high}$ and $HER2^{low}$, i.e. cancer stem cells. On the one hand trastuzumab was used to treat the $HER2^{high}$

subset as it is commonly used in clinics for treating HER2-positive breast cancer patients. On the other hand, *Gupta et al.* have recently found that salinomycin specifically kills the cancer stem cell population of tumors [110]. Therefore we analyzed whether it is effective against the $HER2^{low}$ subset. As expected, $HER2^{high}$ cells exhibited a dose dependent response to trastuzumab. On the contrary, $HER2^{low}$ cells were unaffected by trastuzumab treatment. Salinomycin showed exactly the opposite effect as it killed $HER2^{low}$ cells in a dose dependent manner (Figure 25 a and b). Furthermore, the $HER2^{low}$ fraction was more resistant to the classical chemotherapeutic drug doxorubicin than the $HER2^{high}$ fraction (Figure 25 c). Thus, we authenticated our hypothesis that $HER2^{low}$ fraction constitutes cancer stem cells that are effectively killed by salinomycin.

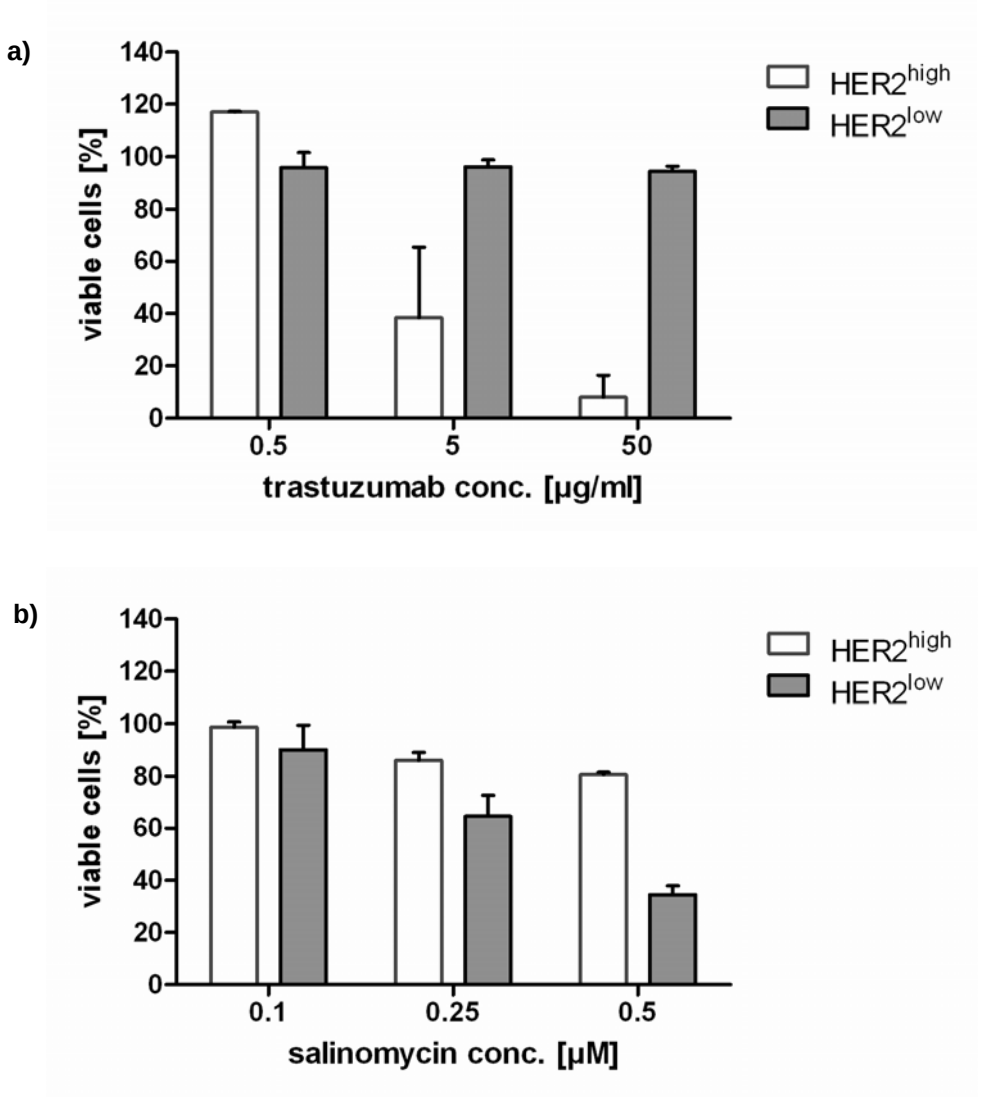

c)

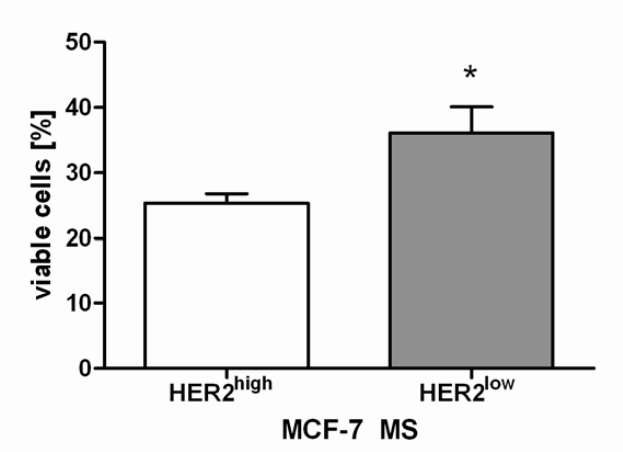

Figure 25. Specific treatments of sorted populations. (a) $HER2^{high}$ and $HER2^{low}$ sorted cell populations of MCF-7 mammospheres were treated with trastuzumab (0.5µg/ml, 5µg/ml and 50µg/ml) for 7d. A cell viability assay was performed subsequently. (b) $HER2^{high}$ and $HER2^{low}$ sorted cell populations of MCF-7 mammospheres were treated with salinomycin (0.5µM, 0.25µM, 0.1µM) for 7 days. A cell viability assay was performed subsequently. (c) Sorted $HER2^{low}$ and $HER2^{high}$ cells from 7 day old MCF-7 mammospheres were treated with 1µM doxorubicin for 72 hrs. Cell viability was performed. All set of experiments were performed in triplicates (n=3). Student's t test is performed to determine the significance (* P-values <0.05).

Furthermore, to confirm the effect of salinomycin on cancer stem cells, quantification of SOX2 positive population was performed by flow cytometric analysis of MCF-7 mammospheres were treated with salinomycin demonstrated decrease in SOX2 positive fraction as compared mock treated (DMSO) and trastuzumab treated cells from mammospheres. These findings further verify the specific effect of salinomycin against cancer stem cells. On the contrary, trastuzumab treated cells showed an upregulation or equal expression of these markers (Figure 26 a and b).

After manifesting the specific targeting of these two populations from mammospheres, the effect of combinatorial treatment of these two drugs on mammospheres was investigated. Treatment of MCF-7 mammospheres with a combination of trastuzumab and salinomycin demonstrated more cell death as compared to single treatments (Figure 27 a).

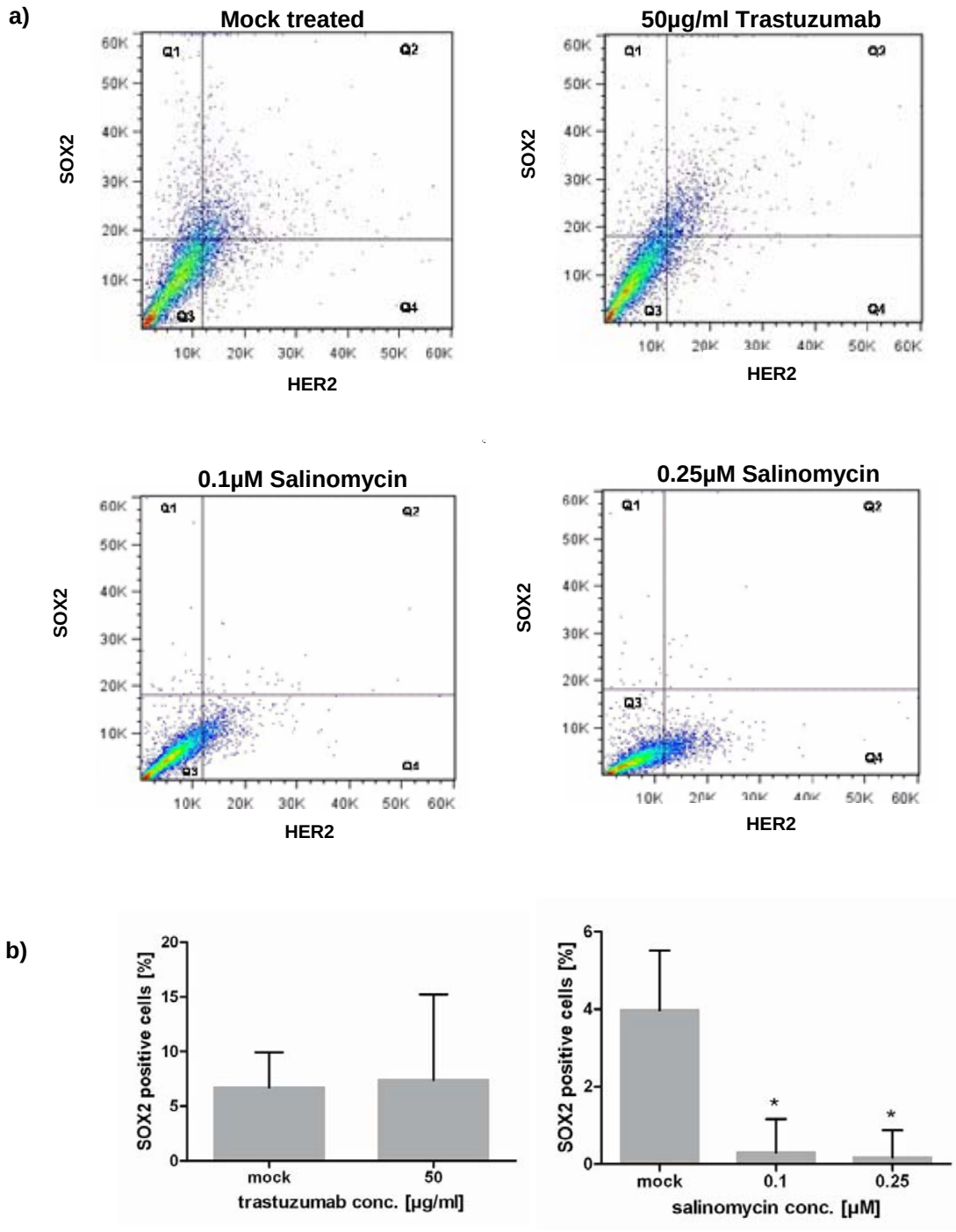

Figure 26. FACS analysis of SOX2 in MCF-7 mammospheres after treatment with trastuzumab and salinomycin. (a) FACS analysis of marker SOX2 (Cy5 tagged secondary antibody) and HER2 (Al-488 tagged secondary antibody) for mock treated (DMSO treated), trastuzumab treated (50µg/ml) and salinomycin treated (0.1µM and 0.25µM) MCF-7 mammosphere. Treatment was performed for 7 days and experiment was done in triplicates (n=3). (b) Quantification of SOX2 positive fraction (Q1) is shown in the bar graph. *Student's t test is performed to determine the significance (* P-values <0.05).*

To open up the scope of study, mammospheres of high HER2 expressing cell lines BT-474 and SKBR-3 were treated in the similar manner. The combination manifested significantly greater effect than single treatments in mammospheres of BT-474 but not in SKBR-3 where a higher dose of trastuzumab would be required for the same (Figure 27 b and c). As expected, no significant increase in cell death was observed in the HER2 negative cell line MDA MB-231 treated with trastuzumab and salinomycin individually and in combination (Figure 27 d). This data supports a novel treatment approach for HER2-positive tumors, which may constitute cancer stem cells in the $HER2^{low}$ fraction which are showing resistance to trastuzumab treatment.

a) MCF-7 MS

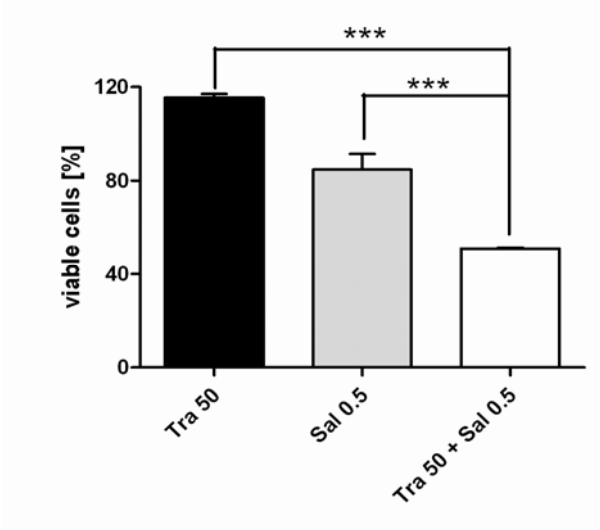

b) BT-474 MS

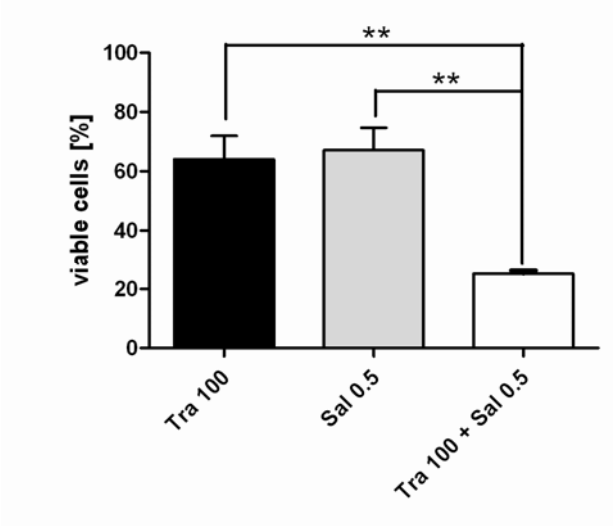

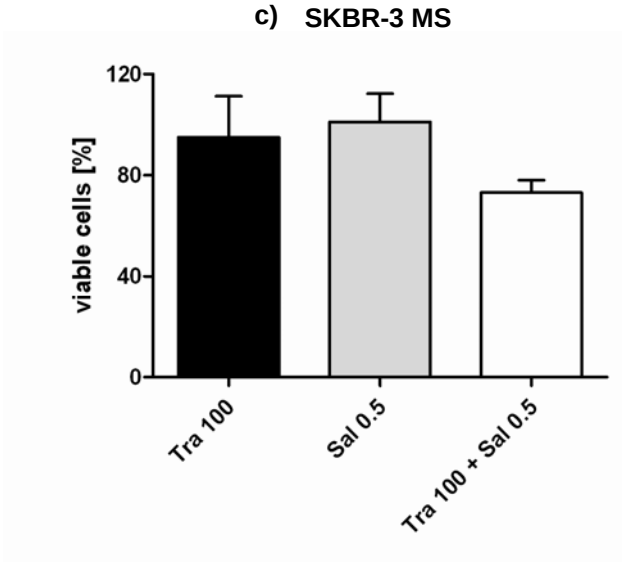

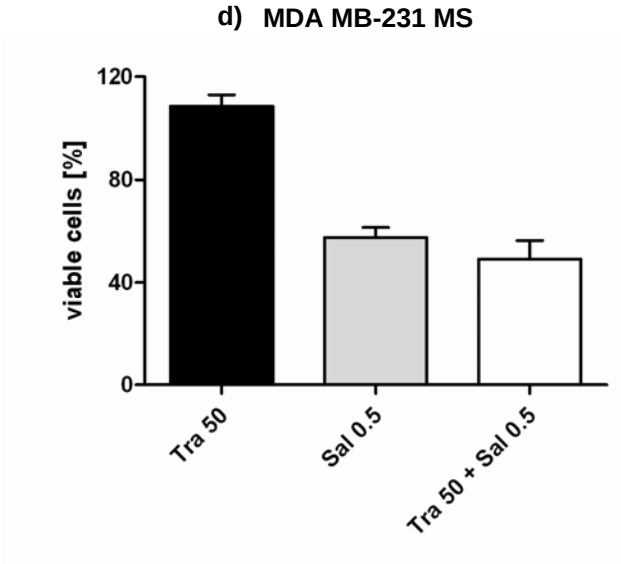

Figure 27. Combinatorial treatment of mammospheres. (a) Cell viability assay of MCF-7 mammospheres was performed after treatment with 50µg/ml trastuzumab and 0.5µM salinomycin individually and in combination. (b) and (c) BT-474 and SKBR-3 mammospheres were treated with 100µg/ml trastuzumab, 0.5µM salinomycin individually and in combination followed by cell viability assay. (d) MDA MB-231 mammospheres were treated with 50µg/ml trastuzumab, 0.5µM salinomycin individually and in combination. Cell viability assay was performed to determine the effect. Tra represents trastuzumab treatment and Sal represents salinomycin treatment. All experiments were performed in triplicates (n=3). Student's t test is performed to determine the significance (*** P-values <0.001, ** P-values <0.01, * P-values <0.05).

3.5 Salinomycin abates migration of mesenchymal-like breast cancer cells

The discovery of salinomycin is based on a screen. Gupta *et al.* knocked down E-cadherin from human mammary epithelial cells hence obtaining a cell type showing upregulation of vimentin. From the vimentin positive cells they further isolated CD44 positive cells as cancer stem cells and a screen of several drugs was performed. Salinomycin was one of the drugs that showed maximum effect against this cancer stem cell population [110]. Furthermore, Basu et al. showed in their study the efficacy of salinomycin on E-cadherin low/ vimentin positive mesenchymal-like cell population [125]. Hence in the current work the effect of salinomycin on the breast cancer cells showing mesenchymal traits was analyzed. To establish this study the epithelial cell line MCF-7 and the mesenchymal-like cell line MDA MB-436 were exploited. As expected classical chemotherapeutics like doxorubicin and paclitaxel were more effective against the epithelial cell line MCF-7 than against the mesenchymal MDA MB-436 (Figure 28 a and b). Likewise, MCF-7 was resistant and mesenchymal-like cell line MDA MB-436 was sensitive to salinomycin (Figure 28 c).

a)

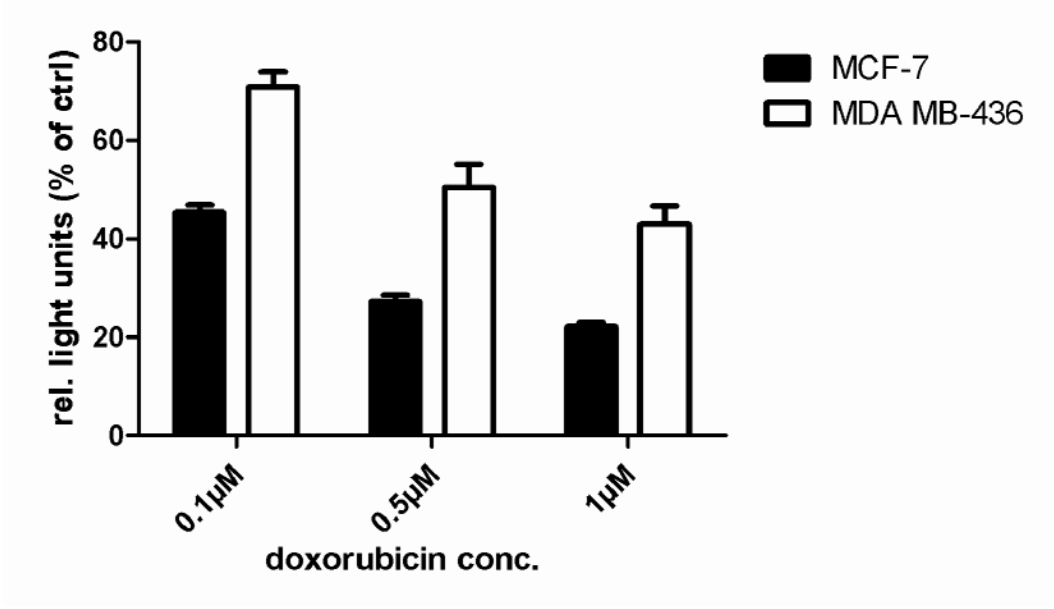

b)

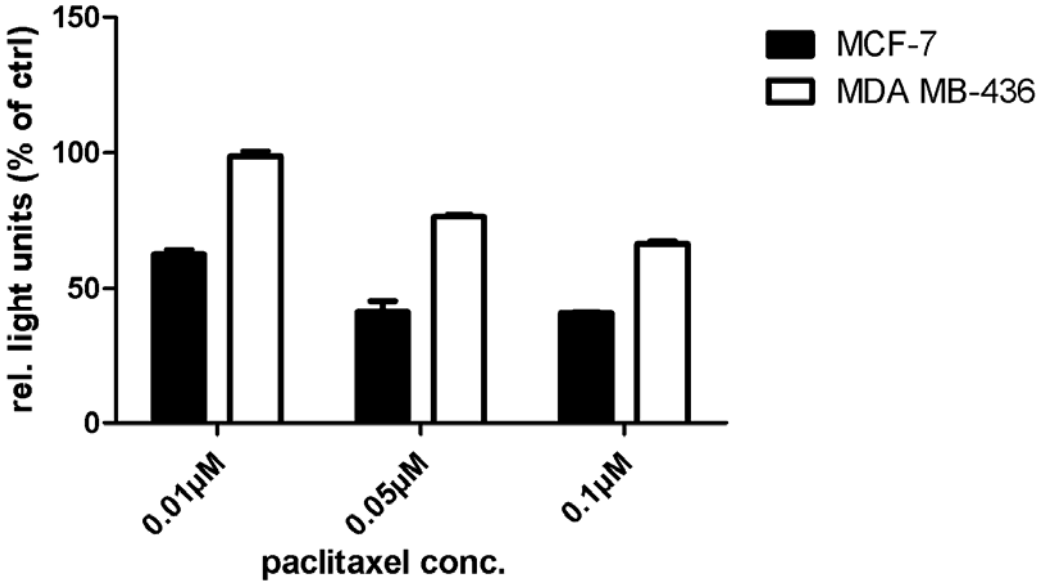

c)

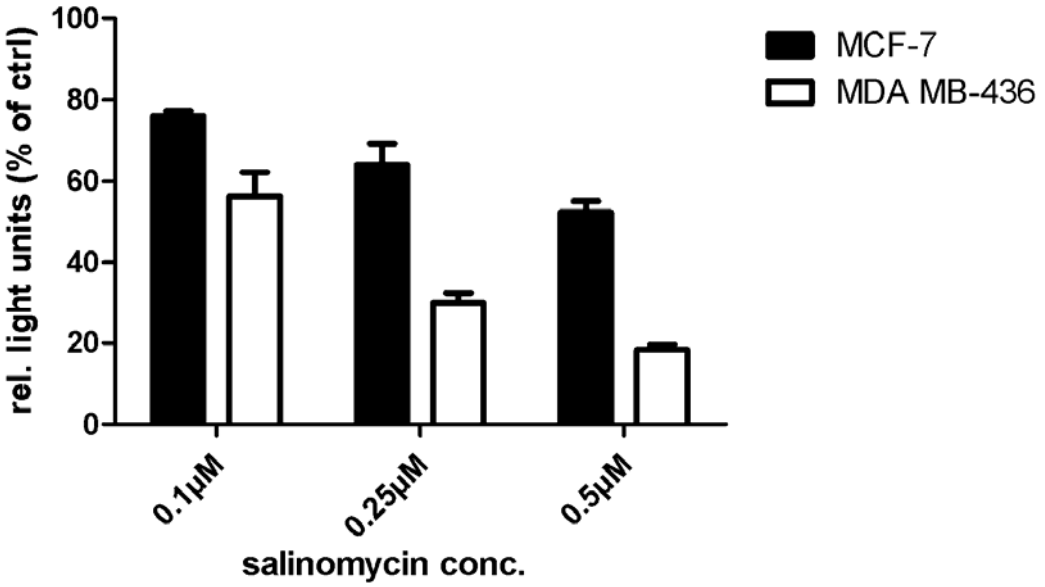

Figure 28. Effect of chemotherapeutics on breast cancer cell lines. (a) Effect of doxorubicin on MCF-7 and MDA MB-436. Treatment was performed for 72 hrs followed by cell viability assay. (b) and (c) Effect of paclitaxel and salinomycin respectively on MCF-7 and MDA MB-436. Treatment was performed for 72 h followed by cell viability assay. Experiment was performed in triplicates (n=3).

Since salinomycin demonstrated the elimination of mesenchymal-like cell line, it was intriguing for us to investigate its effect on migration of these cells which is one of the hallmarks of epithelial to mesenchymal transition (EMT). A scratch assay of MDA

MB-436 cells was performed with or without doxorubicin/ salinomycin. For this assay, concentrations of doxorubicin and salinomycin displaying similar percentage of cell death (15-20% apoptosis) were selected (Figure 29 a). Selecting these concentrations enabled to confirm that the effect on migration of cells was specific and not due to cell death. Figure 29 b displays the results after 0 h and 72 h of treatment. As expected the untreated sample showed migration of cells into the wound leading to wound closure. On the other hand doxorubicin treated cells also showed almost similar migration to untreated ones hence demonstrating induction of aggressiveness after treatment with doxorubicin. On the contrary, salinomycin treated cells showed no or negligible migration of cells leaving the wound open. Furthermore, calculation of the velocities of cells from the three samples showed significant reduction in velocities of cells treated with salinomycin as compared to untreated and doxorubicin treated cells (Figure 29 c). The distance accumulated by cells treated with salinomycin was also significantly reduced as compared to untreated and doxorubicin treated cells (Figure 29 d).

a)

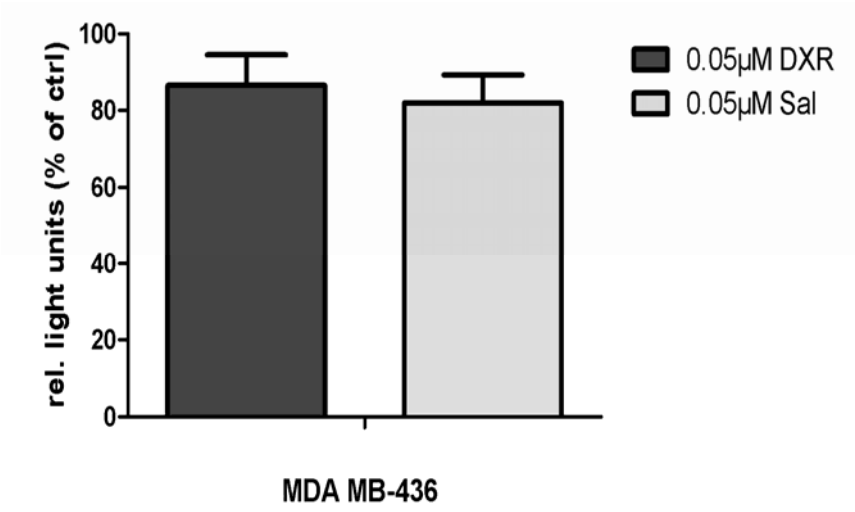

b)

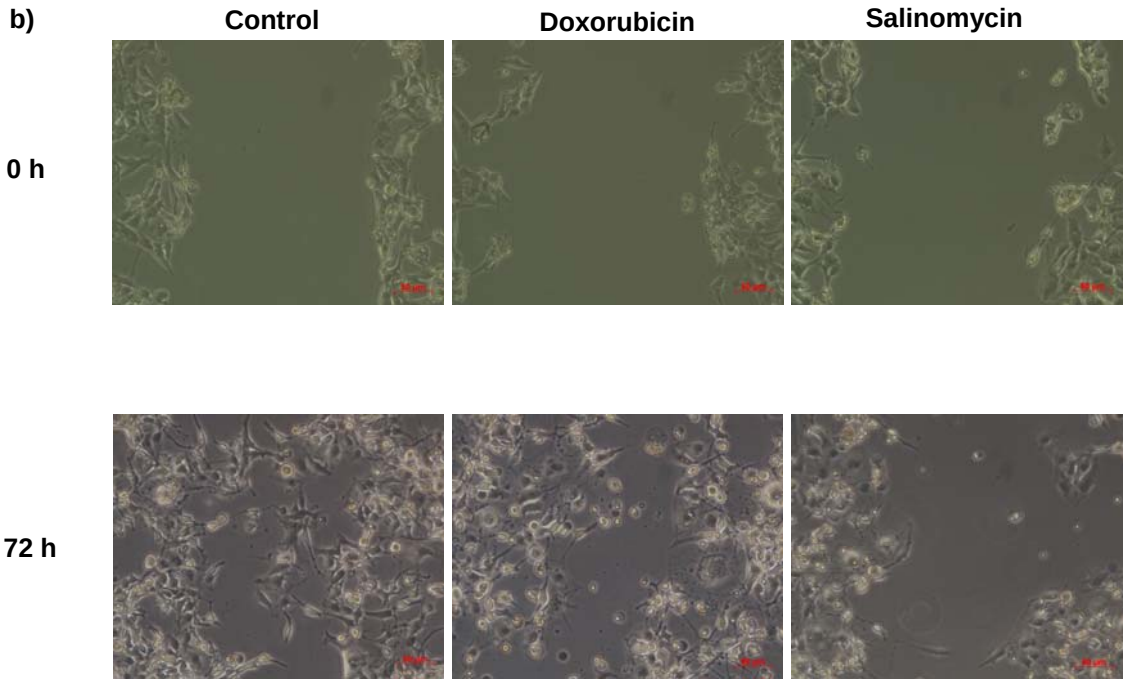
Control
Doxorubicin
Salinomycin
0 h
72 h

c)

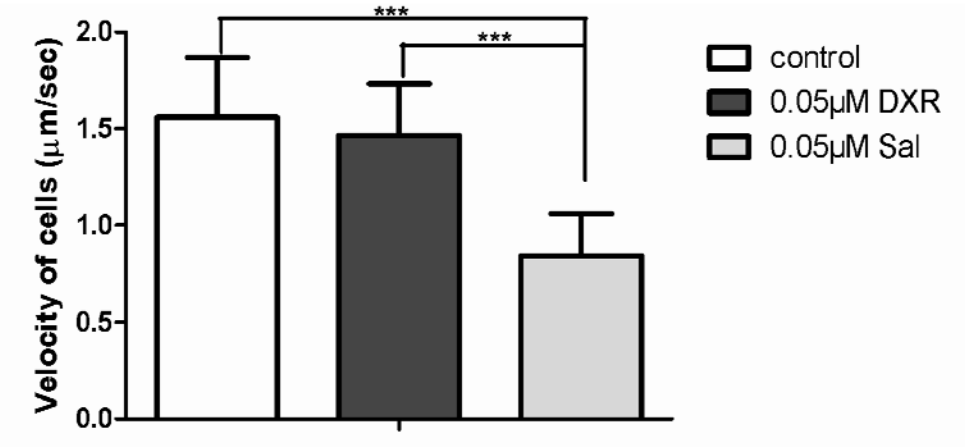
***
***
2.0
1.5
1.0
0.5
0.0
Velocity of cells (μm/sec)
control
0.05μM DXR
0.05μM Sal

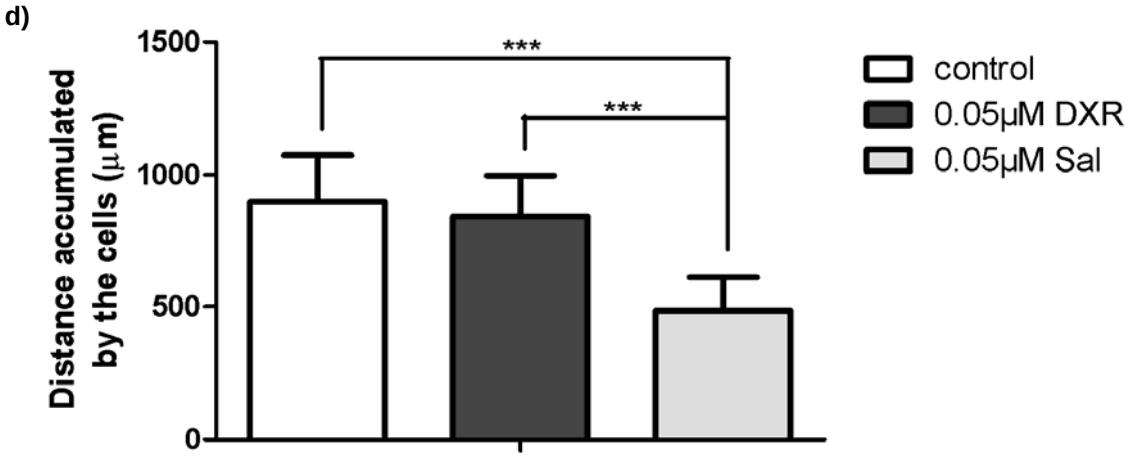

Figure 29. Effect of chemotherapeutics migration of MDA MB-436 cells (scratch assay). (a) Cell viability of MDA MB-436 was performed for 72 hrs and concentrations of doxorubicin and salinomycin showing 15-20% apoptosis/cell death after 72 h were selected for scratch assay. (b) Phase contrast images of MDA MB-436 cells treated with doxorubicin (DXR) and salinomycin (Sal). An untreated set was also kept as control. Samples were treated immediately after a scratch was made and images were taken every 6 hrs. Images of 0 h and 72 h are shown here. A section of 50μm is shown. (c) velocity of 20 random cells (n=20) each sample was calculated. (d) Distance accumulated by 20 random cells/sample (n=20) was also calculated. Student's t test is performed to determine the significance (*** P-values <0.001).

To confirm this observation, a transwell migration assay with MDA MB-436 was performed with or without doxorubicin/ salinomycin treatment. The concentrations of doxorubicin and salinomycin showing 10-15% of apoptosis or cell death in 18 h were selected for this assay for similar reasons mentioned in above paragraph (Figure 30 a). As expected, cells treated with salinomycin showed significantly reduced transwell migration as compared to doxorubicin treated and untreated cells (Figure 30 b).

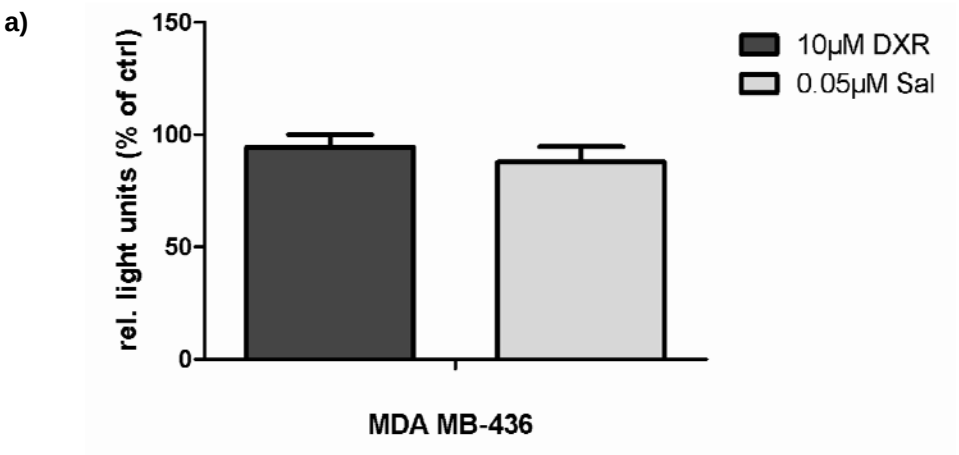

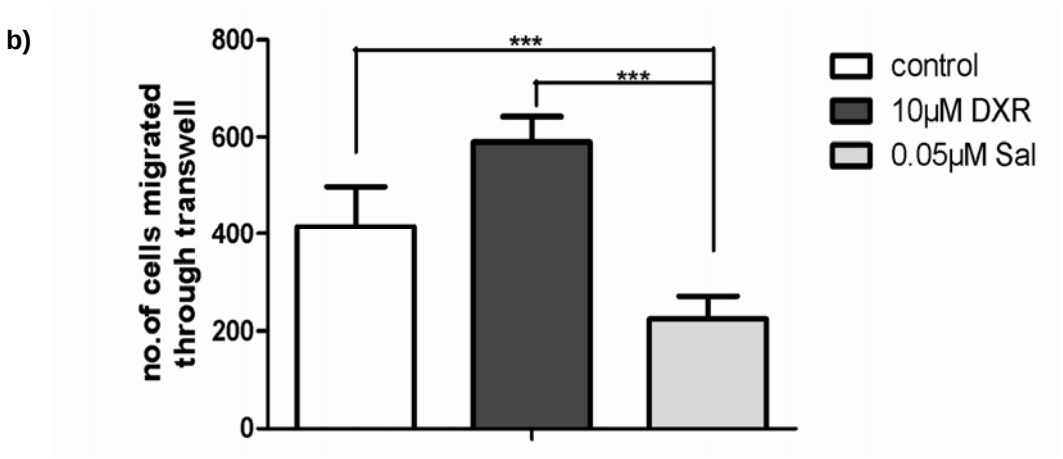

Figure 30. Effect of chemotherapeutics on the migration of MDA MB-436 cells in transwell assay. (a) Cell viability of MDA MB-436 was performed for 72 hrs and concentrations of doxorubicin and salinomycin showing 15-20% apoptosis/cell death after 18 hrs were selected for transwell migration assay. (b) A quantification of number of cells migrated through the transwell after treatment for 18 hrs is shown here. Experiment was performed in triplicates (n=3). Total 15 fields/ transwell were counted. Student's t test is performed to determine the significance (*** P-values <0.001).

Early stages of metastasis demonstrate the phenomenon of EMT that gives rise to mesenchymal-like migrating cells hence configuring a heterogeneous tumor. Since this heterogeneous tumor consist of both epithelial cells and mesenchymal-like cells, it is necessary to target both the population for complete eradication. The results till now display effective targeting of epithelial cells by classical chemotherapeutics like doxorubicin and mesenchymal-like cells by salinomycin. Therefore, the effectiveness of combination of both drugs in treatment of heterogeneous tumors was tested. An establishment of an artificial heterogeneous system was done for this study by mixing epithelial MCF-7 cells and mesenchymal-like MDA MB-436 cells in 1:1 ratio. Figure 31 a shows a phase contrast image displaying both epithelial and mesenchymal morphologies in mixed culture. Red arrows show epithelial like morphology and white arrows demonstrate mesenchymal-like morphology. The samples were further stained for E-cadherin as well as vimentin. Figure 31 b shows presence of both E-cadherin as well as vimentin positive cells in the mixed culture further confirming the heterogeneity.

a)

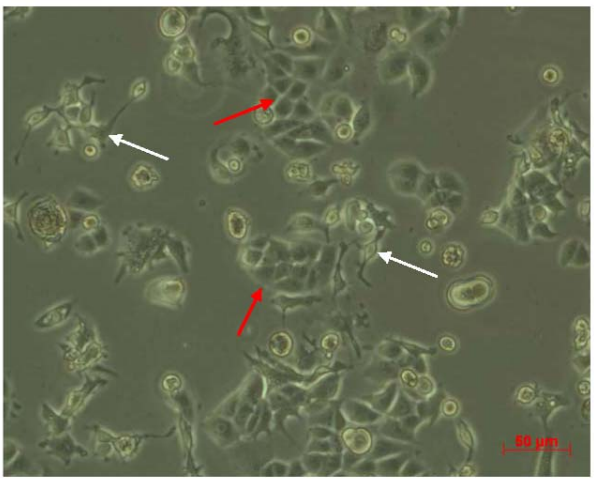

b)

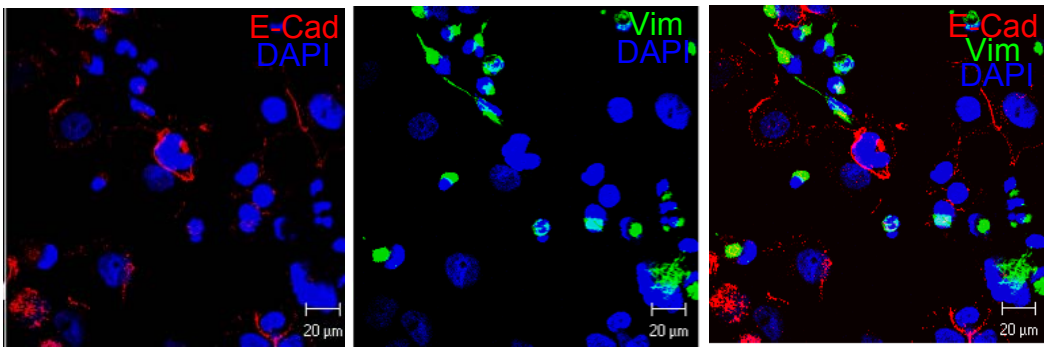

Figure 31. Mixed culture of breast cancer cell lines to mimic early metastatic breast cancer model. (a) Phase contrast microscopic image of MCF-7 and MDA MB-436 cells mixed in 1:1 ratio. Red arrows display epithelial-like morphology and white arrows demonstrate mesenchymal-like morphology. A section of 50µm is shown here. (b) Laser scanning microscopic image of the mixed culture stained for E-cadherin (red) and vimentin (green). Nucleus is stained with DAPI (blue). A section of 20µm is shown here.

Afterwards the effect of chemotherapeutics doxorubicin and salinomycin (individually or in combination) was tested on the established heterogeneous tumor mimic. According to results of Figure 32, there is a significant reduction in number of the cells treated with combination of the two drugs as compared to control, doxorubicin treated and salinomycin treated samples. Hence, the results show synergistic effect of the combination in treating the mimic of metastatic tumor as compared to the single drug treatment. These results open up a new direction for treatment of early metastatic heterogeneous breast cancers.

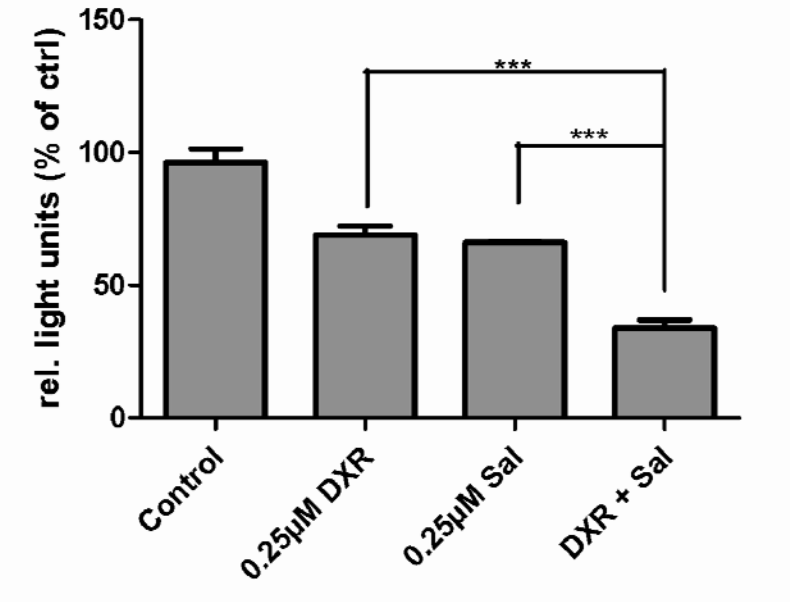

Figure 32 Combinatorial treatment of mimic of early metastatic breast cancer model. (a) As a control MCF-7 and MDA MB-436 cells were treated with doxorubicin (DXR) and salinomycin (Sal) individually or in combination for 72 h and individual drugs. Concentration of drugs showing 20-25% cell death was selected. (b) The mixture of MCF-7 and MDA MB-436 cells discussed above was treated with doxorubicin (DXR) and salinomycin (Sal) individually or in combination for 72 h followed by cell viability assay. Experiment was performed in triplicates. *Student's t test is performed to determine the significance (*** P-values <0.001).*

4. DISCUSSION

4.1 Treatment of breast cancer cell lines with classical chemotherapeutics eventually generates chemoresistance

Resistance to current chemotherapeutic agents account for the failure of the treatment in more than 90% of the patients especially with metastatic cancers [39]. Once the treatment with anthracycline or taxane-based chemotherapy is performed, options are limited as the responses are generally low. Response rates generally range from 30% to 70% but the responses are often not durable, with 6 to 10 months as the time taken for progression [126,127]. This resistance can be innate one i.e. the cells are resistant to the drugs prior to the treatment or it can be acquired over time [128]. A number of mechanisms lead to the chemoresistance. Few are the alterations in the drug pharmacokinetics and metabolism, modification in the genes and protein expressions e.g. overexpression of β-tubulin isotypes, and topoisomerase II mutations, drug compartmentalization in the cellular organelles, altered repair of drug induced DNA damage, changes in the apoptotic signaling pathways (for example, mutated p53), and expression of proteins directly affecting cellular drug transport (efflux pumps) [129,130]. The heterogeneity of the cancer cells, coupled with their high mutation rate, contributes to rapid selection for the drug-resistant clones. To characterize this resistance, a 'molecular evolution assay' (MEA) was developed and utilized in this study (Figure 7). Breast cancer cell lines were treated with the classical chemotherapeutic doxorubicin in cycles. Cell resistant to doxorubicin were allowed to recover and were characterized. This assay aided in characterizing and monitoring the changes in the resistant cells at molecular levels hence characterizing the resistance. A subsequent resistance acquisition over the rounds of MEA was observed along with increase in ABC transporters indicated by side population (Figure 8 and 9). These observations over the course of the cell resistance to doxorubicin are in line with the studies showing involvement of ABC transporter proteins to pump out drugs like doxorubicin hence escaping the treatment [131-133].
Furthermore, mammosphere generating ability of cells recovered from each round of MEA was analyzed. Only cells from R1 and R2 could form mammospheres with a

decreasing potential over the passages. The study by Dittmer *et al*. showed disruption of the intact spheroid structure after the introduction of human mesenchymal stem cells in MCF-7 mammospheres. Additionally, an increase in invasive properties of the cells was observed [134]. Therefore, decrease in MFP could be correlated with the probable increase in invasive properties of resistant cells obtained over the rounds of MEA (Figure 10).

This study demonstrates that the inheritance of chemoresistance is a gradual and eventual process. After exposure to stressful environment e.g. chemotherapeutics, genetically instable cancer cells undergo certain changes that could lead to more aggressive phenotype.

4.2 Heterogeneity and chemoresistance in breast cancer can be explored utilizing mammospheres

Anchorage independent spheroids grown in serum-free media procure the property of heterogeneity and are utilized extensively to study different populations within tumors and enrich the stem cell-like cell population [135-137]. Many studies have shown the association of different markers with different populations in mammospheres proving their heterogeneity. Furthermore, dependency of some cells from mammospheres on extra cellular matrix (ECM) proteins for acquiring 3 dimensional forms further points towards the heterogeneity displayed by spheroid cultures [115]. Similarly, the results of Figure 11 show mammospheres of breast cancer cell lines procuring different morphologies. More aggressive and metastatic cell lines like MDA MB-231, MDA MB-468, MDA MB-435 etc. showed aggregate like appearance of mammospheres. On the other hand, MCF-7 and BT-474 that are epithelial cells displayed tight spheroids. One explanation for this observation could be tight cell-cell contacts due to expression of E-cadherin protein in epithelial cells. This protein is responsible for strong cell-cell interactions hence giving rise to tight spheroids. On the other hand, invasive and metastatic cell line loose the expression of E-cadherin and hence are unable to form tight spheroids and in turn exhibit aggregates [121,122]. Likewise, the results also establish decreasing mammosphere forming potential displayed by invasive and metastatic cell lines as compared to epithelial ones that retain more or less constant MFP (Figure 12). The only exception is MDA MB-435

that shows increasing MFP which can be explained by presence of lectins and antigens required for cell-stromal adhesion and promoting tumor growth and progression [138].

Moreover a coalition between stem cell markers namely CD44+, ALDH1+, MUC1 etc. and mammospheres have been revealed [78,83,90,91]. In support to this finding, the results of figure13 revealed an elevation in NANOG, OCT 4 and SOX 2 levels. Since, the presence of the stem cell-like population in the tumor leads to chemoresistance, the effect of classical chemotherapeutics on mammospheres was analyzed. The results in Figure 14 clarifies that mammospheres acquire the property of chemoresistance along with enrichment of stem cell-like cells. Furthermore, based on the results showing acquisition of stem cell markers and chemoresistance in mammospheres over a period of 7 days, a model to explain involvement of stem cell like cells in resistance can be put forward (Figure 33).

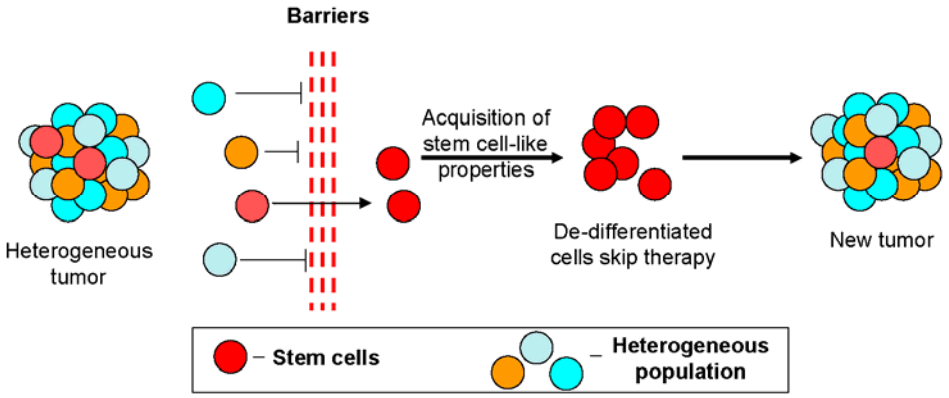

Figure 33. Model depicting dedifferentiation of cells after chemotherapy. This model demonstrates acquisition of stem cell-like properties by cells in tumor after they are exposed to certain barriers as chemotherapy. These dedifferentiated cells then skip therapy and give rise to new tumors.

4.3 HER2 protein is elevated in mammospheres

The EGFR family is one of the receptor tyrosine kinase families involved in the chemoresistance [139]. Additionally, the difference between molecular signalling of HER2 protein in 2D cells as well as in mammospheres shows the flexibility of oncogene switching, which may play an important role in the development of drug resistance [123]. Likewise, in this study elevated HER2 protein levels in mammospheres and xenografts from mammospheres injected in female immunodeficient mice was demonstrated compared to 2D cell lines and xenografts from 2D cells (Figure 15). Additionally, there was a differential expression of HER2 within individual cells of mammospheres, which made it possible to sort for $HER2^{high}$ and $HER2^{low}$ populations.

Furthermore, not all the mechanisms leading to resistance and the cancer progression are explored till date. Being a multistep complex phenomenon, a number of procedures are available for the detection of cancer progression. For this purpose, studies with the 3 dimensional culture systems are extensively used to understand pathways regulating glandular morphogenesis and the epithelial cancer development [140]. For the formation of these 3D anchorage independent spheroids, the cells must acquire anoikis resistance. Anoikis resistance is associated with many factors and its association with HER2 over expression is the latest highlight [141]. HER2 mediated anoikis resistance can be correlated with increased Erk activation and decreased pro apoptotic protein Bim expression [142]. Besides, a recent study demonstrated that integrin α5 is highly upregulated in the HER2 overexpressing 3D spheroids and is required for HER2 mediated anoikis resistance [124]. Likewise, results of Figure 18 demonstrate nearly 3-fold more mammospheres at passage 0 in $HER2^{high}$ sorted population from MCF-7 as compared to $HER2^{low}$ sorted cells that eventually showed decrease in MFP till passage 2. This data displays succumbing of $HER2^{low}$ cells to anoikis hence strongly indicating involvement of HER2 in anoikis resistance and formation of mammospheres. HER2 over expression in the spheroids and its association with anoikis resistance makes it a key player in detection of circulating tumors cells (CTCs) [143-146]**.** Additionally, the interconnection between HER2 overexpression and autophagy provides a perfect environment to circumvent trastuzumab therapy hence giving rise to therapy resistance [147].

4.4 Combinatorial treatment with salinomycin and trastuzumab eradicates cancer stem cells and HER2 positive cells of mammospheres

20-25% of the breast cancers show amplification of HER2 protein and this genomic alteration is predictive of a poor clinical outcome [54,148]. This overexpression leads to the cancer progression, aggressiveness and chemoresistance in breast cancers [149]. Moreover, HER2 amplification results in 50-100 fold increase in the receptors on the cancer cells as compared to normal cells therefore making it a prime target for therapies [150]. Trastuzumab (Herceptin) is a humanized recombinant monoclonal antibody establishing a significant clinical treatment against HER2 positive breast cancers [151]. Moreover, the primary adjuvant therapy for the HER2 positive cancers is treatment with trastuzumab which targets HER2. Although it is one of the most effective treatments in oncology, a significant number of patients show resistance to this treatment [59,152].

Furthermore, a new concept of drug resistance is coming in limelight that describes affiliation of cancer stem cells or stem cell-like cells to chemoresistance. Studies show that the cancer stem cells from leukemia displayed the resistance to duanorubicin and Ara-C [153]. Similarly cancer stem cells from breast, pancreas and colon cancer also show resistance to chemotherapeutics [68,154,155]. These findings indicate that the selection barriers conferring dedifferentiation of cells and heterogeneity of the tumors pave a way for escaping therapies. Hence, targeting cancer stem cells and subpopulations manifesting therapy resistance will achieve definitive curative benefits. Korkaya *et al.* in their study, revealed a correlation between HER2 gene amplification and the upregulation of stem cell markers [90]. Moreover, a similar study displays effective targeting of tumor initiating cells (TICs) utilizing trastuzumab antibody [106]. Since cancer stem cells or dedifferentiated cells are the future targets for effective therapies, elucidation of the cancer stem cell population from mammospheres was performed in this study. Figure 19 displays upregulation of stem cell markers in $HER2^{low}$ immunosorted population as compared to $HER2^{high}$ population. Comparison of this upregulation in 2D MCF-7 cells, 24 hrs old MCF-7 mammospheres and 7 days old mammospheres indicates a time dependent increase in stem cell markers in the $HER2^{low}$ population. This observation suggests an acquisition of stem cell like properties eventually over the time hence indicating a dedifferentiation process. Likewise, the results in Figures 20 and 21 confirm the stem cell like behavior of $HER2^{low}$ cells. Furthermore, the tissue sections

of the xenografts from female immunodeficient mice developed from injection of $HER2^{low}$ cells showed augmented expression of NANOG, OCT4 and SOX2 as compared to xenografts of $HER2^{high}$ (Figure 23 and 24). Moreover, a recent study depicted that sorted $CD44^{high}/CD24^{low}$ cells that are regarded as the stem cell fraction of the immunoselected MCF-7 cell line are enriched in $HER2^{low}$ cells. This also supports the fact that MCF-7 contains a cancer stem cell fraction that displays reduced HER2 expression [156]. A recent study indicates the possibility of heterogeneous HER2 amplified tumors harbouring the $HER2^{low}$ CSCs [157]. Hence, eradication of HER2 positive cells by trastuzumab could give rise to cancer stem cells expressing low or no HER2. Our finding therefore might explain the resistance of some HER2 positive tumors to trastuzumab therapies leading to poor prognosis in relapsed patients.

One step forward in the treatment of the cancer stem cells was the discovery of salinomycin that significantly reduces cell viability of human breast cancer stem-cell-like cells resistant to chemotherapeutic drugs such as paclitaxel, doxorubicin, actinomycin D and campthotecin [110]. One of the most common mechanisms of the drug resistance by CSC is overexpression of ABC transporters. Salinomycin can overcome this ABC transporter mediated therapy and apoptosis resistance in human leukemia and breast cancer stem cell-like cells [158,159]. The data in Figure 25 and 26 supports the above findings. $HER2^{high}$ cells display resistance to salinomycin but as expected are susceptible to trastuzumab. On the other hand, $HER2^{low}$ cells i.e. stem cells that are resistant to trastuzumab could be targeted using salinomycin. Salinomycin also effectively reduced the SOX2 positive stem cell population from MCF-7 mammospheres supporting the specific targeting of cancer stem cells. Since specific targeting of two populations of mammospheres using trastuzumab and salinomycin individually was successful, it was intriguing to check the combinatorial treatment of these two drugs. The results of Figure 27 suggest an additive or synergistic effect of the combination trastuzumab and salinomycin in eradicating most of the cells from mammospheres.

Keeping in mind that in past two decades more than 30 new anticancer drugs have been introduced, but survival rates have improved only marginally for many types of cancers including breast cancer, it is necessary to formulate new and efficient strategies of treatment [160]. To explore this field, a novel combinatorial treatment method that targets most of the cells of heterogeneous mammospheres is

demonstrated for the first time in this thesis (Figure 34). Hence, the results of *in vitro* experiments open up a new horizon for combinatorial therapy eradicating most of the cells and can be considered as a baseline to develop novel treatment strategies targeting different heterogeneous cell populations in breast tumors.

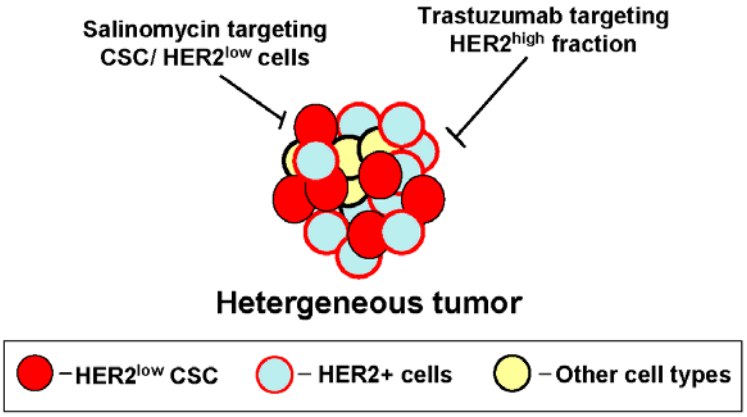

Figure 34. Combinatorial treatment of mammospheres. This model shows a novel combinatorial treatment strategy targeting HER2^{low} or cancer stem cells with salinomycin and HER2^{high} population utiling trastuzumab.

4.5 Salinomycin reduces migration and targets mesenchymal-like cell population of breast cancer cell lines

The results from the previous section showed a potential of salinomycin in targeting the cancer stem cell population from mammospheres. Recently Basu *et al.* gave a new dimension to salinomycin treatment as they established its efficacy against mesenchymal-like cells from head and neck squamous cell carcinoma. These cells expressed vimentin and were E-cadherin low hence suggesting a new target population for salinomycin [125]. Additionally, a recent publication determined potential of salinomycin as an antagonist to wnt signalling pathway, a key player in stem cell signalling and metastasis [161]. Therefore, we scrutinized the effect of salinomycin on breast cancer cells that have undergone EMT and hence are an inherent cause of metastasis. Our results in Figure 29 denote the escape of mesenchymal-like MDA MB-436 cells from classical chemotherapeutic treatment which, in turn affects

epithelial cells MCF-7. On the other hand, salinomycin effectively targets mesenchymal-like cells.

The effect of salinomycin on mesenchymal-like population of breast cancer provoked to check its efficacy in targeting one of the hallmarks of the process of EMT i.e. migration of the mesenchymal cells. In fact, salinomycin affected the migration of cells as compared to doxorubicin treated and untreated MDA MB-436 cells. Furthermore, salinomycin also reduced the velocity of migrating mesenchymal–like cells. On the other hand, doxorubicin that is frequently used clinical drug to treat breast cancer showed no significant effect against migration. Moreover, the migration of the cells treated with doxorubicin was equivalent to the migration of the cells in untreated sample (Figure 29 and 30). These results are in accordance with a recent paper that shows treatment with salinomycin induces the E-cadherin expression in prostrate cancer cells and reduces their transwell migration [112]. This data suggest that treatment of metastatic breast cancers with classical chemotherapeutic will not efficiently target the mesenchymal-like migrating cells causing metastasis but in turn will enhance the process. The migrating cells should be targeted for a complete cure and hence salinomycin could be used as a novel drug for treating the same.

Furthermore, the metastatic tumor undergoes certain physiological changes and the key player in triggering this process is EMT. Consequently, this tumor comprises epithelial cells as well as mesenchymal-like cells. To mimic this condition, a mixture of MCF-7 cells and MDA MB-436 cells was performed in a 1:1 ratio. Since the classical chemotherapeutics target epithelial cells and salinomycin targets mesenchymal-like cells, a combination of both drugs is expected to augment the effect and kill most of the tumor cells. The results in Figure 32 manifest the same. The *in vitro* data of this section, exhibits a new and novel combinatorial treatment to target metastatic breast tumors consisting of epithelial as well as mesenchymal cells (Figure 35). These results pave a gateway for *in vivo* and clinical studies utilizing salinomycin as one of the drugs for combinatorial treatment.

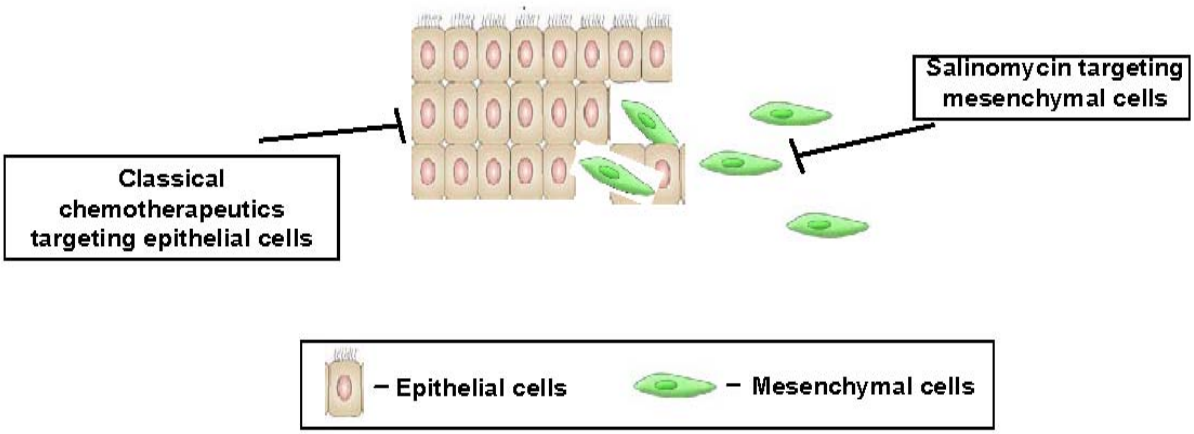

Figure 35. Model depicting combinatorial treatment of early metastatic breast cancer cells. This model puts forward a combinatorial treatment of metastatic breast tumors. Salinomycin targets the mesenchymal-like cells from the metastasizing tumors and epithelial cells are targeted by classical chemotherapeutics like doxorubicin.

5. SUMMARY

One of the reasons for the chemoresistance of breast tumors could be their great degree of heterogeneity as they are composed of various histological subtypes, have variable clinical manifestations and underlying molecular signatures. Cancer cells surviving the therapy and giving rise to new tumors also comprise of dedifferentiated cells or cancer stem cells with a more aggressive phenotype. The persistence of tumorigenic cancer stem cells in locally invasive and metastatic cancer is responsible for the relapse of the disease. Since most of the chemotherapeutics used now-a-days target more differentiated and proliferating population, there is a need to discover and design novel improved treatment strategies targeting aggressive tumor initiating subpopulation.

This study characterized the evolution of resistance to classical chemotherapeutics in breast cancer cell lines with respect to their chemosensitivity, upregulation of stem cell markers, mammosphere formation and side population characteristics. Furthermore, analysis of 3 dimensional cultures (mammospheres) confirmed the involvement of heterogeneity and dedifferentiated cancer stem cells, in acquiring the resistance to classical therapies. Upregulaton and differential expression of receptor tyrosin kinase HER2 in mammospheres enabled the FACS sorting into $HER2^{high}$ and $HER2^{low}$ population. This in turn facilitated the identification of $HER2^{low}$ population as the cancer stem cell population showing resistance to classical trastuzumab (monoclonal antibody against HER2) treatment. Furthermore, $HER2^{low}$ cells remained unaffected to classical chemotherapeutic doxorubicin treatment suggesting their role in chemoresistance. However, eradication of this stem cell-like cell population was efficiently performed by the drug salinomycin. Its specificity was further verified by effective reduction the SOX2 (stem cell marker) subset after treatment of mammospheres. Additionally, the combination of two drugs trastuzumab targeting $HER2^{high}$ cells and salinomycin targeting $HER2^{low}$ cancer stem cells demonstrated abolishment of most of the tumorigenic cells from mammospheres.

Furthermore, effect of salinomycin on mesenchymal-like subset from beast cancer was also studied. The data demonstrate specific killing of epithelial cells by doxorubicin and mesenchymal-like cells using salinomycin. Besides, salinomycin also controlled the migration (one of the hallmarks of EMT) of mesenchymal-like cells. In contrast, doxorubicin treatment led to increased migration displaying a more

aggressive phenotype after treatment suggesting a reason for chemoresistance of metastatic tumors. Additionally, the combinatorial treatment of salinomycin and doxorubicin was superior to the individual treatment of an *in vitro* mimic of metastatic breast cancer.

To summarize, this study puts forward new approaches of combinatorial treatments eradicating the tumor initiating cells from the heterogenic breast tumor models (mammospheres and epithelial-mesenchymal cell mixture). It also demonstrates the effect of salinomycin as an eliminator of resistant tumor subpopulations *in vitro*. Furthermore, *in vivo* and clinical studies need to be performed to validate its specificity, toxicity and efficacy as a potential drug. Likewise, studies on dosage, specific targeting and less toxic analogues of salinomycin should be accomplished for its approval in clinical usage. However, these findings pave the way to novel therapeutic strategies targeting most of the cells from heterogeneous breast tumors.

6 APPENDIX

6.1 Appendix 1: Abbreviations

5FU	5- Fluorouracil
ADH	Atypical ductal hyperplasia
ALDH1	Aldehyde dehydrogenase 1
ALH	Atypical lobular hyperplasia
cDNA	Complementary DNA
CSCs	Cancer stem cells
CTCs	Circulating tumor cells
DAPI	4′,6-Diamidin-2-phenylindol
DCIS	Ductal carcinoma *in situ*
DDR1	Discoidin domain receptor 1
DMSO	Dimethyl sulfoxide
DNA	Deoxyribonucleic acid
DXR	Doxorubicin
ECM	Extra cellular matrix
EDTA	Ethylenediaminetetraacetic acid
EMT	Epithelial to mesenchymal transition
ER	Estrogen receptor
FACS	Fluorescent antibody cell sorter
FBS	Fetal bovine serum
GAPDH	Glyceraldehyde-3-phosphate dehydrogenase
HEPES	N-(2-hydroxyethyl) piperazine-N'-(2-ethansulfonic acid)
HER2	Human Epidermal growth factor receptor
IAP	Inhibitor of apoptosis protein
IBC	Inflammatory breast disease
IDC	Invasive ductal carcinoma
ILC	Invasive lobular carcinoma
LCIS	Lobular carcinoma *in situ*
LSM	Laser scanning microscope
MBC	Metastatic breast cancer

MEA	Molecular evolution assay
MET	Mesenchymal to epithelial transition
MFP	Mammosphere forming potential
mRNA	Messenger RNA
MS	Mammospheres
NOS	NANOG, OCT4, SOX2
P0, P1, P2	Passage 0, 1, 2
PCR	Polymerase chain reaction
PolyHEMA	Poly-2-hydroxyethyl methacrylate
R1, R2, R3, R4	Round 1, 2, 3, 4
RNA	Ribonucleic acid
ROS	Reactive oxygen species
RTKs	Receptor tyrosine kinases
Sal	Salinomycin
SP	Side population
Tax	Paclitaxel
Tra	Trastuzumab
VEGF	Vascular endothelial growth factor
XIAP	X-linked IAP

6.2 Appendix 2: Formulation of solutions

DMEM media for SP	DMEM + 2% FBS + 10mM HEPES
PBS solution for SP	1X PBS + 2% FBS + 10mM HEPES
Permeabilization solution	0.2% Triton X 100 in 1X PBS
Blocking solution	10% FCS + 1% Gelatin + 0.05% Triton X 100 in 1X PBS

6.3 Appendix 3: Publications

A. Poster Presentations

Prajakta S. Oak, Florian Kopp, Chitra Thakur, Joachim Ellwart, Ulf R. Rapp, Axel Ullrich, Ernst Wagner, Pjotr Knyazev and Andreas Roidl: *Salinomycin as an effective drug in combinatorial treatment of breast carcinoma.* ABSTRACT in **AACR special conference on "Advances in breast cancer research: Genetics, Biology and Clinical applications"**, 12-15 Oct 2011, San Francisco, CA, USA.

B. Publications

i) Prajakta S. Oak, Florian Kopp, Chitra Thakur, Joachim W. Ellwart, Ulf R. Rapp, Axel Ullrich, Ernst Wagner, Pjotr Knyazev and Andreas Roidl: *Combinatorial treatment of mammospheres with trastuzumab and salinomycin efficiently eradicates HER2-positive cancer cells and cancer stem cells.* **In Press.**

ii) Prajakta S. Oak, Florian Kopp, Chitra Thakur, Axel Ullrich, Pjotr Knyazev, Ulf R. Rapp, Ernst Wagner, Rajkumar Savai, and Andreas Roidl: *Treatment of salinomycin targets metastatic breast cancer cells and reduces their migration.* **In preparation.**

7. REFERENCES

1. Jemal, A.*, et al.* Global cancer statistics. *CA Cancer J Clin* **61**, 69-90 (2011).
2. Society, A.C. Cancer Facts & Figures 2011. *Atlanta: American Cancer Society*, 1-55 (2011).
3. Richie, R.C. & Swanson, J.O. Breast cancer: a review of the literature. *J Insur Med* **35**, 85-101 (2003).
4. Visvanathan, K. The challenges of treating lobular carcinoma in situ. *Oncology (Williston Park)* **25**, 1058, 1061, 1066 (2011).
5. Evans, W.P., Warren Burhenne, L.J., Laurie, L., O'Shaughnessy, K.F. & Castellino, R.A. Invasive lobular carcinoma of the breast: mammographic characteristics and computer-aided detection. *Radiology* **225**, 182-189 (2002).
6. Perou, C.M.*, et al.* Molecular portraits of human breast tumours. *Nature* **406**, 747-752 (2000).
7. Hu, Z.*, et al.* The molecular portraits of breast tumors are conserved across microarray platforms. *BMC Genomics* **7**, 96 (2006).
8. Sorlie, T.*, et al.* Gene expression patterns of breast carcinomas distinguish tumor subclasses with clinical implications. *Proceedings of the National Academy of Sciences of the United States of America* **98**, 10869-10874 (2001).
9. Schnitt, S.J. Classification and prognosis of invasive breast cancer: from morphology to molecular taxonomy. *Mod Pathol* **23 Suppl 2**, S60-64 (2010).
10. Lakhani, P.S.a.S.R. Recent Developments in the Molecular Pathology of Breast Cancer. *Breast cancer Connection*, 23-27 (2009).
11. Apantaku, L.M. Breast-conserving surgery for breast cancer. *Am Fam Physician* **66**, 2271-2278 (2002).
12. Fisher, B.*, et al.* Tamoxifen, radiation therapy, or both for prevention of ipsilateral breast tumor recurrence after lumpectomy in women with invasive breast cancers of one centimeter or less. *Journal of Clinical Oncology* **20**, 4141-4149 (2002).
13. Boughey, J.C., Buzdar, A.U. & Hunt, K.K. Recent advances in the hormonal treatment of breast cancer. *Curr Probl Surg* **45**, 13-55 (2008).
14. Mukai, H. Targeted therapy in breast cancer: current status and future directions. *Jpn J Clin Oncol* **40**, 711-716 (2010).
15. Hanahan, D. & Weinberg, R.A. Hallmarks of cancer: the next generation. *Cell* **144**, 646-674 (2011).
16. Wolff, A.C. & Davidson, N.E. Primary systemic therapy in operable breast cancer. *Journal of Clinical Oncology* **18**, 1558-1569 (2000).
17. Linn, S.C.*, et al.* Expression of drug resistance proteins in breast cancer, in relation to chemotherapy. *International journal of cancer. Journal international du cancer* **71**, 787-795 (1997).
18. Siddik, Z.H. Biochemical and molecular mechanisms of cisplatin resistance. *Cancer Treat Res* **112**, 263-284 (2002).
19. Prestayko, A.W., D'Aoust, J.C., Issell, B.F. & Crooke, S.T. Cisplatin (cis-diamminedichloroplatinum II). *Cancer treatment reviews* **6**, 17-39 (1979).
20. Lawley, P.D. & Brookes, P. Molecular mechanism of the cytotoxic action of difunctional alkylating agents and of resistance to this action. *Nature* **206**, 480-483 (1965).

21. Sparreboom, A.*, et al.* Clinical pharmacokinetics of doxorubicin in combination with GF120918, a potent inhibitor of MDR1 P-glycoprotein. *Anti-cancer drugs* **10**, 719-728 (1999).
22. Gluck, S. Adjuvant chemotherapy for early breast cancer: optimal use of epirubicin. *Oncologist* **10**, 780-791 (2005).
23. Knight, W.A., 3rd*, et al.* Mitoxantrone in advanced breast cancer: a phase II trial of the Southwest Oncology Group. *Invest New Drugs* **1**, 181-184 (1983).
24. Farber, S. & Diamond, L.K. Temporary remissions in acute leukemia in children produced by folic acid antagonist, 4-aminopteroyl-glutamic acid. *The New England journal of medicine* **238**, 787-793 (1948).
25. Kaye, S.B. New antimetabolites in cancer chemotherapy and their clinical impact. *British journal of cancer* **78 Suppl 3**, 1-7 (1998).
26. Schiff, P.B. & Horwitz, S.B. Taxol stabilizes microtubules in mouse fibroblast cells. *Proceedings of the National Academy of Sciences of the United States of America* **77**, 1561-1565 (1980).
27. Seruga, B., Ocana, A. & Tannock, I.F. Drug resistance in metastatic castration-resistant prostate cancer. *Nat Rev Clin Oncol* **8**, 12-23 (2011).
28. Sui, M., Huang, Y., Park, B.H., Davidson, N.E. & Fan, W. Estrogen receptor alpha mediates breast cancer cell resistance to paclitaxel through inhibition of apoptotic cell death. *Cancer research* **67**, 5337-5344 (2007).
29. Sui, M., Zhang, H. & Fan, W. The role of estrogen and estrogen receptors in chemoresistance. *Curr Med Chem* **18**, 4674-4683 (2011).
30. Maehara, Y.*, et al.* Estrogen-receptor-negative breast cancer tissue is chemosensitive in vitro compared with estrogen-receptor-positive tissue. *Eur Surg Res* **22**, 50-55 (1990).
31. Violette, S.*, et al.* Resistance of colon cancer cells to long-term 5-fluorouracil exposure is correlated to the relative level of Bcl-2 and Bcl-X(L) in addition to Bax and p53 status. *International journal of cancer. Journal international du cancer* **98**, 498-504 (2002).
32. Williams, J.*, et al.* Expression of Bcl-xL in ovarian carcinoma is associated with chemoresistance and recurrent disease. *Gynecol Oncol* **96**, 287-295 (2005).
33. Witham, J.*, et al.* The Bcl-2/Bcl-XL family inhibitor ABT-737 sensitizes ovarian cancer cells to carboplatin. *Clinical cancer research : an official journal of the American Association for Cancer Research* **13**, 7191-7198 (2007).
34. Heere-Ress, E.*, et al.* Bcl-X(L) is a chemoresistance factor in human melanoma cells that can be inhibited by antisense therapy. *International journal of cancer. Journal international du cancer* **99**, 29-34 (2002).
35. Klasa, R.J., Gillum, A.M., Klem, R.E. & Frankel, S.R. Oblimersen Bcl-2 antisense: facilitating apoptosis in anticancer treatment. *Antisense Nucleic Acid Drug Dev* **12**, 193-213 (2002).
36. Li Y, J.Z., Xia K, Li X, Lv X, Pei H, Chen Z, Li J. XIAP is related to the chemoresistance and inhibited its expression by RNA interference sensitize pancreatic carcinoma cells to chemotherapeutics. *Pancreas* **32**, 288-296 (2006).
37. Tran, J.*, et al.* A role for survivin in chemoresistance of endothelial cells mediated by VEGF. *Proceedings of the National Academy of Sciences of the United States of America* **99**, 4349-4354 (2002).
38. Sharom, F.J. ABC multidrug transporters: structure, function and role in chemoresistance. *Pharmacogenomics* **9**, 105-127 (2008).
39. Longley, D.B. & Johnston, P.G. Molecular mechanisms of drug resistance. *J Pathol* **205**, 275-292 (2005).

40. Holen, N.S.W.a.I. Multidrug Resistance in Breast Cancer: FromIn Vitro Models to Clinical Studies. *International Journal of Breast Cancer* **2011**(2011).
41. Grothey, A.*, et al.* The role of insulin-like growth factor I and its receptor in cell growth, transformation, apoptosis, and chemoresistance in solid tumors. *J Cancer Res Clin Oncol* **125**, 166-173 (1999).
42. Roidl, A.*, et al.* The FGFR4 Y367C mutant is a dominant oncogene in MDA-MB453 breast cancer cells. *Oncogene* **29**, 1543-1552 (2010).
43. Chen X, Y.T., Wang Z. Enhanced drug resistance in cells coexpressing ErbB2 with EGF receptor or ErbB3. *Biochem. Biophys. Res. Commun* **277**, 757-763 (2000).
44. Zhang, L.*, et al.* Vascular endothelial growth factor overexpression by soft tissue sarcoma cells: implications for tumor growth, metastasis, and chemoresistance. *Cancer research* **66**, 8770-8778 (2006).
45. Au, Y.W.a.J.L.-S. Role of Tumour Microenvironment in Chemoresistance. *Integration/Interaction of Oncologic Growth*, 285-321 (2005).
46. Teicher, B.A.*, et al.* Tumor resistance to alkylating agents conferred by mechanisms operative only in vivo. *Science* **247**, 1457-1461 (1990).
47. Kuo, T.H.*, et al.* Site-specific chemosensitivity of human small-cell lung carcinoma growing orthotopically compared to subcutaneously in SCID mice: the importance of orthotopic models to obtain relevant drug evaluation data. *Anticancer Res* **13**, 627-630 (1993).
48. Fidler, I.J.*, et al.* Modulation of tumor cell response to chemotherapy by the organ environment. *Cancer Metastasis Rev* **13**, 209-222 (1994).
49. Ahn, K.S., Jung, Y.S., Kim, J., Lee, H. & Yoon, S.S. Behavior of murine renal carcinoma cells grown in ectopic or orthotopic sites in syngeneic mice. *Tumour Biol* **22**, 146-153 (2001).
50. Sanjeev Das, P.P.O., Yoon Sun Yang,Jin-Mo Park,Stuart A. Aaronson, & Lee, a.S.W. Discoidin Domain Receptor 1 Receptor Tyrosine Kinase Induces Cyclooxygenase-2 and Promotes Chemoresistance through Nuclear Factor-KB Pathway Activation. *Cancer research* **66**, 8123-8130 (2006).
51. Ischenko, I.*, et al.* Inhibition of Src tyrosine kinase reverts chemoresistance toward 5-fluorouracil in human pancreatic carcinoma cells: an involvement of epidermal growth factor receptor signaling. *Oncogene* **27**, 7212-7222 (2008).
52. el-Deiry, W.S. Role of oncogenes in resistance and killing by cancer therapeutic agents. *Curr Opin Oncol* **9**, 79-87 (1997).
53. Chun-Ming Tsai, D.Y., Kuo-Ting Chang, Li-Hwa Wu, Reury-Perng Perng, Nuhad K. Ibrahim, Mien-Chie Hung. Enhanced Chemoresistance by Elevation of pl85neu Levels in HER-2/neu-Transfected Human Lung Cancer Cells. *Journal of the National Cancer Institute* **87**, 682-684 (1995).
54. Slamon, D.J.*, et al.* Human breast cancer: correlation of relapse and survival with amplification of the HER-2/neu oncogene. *Science* **235**, 177-182 (1987).
55. Ginestier, C.*, et al.* ALDH1 is a marker of normal and malignant human mammary stem cells and a predictor of poor clinical outcome. *Cell stem cell* **1**, 555-567 (2007).
56. Yaziji, H.*, et al.* HER-2 testing in breast cancer using parallel tissue-based methods. *JAMA* **291**, 1972-1977 (2004).
57. Sasaki, N.*, et al.* Effect of HER-2/neu overexpression on chemoresistance and prognosis in ovarian carcinoma. *J Obstet Gynaecol Res* **33**, 17-23 (2007).
58. Saal, L.H.*, et al.* PIK3CA mutations correlate with hormone receptors, node metastasis, and ERBB2, and are mutually exclusive with PTEN loss in human breast carcinoma. *Cancer research* **65**, 2554-2559 (2005).

59. Pohlmann, P.R., Mayer, I.A. & Mernaugh, R. Resistance to Trastuzumab in Breast Cancer. *Clinical cancer research : an official journal of the American Association for Cancer Research* **15**, 7479-7491 (2009).
60. Miguel A. Molina, R.S.e., Elizabeth E. Ramsey, Marı´a-Jose´ Garcia-Barchino, Federico Rojo, Adam J. Evans, Joan Albanell, Edward J. Keenan, Ana Lluch, Javier Garcı´a-Conde, Jose´ Baselga, and Gail M. Clinton. NH2-terminal Truncated HER-2 Protein but not Full-Length Receptor Is Associated with Nodal Metastasis in Human Breast Cancer. *Clinical Cancer Research* **8**, 347-353 (2002).
61. Jasnis, G.L.F.a.M.A. Molecular Mechanisms of Trastuzumab Resistance in HER2 Overexpressing Breast Cancer. *International Journal of Breast Cancer* **2011**, 1-11 (2011).
62. Dean, M., Fojo, T. & Bates, S. Tumour stem cells and drug resistance. *Nature reviews. Cancer* **5**, 275-284 (2005).
63. Chaudhary, P.M. & Roninson, I.B. Expression and activity of P-glycoprotein, a multidrug efflux pump, in human hematopoietic stem cells. *Cell* **66**, 85-94 (1991).
64. Zinovyeva, M.V., Zijlmans, J.M., Fibbe, W.E., Visser, J.W. & Belyavsky, A.V. Analysis of gene expression in subpopulations of murine hematopoietic stem and progenitor cells. *Experimental hematology* **28**, 318-334 (2000).
65. Scharenberg, C.W., Harkey, M.A. & Torok-Storb, B. The ABCG2 transporter is an efficient Hoechst 33342 efflux pump and is preferentially expressed by immature human hematopoietic progenitors. *Blood* **99**, 507-512 (2002).
66. Gong, C.*, et al.* Markers of tumor-initiating cells predict chemoresistance in breast cancer. *PloS one* **5**, e15630 (2010).
67. Phillips, T.M., McBride, W.H. & Pajonk, F. The response of CD24(-/low)/CD44+ breast cancer-initiating cells to radiation. *J Natl Cancer Inst* **98**, 1777-1785 (2006).
68. Dylla, S.J.*, et al.* Colorectal cancer stem cells are enriched in xenogeneic tumors following chemotherapy. *PloS one* **3**, e2428 (2008).
69. Bao, F.*, et al.* Comparative gene expression analysis of a chronic myelogenous leukemia cell line resistant to cyclophosphamide using oligonucleotide arrays and response to tyrosine kinase inhibitors. *Leuk Res* **31**, 1511-1520 (2007).
70. Bertucci, F. & Birnbaum, D. Reasons for breast cancer heterogeneity. *J Biol* **7**, 6 (2008).
71. Villadsen, R.*, et al.* Evidence for a stem cell hierarchy in the adult human breast. *The Journal of cell biology* **177**, 87-101 (2007).
72. Shipitsin, M.*, et al.* Molecular definition of breast tumor heterogeneity. *Cancer Cell* **11**, 259-273 (2007).
73. Lobo, N.A., Shimono, Y., Qian, D. & Clarke, M.F. The biology of cancer stem cells. *Annual review of cell and developmental biology* **23**, 675-699 (2007).
74. Casarsa, C., Oriana, S. & Coradini, D. The controversial clinicobiological role of breast cancer stem cells. *J Oncol* **2008**, 492643 (2008).
75. Chuthapisith, S., Eremin, J., El-Sheemey, M. & Eremin, O. Breast cancer chemoresistance: emerging importance of cancer stem cells. *Surg Oncol* **19**, 27-32 (2010).
76. Al-Hajj M, W.M., Benito-Hernandez A, Morrison SJ, Clarke MF. Prospective identification of tumorigenic breast cancer cells. *Proc. Natl. Acad. Sci. U.S.A.* **100**, 3983-3988 (2003).

77. Morrison, B.J., Schmidt, C.W., Lakhani, S.R., Reynolds, B.A. & Lopez, J.A. Breast cancer stem cells: implications for therapy of breast cancer. *Breast cancer research : BCR* **10**, 210 (2008).
78. Croker, A.K.*, et al.* High aldehyde dehydrogenase and expression of cancer stem cell markers selects for breast cancer cells with enhanced malignant and metastatic ability. *J Cell Mol Med* **13**, 2236-2252 (2009).
79. Dontu, G. Breast cancer stem cell markers - the rocky road to clinical applications. *Breast cancer research : BCR* **10**, 110 (2008).
80. Bouras, T.*, et al.* Notch signaling regulates mammary stem cell function and luminal cell-fate commitment. *Cell stem cell* **3**, 429-441 (2008).
81. Zhang, M.*, et al.* Identification of tumor-initiating cells in a p53-null mouse model of breast cancer. *Cancer research* **68**, 4674-4682 (2008).
82. Shackleton, M.*, et al.* Generation of a functional mammary gland from a single stem cell. *Nature* **439**, 84-88 (2006).
83. Engelmann, K., Shen, H. & Finn, O.J. MCF7 side population cells with characteristics of cancer stem/progenitor cells express the tumor antigen MUC1. *Cancer research* **68**, 2419-2426 (2008).
84. Grange, C., Lanzardo, S., Cavallo, F., Camussi, G. & Bussolati, B. Sca-1 identifies the tumor-initiating cells in mammary tumors of BALB-neuT transgenic mice. *Neoplasia* **10**, 1433-1443 (2008).
85. Ben-Porath I, T.M., Carey VJ, et al. An embryonic stem cell-like gene expression signature

in poorly differentiated aggressive human tumors. *Nature genetics* **40**, 499-507 (2008).
86. Zhou, H.*, et al.* Generation of induced pluripotent stem cells using recombinant proteins. *Cell stem cell* **4**, 381-384 (2009).
87. Glinsky, G.V. "Stemness" genomics law governs clinical behavior of human cancer: implications for decision making in disease management. *J Clin Oncol* **26**, 2846-2853 (2008).
88. Ma L, L.D., Liu T, Cheng W, Guo L. . Cancer stem-like cells can be isolated with drug selection in human ovarian cancer cell line SKOV3. *Acta Biochim Biophys Sin (Shanghai)* **42**, 593-602 (2010).
89. Tang, Q.L.*, et al.* Salinomycin inhibits osteosarcoma by targeting its tumor stem cells. *Cancer Lett* **311**, 113-121 (2011).
90. Korkaya, H., Paulson, A., Iovino, F. & Wicha, M.S. HER2 regulates the mammary stem/progenitor cell population driving tumorigenesis and invasion. *Oncogene* **27**, 6120-6130 (2008).
91. Grimshaw, M.J.*, et al.* Mammosphere culture of metastatic breast cancer cells enriches for tumorigenic breast cancer cells. *Breast cancer research : BCR* **10**, R52 (2008).
92. Thompson, E.W.*, et al.* Association of increased basement membrane invasiveness with absence of estrogen receptor and expression of vimentin in human breast cancer cell lines. *J Cell Physiol* **150**, 534-544 (1992).
93. Savagner, P. The epithelial-mesenchymal transition (EMT) phenomenon. *Ann Oncol* **21 Suppl 7**, vii89-92 (2010).
94. Hugo, H.*, et al.* Epithelial--mesenchymal and mesenchymal--epithelial transitions in carcinoma progression. *J Cell Physiol* **213**, 374-383 (2007).
95. Berx, G., Raspe, E., Christofori, G., Thiery, J.P. & Sleeman, J.P. Pre-EMTing metastasis? Recapitulation of morphogenetic processes in cancer. *Clin Exp Metastasis* **24**, 587-597 (2007).

96. Come, C.*, et al.* Snail and slug play distinct roles during breast carcinoma progression. *Clinical cancer research : an official journal of the American Association for Cancer Research* **12**, 5395-5402 (2006).
97. Glinsky, G.V., Berezovska, O., and Glinskii, A.B. Microarray analysis identifies a death-from-cancer signature predicting therapy
failure in patients with multiple types of cancer. *J. Clin. Invest.* **115**, 1503–1521 (2005).
98. Lapidot, T.*, et al.* A cell initiating human acute myeloid leukaemia after transplantation into SCID mice. *Nature* **367**, 645-648 (1994).
99. Stingl, J. & Caldas, C. Molecular heterogeneity of breast carcinomas and the cancer stem cell hypothesis. *Nature reviews. Cancer* **7**, 791-799 (2007).
100. Singh, S.K.*, et al.* Identification of a cancer stem cell in human brain tumors. *Cancer research* **63**, 5821-5828 (2003).
101. Ricci-Vitiani, L.*, et al.* Identification and expansion of human colon-cancer-initiating cells. *Nature* **445**, 111-115 (2007).
102. Patrawala, L.*, et al.* Highly purified CD44+ prostate cancer cells from xenograft human tumors are enriched in tumorigenic and metastatic progenitor cells. *Oncogene* **25**, 1696-1708 (2006).
103. Sheridan, C.*, et al.* CD44+/CD24- breast cancer cells exhibit enhanced invasive properties: an early step necessary for metastasis. *Breast cancer research : BCR* **8**, R59 (2006).
104. Liu, H.*, et al.* Cancer stem cells from human breast tumors are involved in spontaneous metastases in orthotopic mouse models. *Proceedings of the National Academy of Sciences of the United States of America* **107**, 18115-18120 (2010).
105. Takahashi-Yanaga, F. & Kahn, M. Targeting Wnt signaling: can we safely eradicate cancer stem cells? *Clinical cancer research : an official journal of the American Association for Cancer Research* **16**, 3153-3162 (2010).
106. Magnifico, A.*, et al.* Tumor-initiating cells of HER2-positive carcinoma cell lines express the highest oncoprotein levels and are sensitive to trastuzumab. *Clinical cancer research : an official journal of the American Association for Cancer Research* **15**, 2010-2021 (2009).
107. Wilson, C.A.*, et al.* HER-2 overexpression differentially alters transforming growth factor-beta responses in luminal versus mesenchymal human breast cancer cells. *Breast cancer research : BCR* **7**, R1058-1079 (2005).
108. Mitani, M., Yamanishi, T., Miyazaki, Y. & Otake, N. Salinomycin effects on mitochondrial ion translocation and respiration. *Antimicrobial agents and chemotherapy* **9**, 655-660 (1976).
109. Matsumori, N., Morooka, A. & Murata, M. Conformation and location of membrane-bound salinomycin-sodium complex deduced from NMR in isotropic bicelles. *Journal of the American Chemical Society* **129**, 14989-14995 (2007).
110. Gupta, P.B.*, et al.* Identification of selective inhibitors of cancer stem cells by high-throughput screening. *Cell* **138**, 645-659 (2009).
111. Zhang, G.N.*, et al.* Combination of salinomycin and gemcitabine eliminates pancreatic cancer cells. *Cancer Lett* **313**, 137-144 (2011).
112. Dong, T.T.*, et al.* Salinomycin selectively targets 'CD133+' cell subpopulations and decreases malignant traits in colorectal cancer lines. *Ann Surg Oncol* **18**, 1797-1804 (2011).
113. Kim, J.H.*, et al.* Salinomycin sensitizes cancer cells to the effects of doxorubicin and etoposide treatment by increasing DNA damage and reducing p21 protein. *British journal of pharmacology* **162**, 773-784 (2011).

114. Kim, K.Y.*, et al.* Salinomycin-induced apoptosis of human prostate cancer cells due to accumulated reactive oxygen species and mitochondrial membrane depolarization. *Biochemical and biophysical research communications* **413**, 80-86 (2011).
115. Dontu, G.*, et al.* In vitro propagation and transcriptional profiling of human mammary stem/progenitor cells. *Genes Dev* **17**, 1253-1270 (2003).
116. Ponti, D.*, et al.* Isolation and in vitro propagation of tumorigenic breast cancer cells with stem/progenitor cell properties. *Cancer research* **65**, 5506-5511 (2005).
117. LaBarge, M.A.*, et al.* Human mammary progenitor cell fate decisions are products of interactions with combinatorial microenvironments. *Integr Biol (Camb)* **1**, 70-79 (2009).
118. Cowell, L.N., Graham, J.D., Bouton, A.H., Clarke, C.L. & O'Neill, G.M. Tamoxifen treatment promotes phosphorylation of the adhesion molecules, p130Cas/BCAR1, FAK and Src, via an adhesion-dependent pathway. *Oncogene* **25**, 7597-7607 (2006).
119. Goodell, M.A. Introduction: Focus on hematology. CD34(+) or CD34(-): does it really matter? *Blood* **94**, 2545-2547 (1999).
120. Rapp, U.R.*, et al.* MYC is a metastasis gene for non-small-cell lung cancer. *PloS one* **4**, e6029 (2009).
121. Ivascu, A. & Kubbies, M. Diversity of cell-mediated adhesions in breast cancer spheroids. *Int J Oncol* **31**, 1403-1413 (2007).
122. Shaw, K.R., Wrobel, C.N. & Brugge, J.S. Use of three-dimensional basement membrane cultures to model oncogene-induced changes in mammary epithelial morphogenesis. *J Mammary Gland Biol Neoplasia* **9**, 297-310 (2004).
123. Pickl, M. & Ries, C.H. Comparison of 3D and 2D tumor models reveals enhanced HER2 activation in 3D associated with an increased response to trastuzumab. *Oncogene* **28**, 461-468 (2009).
124. Haenssen, K.K.*, et al.* ErbB2 requires integrin alpha5 for anoikis resistance via Src regulation of receptor activity in human mammary epithelial cells. *Journal of cell science* **123**, 1373-1382 (2010).
125. Basu, D.*, et al.* Detecting and targeting mesenchymal-like subpopulations within squamous cell carcinomas. *Cell Cycle* **10**, 2008-2016 (2011).
126. O'Shaughnessy, J. Extending survival with chemotherapy in metastatic breast cancer. *Oncologist* **10 Suppl 3**, 20-29 (2005).
127. Cortes, J. & Baselga, J. Targeting the microtubules in breast cancer beyond taxanes: the epothilones. *Oncologist* **12**, 271-280 (2007).
128. Giaccone, G. & Pinedo, H.M. Drug Resistance. *Oncologist* **1**, 82-87 (1996).
129. Leonessa, F. & Clarke, R. ATP binding cassette transporters and drug resistance in breast cancer. *Endocr Relat Cancer* **10**, 43-73 (2003).
130. Rivera, E. & Gomez, H. Chemotherapy resistance in metastatic breast cancer: the evolving role of ixabepilone. *Breast cancer research : BCR* **12 Suppl 2**, S2 (2010).
131. Choi, C.H. ABC transporters as multidrug resistance mechanisms and the development of chemosensitizers for their reversal. *Cancer Cell Int* **5**, 30 (2005).
132. Dean, M., Hamon, Y. & Chimini, G. The human ATP-binding cassette (ABC) transporter superfamily. *Journal of lipid research* **42**, 1007-1017 (2001).
133. Chang, G. Multidrug resistance ABC transporters. *FEBS letters* **555**, 102-105 (2003).

134. Dittmer, A.*, et al.* Mesenchymal stem cells and carcinoma-associated fibroblasts sensitize breast cancer cells in 3D cultures to kinase inhibitors. *Int J Oncol* **39**, 689-696 (2011).
135. Reynolds, B.A. & Weiss, S. Generation of neurons and astrocytes from isolated cells of the adult mammalian central nervous system. *Science* **255**, 1707-1710 (1992).
136. Lan, L., Cui, D., Nowka, K. & Derwahl, M. Stem cells derived from goiters in adults form spheres in response to intense growth stimulation and require thyrotropin for differentiation into thyrocytes. *The Journal of clinical endocrinology and metabolism* **92**, 3681-3688 (2007).
137. Shi, X., Gipp, J. & Bushman, W. Anchorage-independent culture maintains prostate stem cells. *Developmental biology* **312**, 396-406 (2007).
138. Vladislav V. Glinsky, G.V.G., Kate Rittenhouse-Olson, Margaret E. Huflejt, Olga V. Glinskii, & Susan L. Deutscher, a.T.P.Q. The Role of Thomsen-Friedenreich Antigen in Adhesion of Human Breast and Prostate Cancer Cells to the Endothelium. *Cancer research* **61**, 4851–4857 (2001).
139. Hynes, N.E. & Lane, H.A. ERBB receptors and cancer: the complexity of targeted inhibitors. *Nature reviews. Cancer* **5**, 341-354 (2005).
140. Debnath, J. & Brugge, J.S. Modelling glandular epithelial cancers in three-dimensional cultures. *Nature reviews. Cancer* **5**, 675-688 (2005).
141. Reginato, M.J.*, et al.* Integrins and EGFR coordinately regulate the pro-apoptotic protein Bim to prevent anoikis. *Nat Cell Biol* **5**, 733-740 (2003).
142. Reginato, M.J.*, et al.* Bim regulation of lumen formation in cultured mammary epithelial acini is targeted by oncogenes. *Molecular and cellular biology* **25**, 4591-4601 (2005).
143. Riethdorf, S.*, et al.* Detection and HER2 expression of circulating tumor cells: prospective monitoring in breast cancer patients treated in the neoadjuvant GeparQuattro trial. *Clinical cancer research : an official journal of the American Association for Cancer Research* **16**, 2634-2645 (2010).
144. Fehm, T. & Sauerbrei, W. Information from CTC measurements for metastatic breast cancer prognosis-we should do more than selecting an "optimal cut point". *Breast cancer research and treatment* **122**, 219-220 (2010).
145. Muller, V. & Pantel, K. HER2 as marker for the detection of circulating tumor cells. *Breast cancer research and treatment* **117**, 535-537 (2009).
146. Meng, S.*, et al.* HER-2 gene amplification can be acquired as breast cancer progresses. *Proceedings of the National Academy of Sciences of the United States of America* **101**, 9393-9398 (2004).
147. Vazquez-Martin, A., Oliveras-Ferraros, C. & Menendez, J.A. Autophagy facilitates the development of breast cancer resistance to the anti-HER2 monoclonal antibody trastuzumab. *PloS one* **4**, e6251 (2009).
148. Slamon, D.J.*, et al.* Studies of the HER-2/neu proto-oncogene in human breast and ovarian cancer. *Science* **244**, 707-712 (1989).
149. Harari, D. & Yarden, Y. Molecular mechanisms underlying ErbB2/HER2 action in breast cancer. *Oncogene* **19**, 6102-6114 (2000).
150. Aguilar, Z.*, et al.* Biologic effects of heregulin/neu differentiation factor on normal and malignant human breast and ovarian epithelial cells. *Oncogene* **18**, 6050-6062 (1999).
151. Hudis, C.A. Trastuzumab--mechanism of action and use in clinical practice. *The New England journal of medicine* **357**, 39-51 (2007).
152. O'Brien, N.A.*, et al.* Activated phosphoinositide 3-kinase/AKT signaling confers resistance to trastuzumab but not lapatinib. *Mol Cancer Ther* **9**, 1489-1502 (2010).

153. Ailles, L.E. & Weissman, I.L. Cancer stem cells in solid tumors. *Curr Opin Biotechnol* **18**, 460-466 (2007).
154. Wright, M.H.*, et al.* Brca1 breast tumors contain distinct CD44+/CD24- and CD133+ cells with cancer stem cell characteristics. *Breast cancer research : BCR* **10**, R10 (2008).
155. Hermann, P.C.*, et al.* Distinct populations of cancer stem cells determine tumor growth and metastatic activity in human pancreatic cancer. *Cell stem cell* **1**, 313-323 (2007).
156. Reim, F.*, et al.* Immunoselection of breast and ovarian cancer cells with trastuzumab and natural killer cells: selective escape of CD44high/CD24low/HER2low breast cancer stem cells. *Cancer research* **69**, 8058-8066 (2009).
157. Pommier, S.J.*, et al.* Characterizing the HER2/neu status and metastatic potential of breast cancer stem/progenitor cells. *Ann Surg Oncol* **17**, 613-623 (2010).
158. Fuchs, D., Heinold, A., Opelz, G., Daniel, V. & Naujokat, C. Salinomycin induces apoptosis and overcomes apoptosis resistance in human cancer cells. *Biochemical and biophysical research communications* **390**, 743-749 (2009).
159. Fuchs, D., Daniel, V., Sadeghi, M., Opelz, G. & Naujokat, C. Salinomycin overcomes ABC transporter-mediated multidrug and apoptosis resistance in human leukemia stem cell-like KG-1a cells. *Biochemical and biophysical research communications* **394**, 1098-1104 (2010).
160. Weir, H.K.*, et al.* Annual report to the nation on the status of cancer, 1975-2000, featuring the uses of surveillance data for cancer prevention and control. *J Natl Cancer Inst* **95**, 1276-1299 (2003).
161. Lu, D.*, et al.* Salinomycin inhibits Wnt signaling and selectively induces apoptosis in chronic lymphocytic leukemia cells. *Proceedings of the National Academy of Sciences of the United States of America* **108**, 13253-13257 (2011).

8. ACKNOWLEDGEMENTS

Before beginning a new chapter of my life, I would like to extend a heartfelt thanks to the following people who supported, guided and inspired me throughout the journey of my PhD life.

First and foremost I would like to express my profound gratitude to Prof. Dr. Ernst Wagner, Chair of Pharmaceutical Biotechnology (Department of Pharmacy, Ludwig Maximilians University Munich) for providing me the opportunity of completion of my doctoral studies in his department. Thank you for all the discussions and guidance during my thesis work.

I would also like to extend a heartfelt thanks to my supervisor Dr. Andreas Roidl (Groupleader Molecular Biology) for guiding me through the thesis, encouraging and pushing me whenever required. Further, I thank him for providing me the interactive environment that helped me develop the ability of analysis and shaping up the projects independently. Thanks for all the criticism that improved my scientific writing abilities and technical expertise. I further want to acknowledge my group member Florian Kopp for helping me with the qPCR based and *in vivo* experiments. Thanks for all the collaborative work and discussions during meetings/presentations. I further extend my gratitude to Melinda Kiss our technical assistant for providing all the cell culture support during my thesis and guiding me during my initial lab work. I also thanks Rebekka Kubisch one of our 'friday group seminar' member for her suggestions and criticism during the discussions.

Thanks especially to Dr. Manfred Ogris for his suggestions and discussions not only regarding projects but also regarding different dishes, religions and spices.

I am also grateful to Dr. Joachim W. Ellwart (Institute for Molecular Immunology, Helmholtz Zentrum, Munich) for his support in all the Cell sorting experiments. I also epress gratitude to Dr. Stefan Zahler and Dr. Robert Fürst (Pharmaceutical Biology, Department of Pharmacy, LMU, Munich) for their guidance in using Laser scaning microscope and Flow cytometer respectively.

Special thanks to Dr. Axel Ullrich (Director, Molecular biology, Max Planck institute of Biochemistry, Martinred) for supporting us with ideas and expert advice during my doctoral studies. I am very grateful to Dr. Pjotr Knyazev (senior staff scientist, Max Planck institute of Biochemistry, Martinred) for supporting us with certain laboratory materials and for all the discussions in shaping certain parts of the project. Special thanks to Dr. Ulf R Rapp (Department of Molecular Biology 'Cancer metastasis group', Max-Planck-Institute of Biochemistry, Martinsried) for supporting us with mouse breeds for our study. I also extend my gratitude to Dr. Rajkumar Savai (Molecular mechanisms in lung cancer, Max Planck Institut for Heart and Lung Research, Bad nauheim) for his assistance in performing mouse experiments in Bad Nauheim.

I want to extend my special acknowledgements to Chitra thakur (Molecular biology, Max Planck institute of Biochemistry, Martinred) for being a great collaborator and standing by me throughout all the odds. Special thanks to Dr. Vaibhao Janabandhu for guiding me through with certain techniques and being such a wonderful friend.

Thanks to Ursula Biebl and Anna Kulinyak for taking care of all the laboratory consumables. A heartfelt thanks to Miriam Höhn for technical assistance and guidance for cell culture. I would like to acknowledge Markus Kovac for helping me whenever I required and for taking care of our mouse facility. A heartfelt gratitude to Wolfgang Rödl, for patiently sorting out technical problems of instruments, specially related to computer. I extend my thanks to Olga Brück (Secretary) for supporting me in the entire official paper work.

I further acknowledge all the bachelor students who did their bachelor thesis under my supervision Svenja Groeneveld, Rebekka Kosch, Josefine Pott, Simone Schlagmüller and Vanessa Welk for helping me with experiments and providing me with an opportunity to improve my teaching skills.

I owe my sincere gratitude to my parents Mr. Shirish Oak and Mrs. Nisha Oak and my brother Mr. Aditya Oak for their unconditional love, emotional support and belief in my skills and abilities. I dedicate my doctoral thesis to them.

A special thank to ‘coffee break group’ Katarina, Rebekka, Petra, Melinda and Joana for providing me refreshing coffee breaks in between. Special and heartfelt thanks to Rebekka and Petra for supporting me and encouraging me through my low times. Heartfelt thanks to Katarina for sharing lovely movie evenings with Indian chai and homemade Indian and Slovakian food. I would like to acknowledge my ‘German brother’ David and his wife Eva for supporting throughout the stay here and providing me with nice family environment around. I also extend my thanks to all the lab members for all the scientific as well as non-scientific discussions and all the off-work enjoyment in lab and trips.

Last but not least I want to extend my gratitude to all my Indian friends Ganesh, Vaibhao, Bharti, Naresh, Monali, Avinash, Mayur, Amit, Sayantanee, Aditya, Sneha, Chitra, Dity, Megha, Hema, Purvi and Padma for making my stay in Munich smooth and joyful. I owe a heartfelt thank to Shymolie Patil for being such a great and jolly small sister and always being there. Also heartfelt thanks to ‘Team Asha Munich’ for providing me with an opportunity to get involved with NGO ‘Asha for education’ supporting education of underprivileged children in India.

9. CURRICULUM VITAE

Personal Details

Name	Prajakta Shirish Oak
Date of Birth	29.08.1983
Place of Birth	Pune, India
Nationality	Indian

Education

Nov 2008-Till date	Doctoral studies, Dept. of Pharmacy, LMU, Munich, GERMANY. **Supervisors:** Prof. Ernst Wagner, Dr. Andreas Roidl.
Jan 2006- May 2008	Project assistant, National center for cell science, Pune, INDIA. **Supervisor:** Dr. (Mrs.) V. P. Kale.
2003-2005	Master of Science (Microbiology), V.E.S College of Arts, Science and commerce, University of Mumbai, INDIA.
2000-2003	Bachelor of Science (Microbiology), V.E.S College, University of Mumbai, INDIA.

Awards/Scholarships

i) **'AACR Scholar-in-training Award'** funded by Susan G. Komen for the cure for poster presentation in American Association for Cancer Research's special conference on 'Advances in breast cancer research' held in CA, USA.

ii) **'The Dr. Dhala's felicitation fund Eureka Forbes ltd. Scholarship'** for securing the highest marks in 'Master of Science' examination held in March, 2005 (University Topper in Microbiology).

iii) **'Best student'** of the College for the year 2002-2003. Certificate of Merit for All-Round Proficiency awarded by the college.